NAVAL POSTGRADUATE SCHOOL
MONTEREY, CALIFORNIA

THESIS

OPTIMIZATION AND PERFORMANCE ANALYSIS OF WAVERIDER CONFIGURED INTERPLANETARY SPACE VEHICLES

by
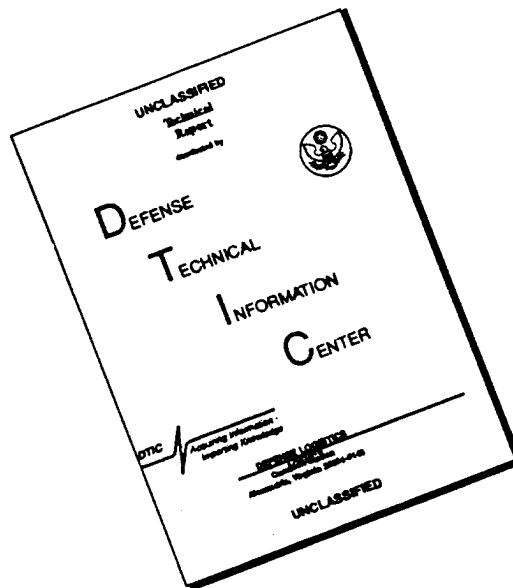
John M. Flynn

June, 1996

Thesis Advisor: Conrad F. Newberry
Co-Advisor: Jeffrey V. Bowles

Approved for public release; distribution is unlimited.

19960910 146

DISCLAIMER NOTICE

THIS DOCUMENT IS BEST QUALITY AVAILABLE. THE COPY FURNISHED TO DTIC CONTAINED A SIGNIFICANT NUMBER OF PAGES WHICH DO NOT REPRODUCE LEGIBLY.

		Form Approved OMB No. 0704-0188

REPORT DOCUMENTATION PAGE

1. AGENCY USE ONLY *(Leave blank)*	2. REPORT DATE June 1996.	3. REPORT TYPE AND DATES COVERED Master's Thesis

4. TITLE AND SUBTITLE TITLE OF THESIS.
OPTIMIZATION AND PERFORMANCE ANALYSIS OF WAVERIDER CONFIGURED INTERPLANETARY SPACE VEHICLES

5. FUNDING NUMBERS

6. AUTHOR(S)
Flynn, John M.

7. PERFORMING ORGANIZATION NAME(S) AND ADDRESS(ES)
Naval Postgraduate School
Monterey CA 93943-5000

8. PERFORMING ORGANIZATION REPORT NUMBER

9. SPONSORING/MONITORING AGENCY NAME(S) AND ADDRESS(ES)

10. SPONSORING/MONITORING AGENCY REPORT NUMBER

11. SUPPLEMENTARY NOTES The views expressed in this thesis are those of the author and do not reflect the official policy or position of the Department of Defense or the U.S. Government.

12a. DISTRIBUTION/AVAILABILITY STATEMENT
Approved for public release; distribution is unlimited.

12b. DISTRIBUTION CODE

13. ABSTRACT *(maximum 200 words)*
   This thesis describes a number of issues associated with waverider configured spacecraft designed for interplanetary missions. The first such issue is the determination of the magnitude of the energies and velocities required for conventional gravity-assist (GA) spaceflight maneuvers contrasted with energies and velocities required for less conventional aero-gravity assisted (AGA) maneuvers for interplanetary spaceflight travel. These comparisons will be made for an Earth-Mars shuttle mission, a mission to Saturn, a mission to Neptune, and a round-trip mission to Saturn. Two additional issues considered for each mission are the fuel requirements and flight time parameters for both gravity-assist and AGA maneuvering spaceflight trajectories. This research includes the use of the patched conic interplanetary trajectory optimization MIDAS (Mission Design and Analysis Software) code for mission flight path analysis developed by the Jet Propulsion Laboratory. Waverider configuration development and off-design aerothermal analysis for each mission was supported by the NASA Ames Research Center's Waverider code (a subset of the Hypersonic Aircraft Vehicle Optimization Code) and a modified AEROSA code employing a Martian atmosphere, respectively. The results of this research showed that by using AGA, launch windows could be widened, flight times could be reduced by 25%, and fuels could be reduced by 30%.

14. SUBJECT TERMS Waveriders, Interplanetary Trajectories, Aero-Gravity-Assist	15. NUMBER OF PAGES 133
	16. PRICE CODE

17. SECURITY CLASSIFICATION OF REPORT Unclassified	18. SECURITY CLASSIFICATION OF THIS PAGE Unclassified	19. SECURITY CLASSIFICATION OF ABSTRACT Unclassified	20. LIMITATION OF ABSTRACT UL

NSN 7540-01-280-5500

Standard Form 298 (Rev. 2-89)
Prescribed by ANSI Std. 239-18 298-102

DTIC QUALITY INSPECTED 3

OPTIMIZATION AND PERFORMANCE ANALYSIS OF WAVERIDER CONFIGURED INTERPLANETARY SPACE VEHICLES

John M. Flynn
Lieutenant, United States Navy
B. S., University of Southern California, 1989

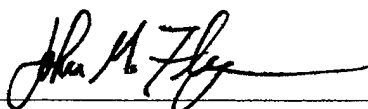Submitted in partial fulfillment
of the requirements for the degree of

MASTER OF SCIENCE IN ASTRONAUTICAL ENGINEERING

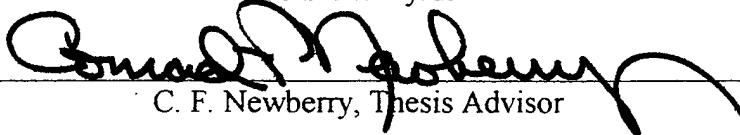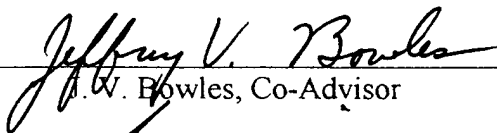from the

NAVAL POSTGRADUATE SCHOOL
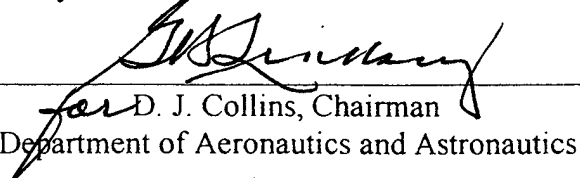
June 1996

Author: _____

John M. Flynn

Approved By: _____

C. F. Newberry, Thesis Advisor

_____

J. V. Bowles, Co-Advisor

_____

D. J. Collins, Chairman
Department of Aeronautics and Astronautics

iii

ABSTRACT

This thesis describes a number of issues associated with waverider configured spacecraft designed for interplanetary missions. The first such issue is the determination of the magnitude of the energies and velocities required for conventional gravity-assist (GA) spaceflight maneuvers contrasted with energies and velocities required for less conventional aero-gravity assisted (AGA) maneuvers for interplanetary spaceflight travel. These comparisons will be made for an Earth-Mars shuttle mission, a mission to Saturn, a mission to Neptune, and a round-trip mission to Saturn. Two additional issues considered for each mission are the fuel requirements and flight time parameters for both gravity-assist and AGA maneuvering spaceflight trajectories. This research includes the use of the patched conic interplanetary trajectory optimization MIDAS (Mission Design and Analysis Software) code for mission flight path analysis developed by the Jet Propulsion Laboratory. Waverider configuration development and off-design aerothermal analysis for each mission was supported by the NASA Ames Research Center's Waverider code (a subset of the Hypersonic Aircraft Vehicle Optimization Code) and a modified AEROSA code employing a Martian atmosphere, respectively. The results of this research showed that by using AGA, launch windows could be widened, flight times could be reduced by 25%, and fuels could be reduced by 30%.

TABLE OF CONTENTS

LIST OF FIGURES

LIST OF TABLES

ACKNOWLEDGMENTS

Before getting into the heart of this thesis, I would like to take this time to show my appreciation to certain people who made this thesis possible. First, and foremost, to Prof. Conrad F. Newberry, my advisor at the Naval Postgraduate School, who was able to steer me clear of unattainable goals. Second, to Jeffrey V. Bowles and Loc Hyunh, both of the NASA Ames Research Center, for going above and beyond the call in order to help me by modifying their complex computer codes to fit my needs. Indeed, my heartfelt appreciation goes to all those at the Systems Analysis Branch at NASA Ames who have put in many extra hours so that I would not. I would also like to show my thanks to the people at the Jet Propulsion Laboratory who started me on the right track towards this ultimate goal. They include Dr. Angus McRonald, Dr. Jim Randolph, Stacey Weinstein, and many others who added their thoughts and inputs towards waveriders and interplanetary travel. Dr. McRonald and Dr. Randolph introduced me to volumes of literature written mostly by themselves dealing with waveriders and the AGA maneuver. Ms. Weinstein was kind enough to teach me the MIDAS code and provide me with previous analyses of low energy trajectories to the outer planets. Without all these contributions from these various sources this thesis would not have been possible.

John M. Flynn, June 1996

Monterey, California

I. INTRODUCTION

Since before the dawn of the space age, man has looked towards space as the new frontier for exploration. However, it was not until July of 1969 that man actually visited another worldly body. In addition, it has been only in the last ten to fifteen years that man has sent deep space probes to the outer planets in order to help quench his desire to explore. In fact, the mission designers for the two Voyager missions that were launched in 1977 were lucky that they had the technology to take advantage of a unique planetary alignment allowing visits to all the outer planets (ending with a flyby of Neptune in 1989) except Pluto. This was known as the grand tour. One of the advantages of this alignment was that every planet visited by Voyager contributed some momentum and a change in the spacecraft's heliocentric velocity vector that enabled Voyager to be pointed towards its next destination without using much fuel. This gravity-assist (GA) maneuver is a much more efficient method of traveling in space to the outer planets than a direct trajectory from Earth.

Generally, a direct trajectory to any celestial body will require an enormous amount of energy (i.e., fuel). In fact, this method will most likely require more fuel than the launch vehicle is capable of carrying. It was determined through celestial and orbital mechanics that GA trajectories to the outer plants offer the advantages of smaller fuel mass along with quicker flight times that would otherwise be the case. One of the many disadvantages of GA is that mission planners have to wait for the correct planetary alignment before launching a given spacecraft. Furthermore, GA bending at the small

1

planets is limited, calling for multiple flybys and longer flight times. With problems in

software development, integration, and other causes of launch delays, mission designers

have to use proven technology rather than risking the development of new technologies

so that their spacecraft can be ready to meet its launch window. This problem could be

solved if there was a way to increase the size of the launch window, and perhaps,

decrease the length of the mission resulting in a reduction in fuel consumption.

A. AERO-GRAVITY-ASSIST

Aero-Gravity-Assist (AGA) is a method currently being studied for long range

inter-planetary travel. It uses the atmosphere of a small planet to provide the spacecraft

with more momentum and a bending of its heliocentric velocity vector relative to the

planet [Ref 1]. The intent of the AGA maneuver is to bend the spacecraft's heliocentric

velocity vector towards the direction the mission planners want the spacecraft to go upon

leaving the planet.

As can be seen in the first three diagrams of Fig. 1.1, simple vector diagrams

show how an AGA maneuver would occur. When the spacecraft approaches the AGA

planet it has a heliocentric velocity of $V_{S/C}$, while the planet is moving around the sun at

a velocity of V_P (Fig. 1.1a). The velocity of the spacecraft relative to the planet is

defined as V_∞. These three velocities are related by the vector equation: $V_{S/C} = V_P + V_\infty$.

During the AGA maneuver the velocity vector $V_{S/C}$ is turned through an angle (ϕ, in Fig.

1.1b and 1.1e) until the spacecraft is on course to its next destination. As $V_{S/C}$ is bent it

increases in magnitude as shown in Fig 1.1c. Note that V_P and V_∞ remain at their initial

magnitude.

2

The AGA maneuver could also be used to slow a spacecraft down and put it into orbit around a planet. This particular maneuver is shown by the three vector diagrams on the right side of Fig. 1.1. Figure 1.1d depicts the initial vector diagram as the spacecraft approaches the AGA planet. In this case $V_{S/C}$ is turned so that V_∞ is in the opposite direction of V_P (Fig 1.1e). From Fig 1.1f, one can see the decrease in the magnitude of the spacecraft's heliocentric velocity ($V_{S/C}$).

Vector Analysis: $V_{S/C} = V_P + V_\infty$
$V_{S/C}$ = Heliocentric Spacecraft Velocity
V_P = Heliocentric Planet Velocity
V_∞ = Velocity of Spacecraft Relative to the Planet as if it were coming from infinity
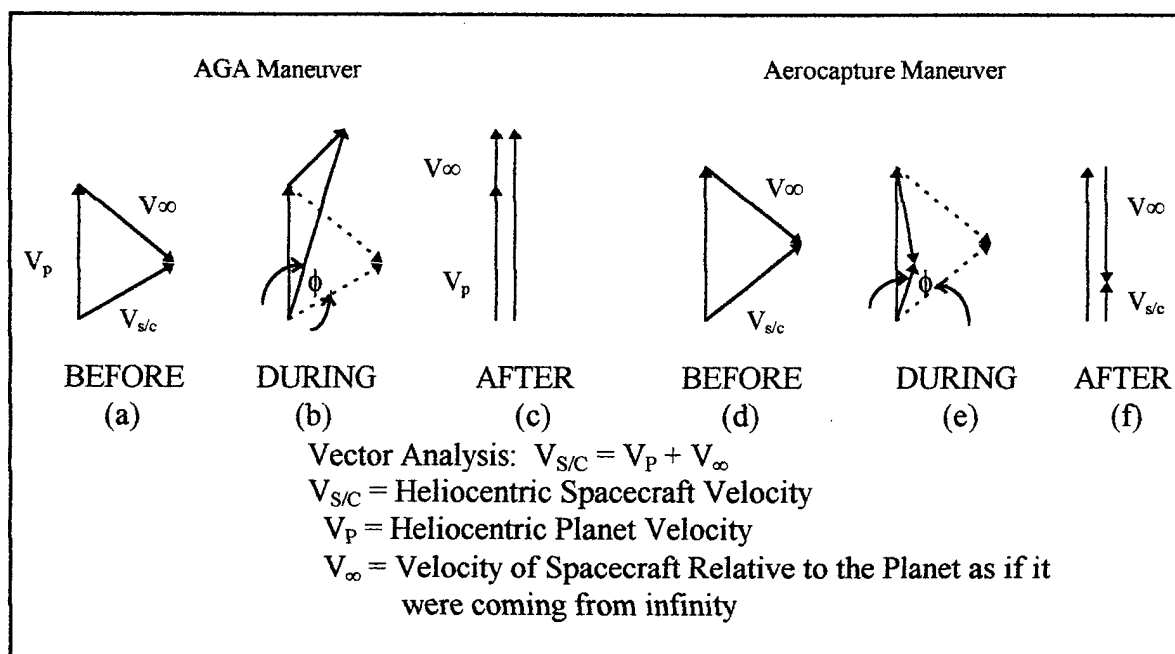
Figure 1.1 Aero-Gravity-Assist Maneuver

The planets currently being studied for possible use of AGA for outer planetary missions are Mars, Venus, and Earth. Theoretically, the AGA maneuver uses the aerodynamic lift from a high lift-to-drag (L/D) vehicle to create the needed force to keep the vehicle in a circular path around a planet with an atmosphere until the desired change in the heliocentric velocity vector is attained. The reason a high L/D vehicle is required can be seen from the following discussion.

3

An approximate equation (Eq. 1.1) can be formulated to describe the balance between the aerodynamic force, gravity and centrifugal force during an AGA maneuver [Ref. 2]:

$$1/2 \, \rho V^2 \, C_L + mg = \frac{m V^2}{R}$$ (1.1)

From this relationship, the atmospheric density can be obtained, almost independent of speed (Eq. 1.2). The atmospheric density identifies the altitude at which the vehicle needs to fly until the required heliocentric velocity is obtained:

$$\rho = \left[1 - \left(\frac{V_c}{V}\right)^2\right] \frac{2 \, m}{R C_L S}$$ (1.2)

V_c is the velocity required to maintain a circular orbit around the given planet and S is the aerodynamic reference area of the vehicle. By integrating the drag along the flight path through the atmosphere, the velocity loss due to aerodynamic drag can be found:

$$\Delta V = -\int \frac{1/2 \, \rho V^2 C_D S}{m} dt$$ (1.3)

Eq. 1.3, can be integrated to obtain the following approximation:

$$\frac{\Delta V}{V} = \frac{-\phi}{C_L / C_D}\left[1 - \left(\frac{V_c}{V}\right)^2\right]$$ (1.4)

With this relationship between V and V_∞, another equation can be written according to the authors of Ref. 2:

$$\frac{\Delta V_\infty}{V_\infty} = -\frac{\phi}{C_L / C_D}\left[1 + \left(\frac{V_c}{V_\infty}\right)^2\right]$$ (1.5)

4

Equation 1.5 represents the velocity loss in the atmosphere due to aerodynamic

drag during an AGA maneuver. In order to minimize the velocity loss (ΔV_∞) in Eq. 1.5,

the L/D ratio must be high. As noted above, Eq. 1.2 can be used as a mission trajectory

design equation for determining the appropriate altitude at which to fly the AGA

maneuver. One of the factors in the Eq. 1.2 is a design factor known as the lift

parameter. Given the lift parameter defined in Eq. 1.6, the value of the density (ρ),

corresponding to the altitude of the AGA maneuver, can be obtained implicitly (V_c is also

a function of altitude) from Eq. 1.2.

$$\textbf{Lift Parameter} = \frac{m}{C_L S} \tag{1.6}$$

An illustration of the forces acting on the vehicle during an AGA maneuver at

Mars is shown in Fig. 1.2. From the preceding equations and the two figures, a "free"

parameter is introduced. This "free" parameter is the bending angle (ϕ). It is considered

a "free" parameter because the mission planners using AGA can adjust this parameter to

whatever value is required to send the spacecraft off to its next planetary destination with

the added benefit of a large increase in the spacecraft's heliocentric velocity. The launch

window for an AGA mission is widened since mission planners are free to adjust the

bending angle at the AGA planet. Again, a high L/D vehicle is required (L/D of at least

five) in order to minimize aerodynamic drag losses and to maintain a circular flight path

around the planet. The waverider design is best suited for this type of mission.
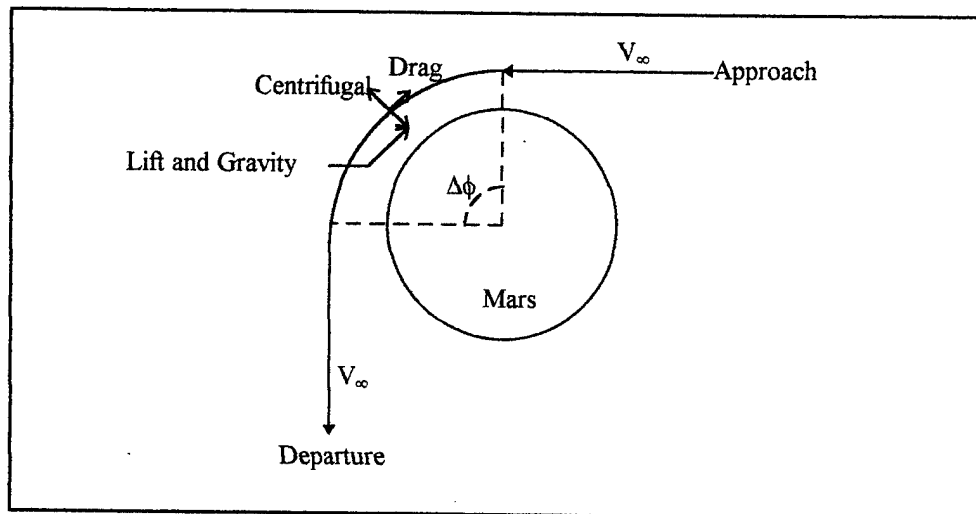
Figure 1.2 Forces Present During an AGA Maneuver

B. WAVERIDERS

Waveriders are configurations designed inversely to fit known flowfields [Ref. 3].

They offer the advantages of increased aerodynamic lift and a decrease in aerodynamic

drag compared to conventionally shaped vehicles in the hypersonic flight regime. Thus,

the waverider's L/D ratio in this hypersonic flight regime is much higher than other

vehicles. Nonweiler pointed out in the Journal of the Royal Aeronautical Society that the

flow fields formed by oblique wedge generated shockwaves define a family of caret-

shaped vehicles. These caret-shaped vehicles are examples of waveriders. One such

vehicle is illustrated in Fig. 1.3. The term "waverider" comes from the fact that the

leading edges of these vehicles ride on the surface of a the attached planar shockwave.

Waveriders increase the lift of the vehicle by capturing the planar shockwave and using

the increased pressure behind the shockwave to provide lift.
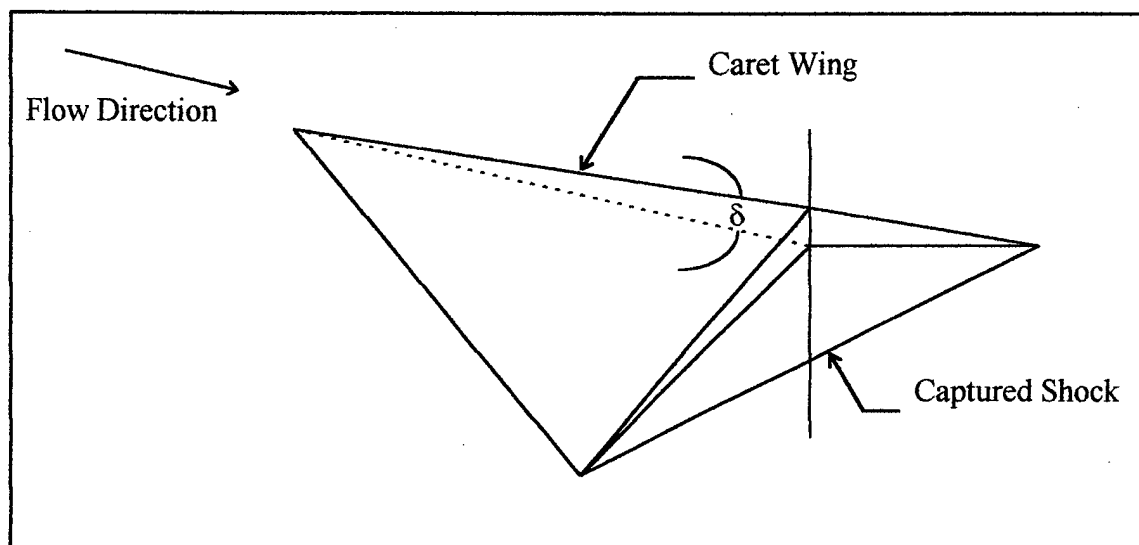
Figure 1.3 Nonweiler's Caret Wing

The concept of using a waverider design for AGA maneuvers was first explored by McRonald and Randolph [Ref. 2] in 1984. These two researchers developed the notion of aero-gravity-assist in order to increase an interplanetary vehicle's heliocentric velocity. They found that typical amounts of change in the heliocentric velocity (ΔV) when using only GA around the terrestrial planets were of the order of 3 to 5 km/s. In order to fly to Pluto in five years a ΔV of 10 to 25 km/s would be required. This number was related to the amount of bending or rotation caused by the planet's size. Therefore, large changes in the bending angle could be expected to yield large changes in ΔV. Of course, only Jupiter offers the advantage of large bending angles using GA because of its large mass. The AGA maneuver using a hypersonic waverider vehicle is today's only apparent option for achieving the kinds of ΔV increments required for missions to the outer planets with a relatively short flight time.

C. RECENT RESEARCH

McRonald and Randolph approached the Association in Scotland to Research into Astronautics (ASTRA) in 1984 about using waveriders for an AGA mission. They were very enthusiastic and showed a continuing interest in the subject by publishing an article in July, 1988 in their ASTRA Spacereport. Today at the Jet Propulsion Laboratory (JPL) in Pasadena, California, both McRonald and Randolph are continuing research related to waverider AGA missions involving the Solar Probe mission, aero-capture missions to Jupiter, missions to Titan, and shuttle missions to Mars. Lewis [Ref. 4] has studied the affects of drag through an atmosphere during an AGA maneuver. He concluded that if a waverider was designed for an AGA mission it must be as long and as wide as possible and to fly at the lowest possible altitude.

With these thoughts in mind, the author has studied and analyzed four different AGA missions. The first mission is a Mars shuttle mission. A one way mission to Saturn is the second mission considered. Third, a long voyage to Neptune is examined. Finally, a round trip mission to Saturn is investigated. Every mission will use an AGA maneuver at Mars, in addition to a GA maneuver at Jupiter (except for the Mars shuttle mission). Comparisons between AGA missions and GA only missions will be addressed, as well as fuel considerations. Moreover, off-design analysis of the AGA maneuver at Mars will be taken into account. This analysis will include sensitivities to changes in angle of attack (AOA), altitude, and Mach number from the design conditions. One aspect of maneuvering through the Martian atmosphere that will not be examined is the heating affects that will be experienced by the waverider.

Vectors are used in Fig 1.4 to depict a typical AGA maneuver at Mars. The velocity vectors have the same definitions as defined above. Before the AGA maneuver, the spacecraft's heliocentric velocity ($V_{S/C}$) is comparable to Mars' (V_P). As the spacecraft turns through an angle ($\Delta\phi$), the magnitude of $V_{S/C}$ is increased until the desired angle is reached (i.e., that angle that will get you to the next planet). At the completion of the AGA maneuver the spacecraft is on a course for its next planetary destination with a large increase in its heliocentric velocity.
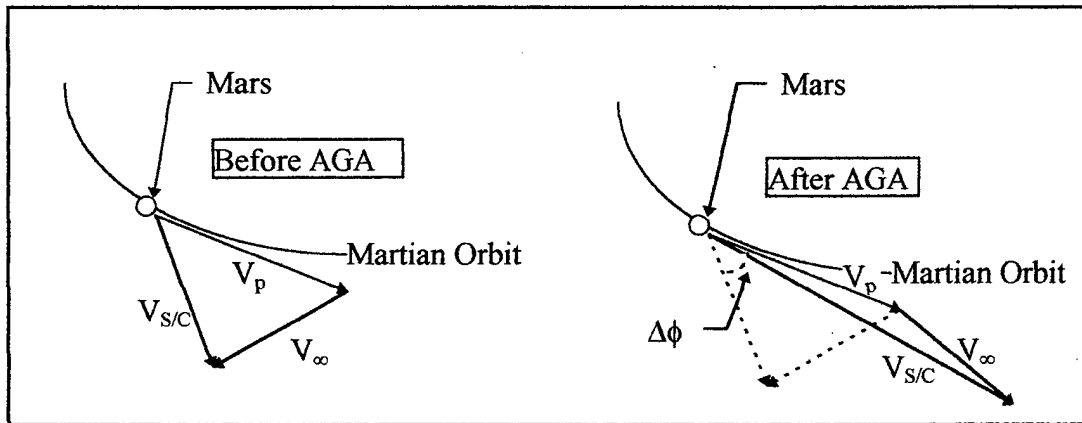
Figure 1.4 The Aero-Gravity-Assist Maneuver at Mars

II. MISSION DESIGN AND ANALYSIS

As a first step towards analyzing an AGA mission, a trajectory to a desired

planetary destination is required. A tool used by the mission planners at JPL is the

Mission Design and Analysis Software for the Optimization of Ballistic Interplanetary

Trajectories, or MIDAS. MIDAS was developed by C. G. Sauer [Refs. 5 and 6] and is

continually being improved to provide essential information to mission planners.

A. MIDAS CODE

MIDAS is a patched conic trajectory optimization program developed to

investigate many complex ballistic heliocentric transfer trajectories. MIDAS can be used

to optimize for a variety of parameters including total velocity change (ΔV), propellant

required, flight times, etc. For this study, MIDAS was used to optimize for minimum ΔV

required for a wide variety of trajectory event times. These include: departure date,

arrival date, flight times between intermediate bodies, launch energies and launch vehicle

parking orbit parameters. The optimization is performed by iterating between a number

of trajectories until it finds the one with the least amount of total velocity change (ΔV).

This total velocity change is the velocity change due to propellant use only, not on the

velocity change due to AGA or GA affects. By knowing ΔV, the amount of required

propellant can be computed by using the rocket equations to be discussed in Chapter IV.

The trajectory can be printed to the computer screen and/or to a post-script printer for a

hard copy. Currently, MIDAS is only available on the SUN Unix computers at the Naval

Postgraduate School (NPS).

In order to run the MIDAS code one must have an input file of the form ***.inp,** where the '*****' represents any word a mission planner might use for his or her proposed mission. One can then run the MIDAS code with a list of 'flags' that represent the kind of output the mission planner requires. Table 2.1 on the following page shows a partial list of the flags available to MIDAS (a full list is available in Ref. 6). An example of the format for running MIDAS is:

midas -bex galileo

The above format has the output flags to the right of the hyphen with the mission name, galileo, at the end (all in lower case). By choosing the flags, the mission planner will have a **galileo.bin** file to be used for plotting the trajectory, and a **galileo.sav** file which displays all the ballistic trajectory data. Additional maneuvers such as deep space propellant burns will be inhibited by using the "x" flag.

b	flag to save a trajectory file of spacecraft state vectors in a binary form
c	flag to print ongoing search information on the computer screen
e	flag for a condensed output file with additional data for perihelion and aphelion
l	flag for a brief appended one line trajectory summary
o	flag to prohibit trajectory updates
x	flag to inhibit addition of maneuvers

Table 2.1 Partial List of MIDAS Output Flags

B. MIDAS INITIAL DATA

A complete list of data for the MIDAS ***.inp** file is available in Ref. 6. Table 2.2 on the following page is a list of such data used for the waverider missions. There is one "trick" that must be performed so that a valid MIDAS trajectory is obtained for waverider missions. All the planet ephemeral data imbedded into the MIDAS code assume that each planet is a point mass. Furthermore, MIDAS was written assuming that only GA

trajectories would be used. Therefore, in the ***.inp** file, one must enter in an erroneous altitude at which to fly the waverider past the prospective AGA planet. This is done by setting the variable 'rcb' to 0.0001. This means that MIDAS will think that the spacecraft is flying at 0.0001 times the radius of the planet; basically, through the planet's core. This appeared to be the only method available, within MIDAS, to achieve the large bending angles that an AGA maneuver will provide.

adate	Arrival date
altb/c/d ...	Altitude constraint for the intermediate bodies (km)
bodyX	Name of the X intermediate body (X=1, 2, 3, etc.)
bulsi	Name of target body
c3	Constrained departure energy C_3 (km^2/s^2)
head	Title or description of trajectory
jdate	Departure time (days)
jdl	Epoch calendar date (year, month, day, hour, minute, second)
nda	Type flag for target body
ndb/c/d/e ...	Type flag for the intermediate bodies
ndl	Type flag for the launch body
ra	Target orbit apoapsis distance (km or radii)
rp	Target orbit periapsis distance (km or radii)
rcb/c/d/e ...	Periapsis distance for swingby of the intermediate bodies (km or radii)
re	circular parking orbit altitude (km)
rn	Trajectory revolution counter
shota	Name of departure body
tend	Flight time (days)
tpb/c/d/e ...	Arrival times at the intermediate bodies (days)
varyi	Independent search variables

Table 2.2 Partial List of MIDAS Initial Data Variables

Although MIDAS is an optimization search code, certain initial data must be present in order to provide an estimate of trajectory event times. If event times can not be met within certain tolerances, the program is unable to calculate a valid trajectory. The mission planner simply changes some of the event dates and/or flight times until these tolerances are met. The author was able to use the code efficiently and effectively

13

for mission planning. Examples of ***.inp** files used for the waverider missions are located in Appendix A.

Some initial data variables in Tab. 2.2 require some further explanation. The term C_3 is a well known energy parameter used for launch vehicles. Equation (2.1) defines C_3.

$$C_3 = V_{char}^2 - V_{esc}^2 \qquad (2.1)$$

V_{char} is the characteristic velocity of the launch vehicle and is dependent on the type of orbit the vehicle is attempting to reach. V_{esc} is the escape velocity of Earth and is equal to 11.19 km/s.

The MIDAS code flags nda/b/c/d... for the target, launch and intermediate bodies (which could be Earth, the sun, asteroids, or other planets) define options available for the mission planner at the various bodies. For the waverider missions, all these variables were set to 2. Accordingly, the MIDAS program models the space vehicle trajectory to include a rendezvous with the destination planet or a powered (propellant used) large body flyby at the intermediate bodies; rather than an unpowered (no propellant used) flyby. The variable "rn" defines the type of trajectory to be followed to each subsequent body along the space flight based on the number of degrees of revolutions around the sun, or intermediate body. Table 2.3 displays the range of "rn" values.

Values of rn	Degrees of Revolution
$-0.5 < rn < 0.0$	$< 180°$
$0.0 < rn < 1.0$	$180° - 360°$
$1.0 < rn < 1.5$	$360° - 540°$
$1.5 < rn < 2.0$	$540° - 720°$

Table 2.3 rn Values

Finally, "varyi" is the list of variables the mission planner wishes to vary for optimization. Usually, "varyi" includes a list of trajectory event times and launch dates.

C. MIDAS RESULTS

Depending on the contents of the initial data file, the MIDAS mission output file will vary. The output is saved in the file *.sav and can be found in Appendix B for all the waverider missions along with the comparison GA missions. After MIDAS has run through a minimization routine to find the smallest ΔV possible for the mission, it will show the *.sav file. Table 2.4 displays a partial list of the various output variables that were used for analysis. Some of the variables shown in the *.sav file were previously defined in Tab. 2.2. A complete list of the MIDAS output variable definitions can be found in Ref. 6.

bend	Total bend angle of the excess velocity vector (degs)
c3	Departure vis-viva energy (km^2/s^2)
dva	Magnitude of arrival velocity vector (km/s)
dvb/c/d ...	Magnitude of powered swingby of the intermediate bodies (km/s)
dvl	Magnitude of departure velocity maneuver (km/s)
fty	Total flight time (years)
rcb/c/d ...	Distance of closest approach for the intermediate bodies (km)
veq	Weighted ΔV, performance parameter for search (km/s)
vhi	Magnitude of incoming excess velocity vector (km/s)
vho	Magnitude of outgoing excess velocity vector (km/s)
x/y/zma	Aphelion position vector (AU)
x/y/zmp	Perihelion position vector (AU)

Table 2.4 Partial List of MIDAS Output Variables

A printout of the MIDAS mission trajectory can be made by using the **plotsc** command and then the **plot-ps** command, some of which are shown on the following pages. An option for showing the trajectory on the screen is also available through the

plot-w command. These plots illustrate the significant events during the mission as Event A, Event B, etc. The events correspond to the significant events in the ***.sav** file.

D. MIDAS TRAJECTORY PLOTS AND ANALYSIS

The next few pages show the trajectory plots of the four waverider missions. There are two comparison missions for each waverider mission. One is a GA mission to the destination planet with a typically low launch energy (C_3, or c3 in the MIDAS code, less than 15 km^2/s^2) and a small ΔV requirement. The other is a GA mission launching on the same day as the waverider and following the same route as the waverider mission. A comparison between the waverider missions and the GA missions are shown through bar charts comparing C_3, flight time, and the total ΔV required for each mission.

2011 Earth–Mars–Earth Waverider Mission

30 day tics on s/c

Earth
Mars
——— Spacecraft
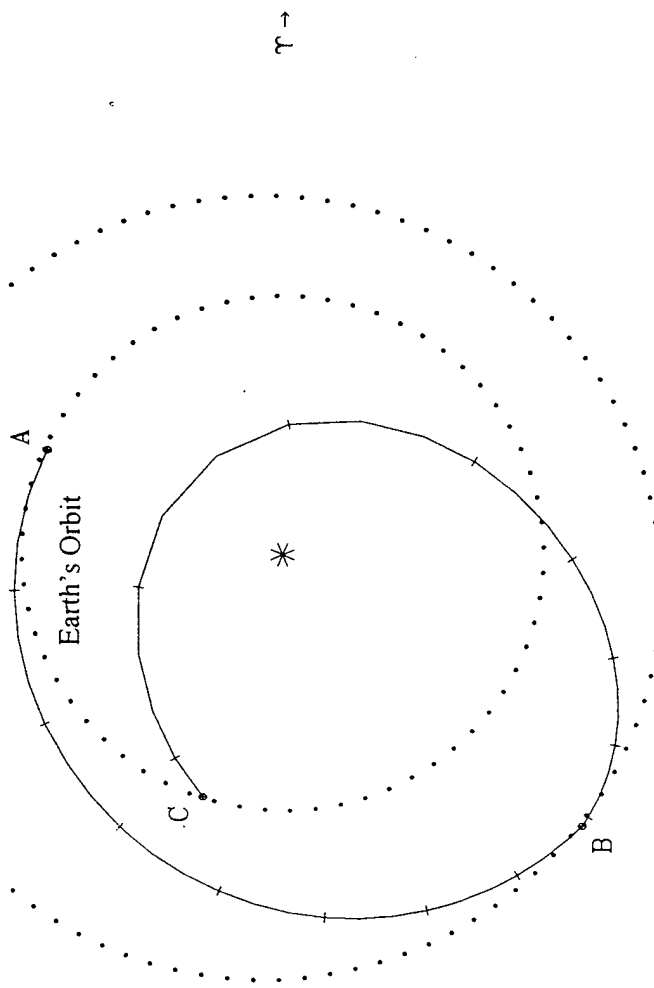
Event Times

A   Nov 28, 2011 Launch Date
B   Jul 21, 2012 Mars Flyby
C   Mar 2, 2013 Arrival Date

Mars' Orbit

Earth's Orbit

A

B

C

Figure 2.1 Trajectory Plot of the Earth-Mars-Earth Waverider Mission

1. The Earth-Mars-Earth Waverider Mission

Figure 2.1 shows the trajectory for the Earth-Mars-Earth (E-M-E) waverider mission. The significant event times are shown on the right side of the figure. Appendix B contains the complete output file results for each mission. From these results, the E-M-E waverider mission is set to launch on November 28, 2011, and perform an AGA maneuver at Mars as it flies by the planet on July 12, 2012. The heliocentric velocity entering the Martian atmosphere (vhi) is 3903 m/s. The AGA maneuver increases the heliocentric velocity leaving the Martian atmosphere (vho) to 7446 m/s while bending the heliocentric velocity vector through an angle (bend) of 50.46°. An aerocapture maneuver (Fig. 1.1) is performed upon the waverider's arrival into Earth orbit on March 2, 2013. The aerocapture maneuver is required to decrease the incoming velocity of the waverider to Earth (vhp) from 16846 m/s to the appropriate circular orbit velocity.

MIDAS calculated the total ΔV (veq) to be 20343 m/s; however, the AGA maneuver at Mars significantly lowers the amount of propellant required to achieve the ΔV at Mars (dvb). The only propellant needed for the AGA maneuver is to make up for the atmospheric drag losses encountered by flying through the Martian atmosphere. As will be shown in Chapt. III, the average velocity loss due to atmospheric drag is about 1000 m/s. Therefore, the ΔV at Mars (dvb) is decreased from 4372 m/s to 1000 m/s. This same argument is used to decrease the ΔV at Earth (dva) from 12317 m/s to 0 m/s by utilizing an aerocapture maneuver. Thus, the total ΔV for this mission has been reduced from 20343 m/s to 4654 m/s (the value of dvl plus the 1000 m/s due to Martian atmospheric drag losses).

2011 Earth–Mars–Jupiter–Saturn Waverider Mission

30 day tics on s/c

Earth
Saturn
Mars
Jupiter
——— Spacecraft

Event Times

A	Oct 26, 2011	Launch Date
B	Jul 7, 2012	Mars Flyby
C	Nov 16, 2014	Jupiter Flyby
D	Dec 8, 2018	Arrival Date

Saturn's Orbit

Jupiter's Orbit

Earth's Orbit

Mars' Orbit

A

B

C

D

♈ →
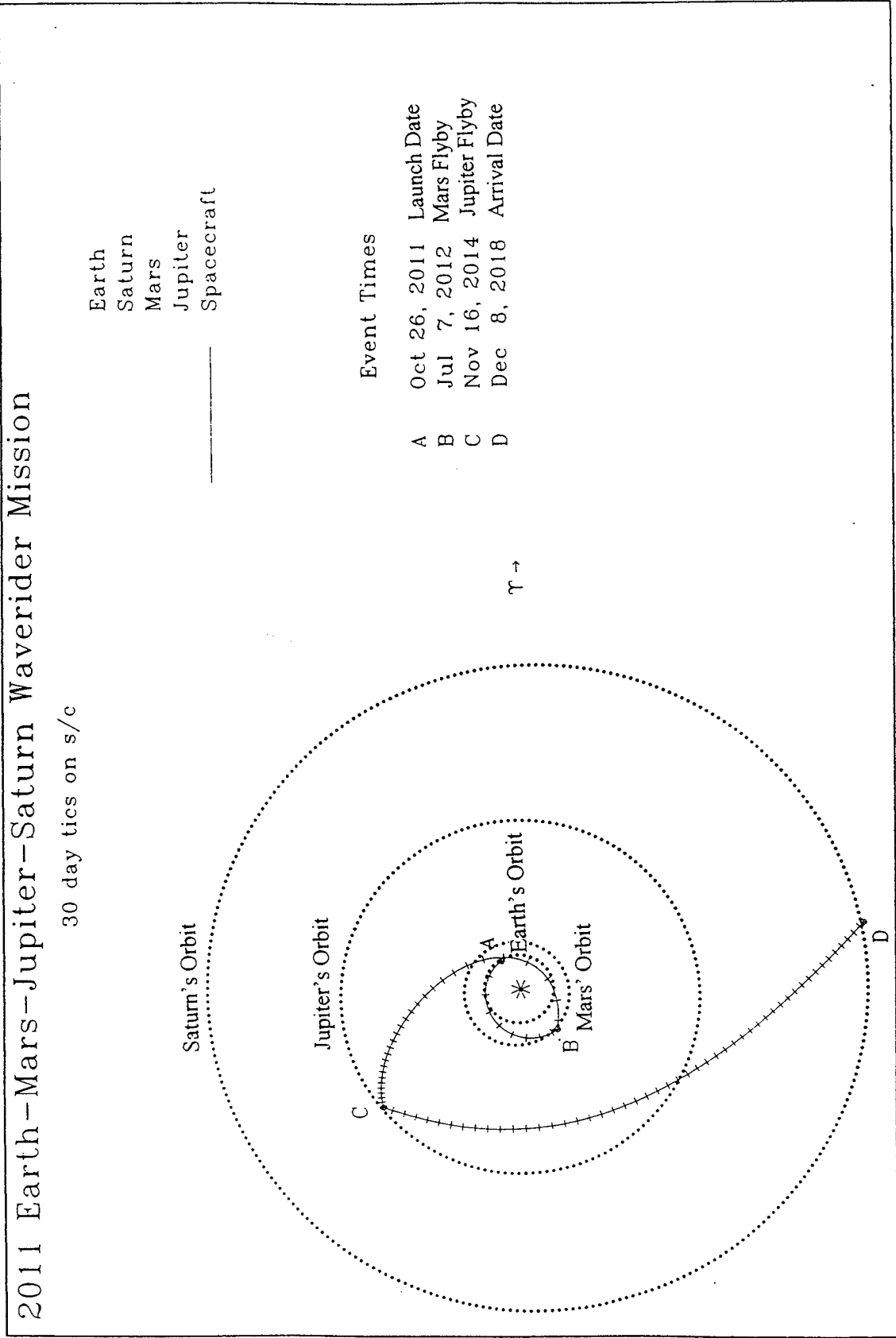
Figure 2.2 Trajectory Plot of the Earth-Mars-Jupiter-Saturn Waverider Mission

19

2. The Earth-Mars-Jupiter-Saturn Waverider Mission

Figure 2.2 shows the trajectory for the Earth-Mars-Jupiter-Saturn (E-M-J-S) waverider mission. The launch date is set for October 26, 2011 with an AGA maneuver at Mars slated for July 7, 2012. The waverider enters the Martian atmosphere at a speed of 4444 m/s (vhi), turning through an angle (bend) of 137°, before leaving at a heliocentric velocity (vho) of 16838 m/s. By bending the heliocentric velocity vector, the waverider is now on a course for a Jupiter flyby on November 16, 2014, where it will undergo a conventional GA maneuver in order to send it towards Saturn. The conventional GA maneuver at Jupiter turns the waverider 136°, and increases the heliocentric velocity from 6799 m/s (vhi) to 10765 m/s (vho). Upon arrival into a Saturn orbit on December 8, 2018, the waverider will have to decrease its velocity (dva) by 2870 m/s.

MIDAS calculated the total ΔV (veq) for this mission to be 9869 m/s. However, as stated before, the AGA maneuver at Mars only requires a ΔV of 1000 m/s. Therefore, the total ΔV is reduced to 8511 m/s (dvl + 1000 + dvc + dva).

2003 Earth–Mars–Jupiter–Neptune Waverider Mission

30 day tics on s/c

Earth
Neptune
Mars
Jupiter
——— Spacecraft

Event Times

A	Jun 27, 2003	Launch Date
B	Oct 27, 2003	Mars Flyby
C	Aug 9, 2005	Jupiter Flyby
D	Jun 27, 2011	Arrival Date

Neptune's Orbit

Jupiter's Orbit

♈→
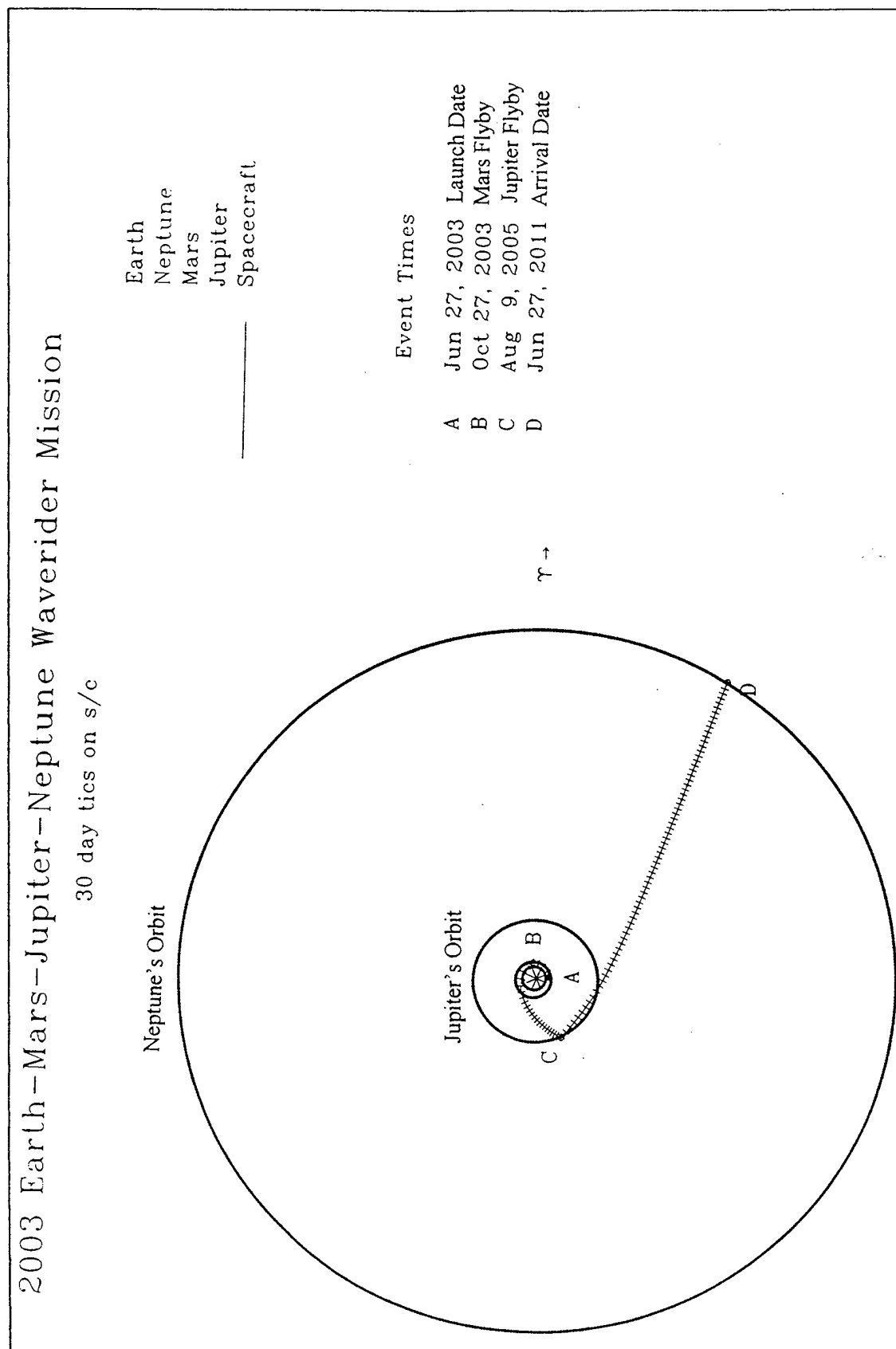
Figure 2.3 Trajectory Plot of the Earth–Mars–Jupiter–Neptune Waverider Mission

3. The Earth-Mars-Jupiter-Neptune Waverider Mission

Figure 2.3 shows the trajectory for the Earth-Mars-Jupiter-Neptune (E-M-J-N) waverider mission. From the results shown in Appendix B, the launch date is set for June 27, 2003 with an AGA maneuver at Mars slated for October 27, 2003 as the waverider flies by the planet. By using an AGA maneuver at Mars, the waverider is bent through an angle (bend) of 165° while increasing its heliocentric velocity from 4993 m/s (vhi) to 13978 m/s (vho). Note, however, that the ΔV at Mars (dvb) is only 573 m/s, but a ΔV of 1000 m/s is required for the atmospheric drag losses. This leads to a conclusion that an AGA maneuver is not effective for this mission. Other problems with this particular mission will be addressed in a later chapter.

Upon leaving Mars, the waverider is sent on a course for a Jupiter flyby on August 9, 2005, where it will undergo a conventional GA maneuver. At Jupiter, the waverider turns through an angle (bend) of 158°, while increasing its heliocentric velocity from 10636 m/s (vhi) to 19561 m/s (vho). The Neptune arrival date is set for June 27, 2011, where the waverider will have to lose 16860 m/s (dva) in order to be placed in orbit around Neptune.

2014 Earth–Mars–Jupiter–Saturn–Earth Waverider Mission

30 day tics on s/c

Earth
Mars
Jupiter
Saturn
——— Spacecraft
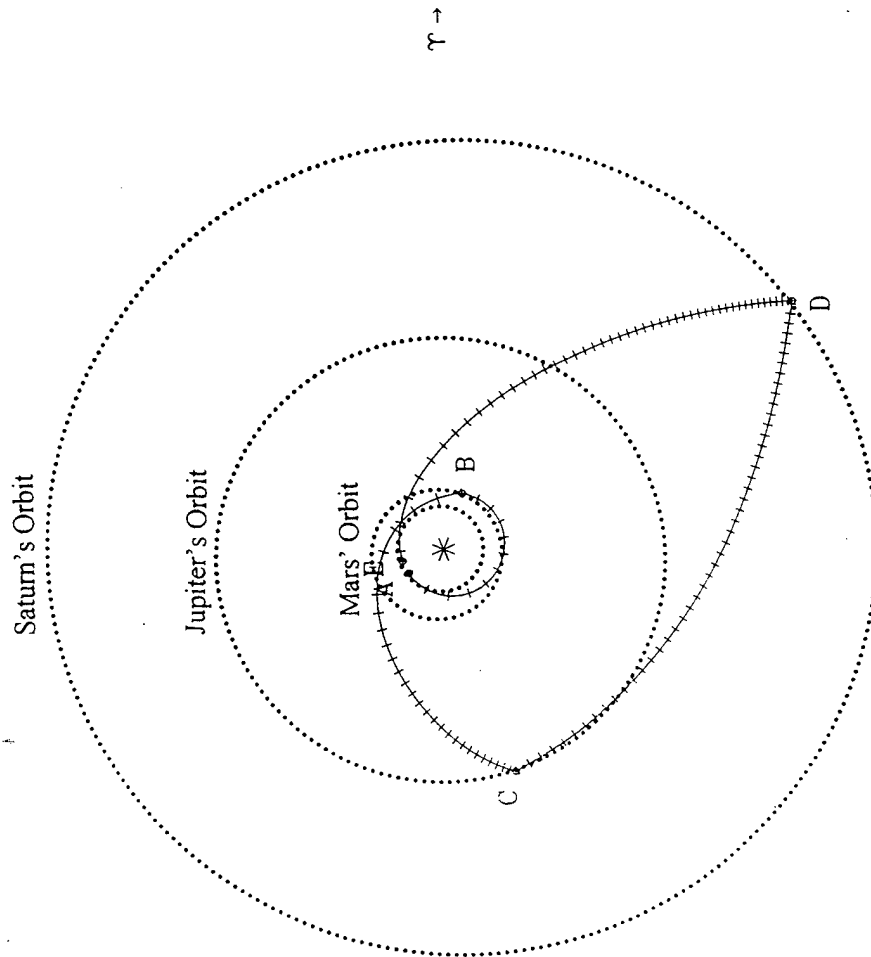
Event Times

A   Jan 24, 2014   Launch Date
B   Dec 19, 2014   Mars Flyby
C   Apr 4, 2017   Jupiter Flyby
D   Feb 25, 2021   Saturn Flyby
E   Jan 6, 2025   Arrival Date

Saturn's Orbit

Jupiter's Orbit

Mars' Orbit

Figure 2.4 Trajectory Plot of the Earth-Mars-Jupiter-Saturn-Earth Waverider Mission

4. The Earth-Mars-Jupiter-Saturn-Earth Waverider Mission

Figure 2.4 shows the trajectory for the Earth-Mars-Jupiter-Saturn-Earth (E-M-J-S-E) waverider mission. The launch date is set for January 24, 2014 with an AGA maneuver at Mars slated for December 19, 2014. The waverider enters the Martian atmosphere with a heliocentric velocity (vhi) of 5245 m/s, turns through an angle (bend) of 53°, before leaving the Martian atmosphere with a heliocentric velocity (vho) of 12827 m/s. The ΔV required for the AGA maneuver is reduced from 4530 m/s (dvb) to the average value of 1000 m/s which is due to the atmospheric drag losses.

After leaving Mars, the waverider is headed for a Jupiter flyby where it will undergo a conventional GA maneuver in order to send it towards Saturn. The Jupiter flyby is set for April 4, 2017, when the waverider turns through an angle (bend) of 166°. Note that the heliocentric velocity is decreased from 6888 m/s (vhi) to 6014 m/s (vho). This can be seen in the figure as the waverider turns around Jupiter and is no longer heading directly away from the sun.

When the waverider flies by Saturn on February 25, 2021, it can release its payload and return to Earth. The arrival date at Earth is slated for January 6, 2025, when the waverider will undergo an aerocapture maneuver before going into a circular orbit around Earth where it can be refurbished for the next mission.

The total ΔV (veq) calculated by MIDAS for this mission is 27609 m/s. However, by using AGA and aerocapture, the total ΔV is reduced to 16137 m/s (dvl + 1000 + dvc + dvd).

Low Energy Trajectory Non-Waverider Roundtrip Mission to Mars

30 day tics on s/c

Earth

Mars

—————— Spacecraft

Mars' Orbit

Earth's Orbit

Event Times

A	Dec 21, 2013	Launch Date
B	Aug 3, 2014	Mars Flyby
C	Apr 5, 2015	Arrival Date
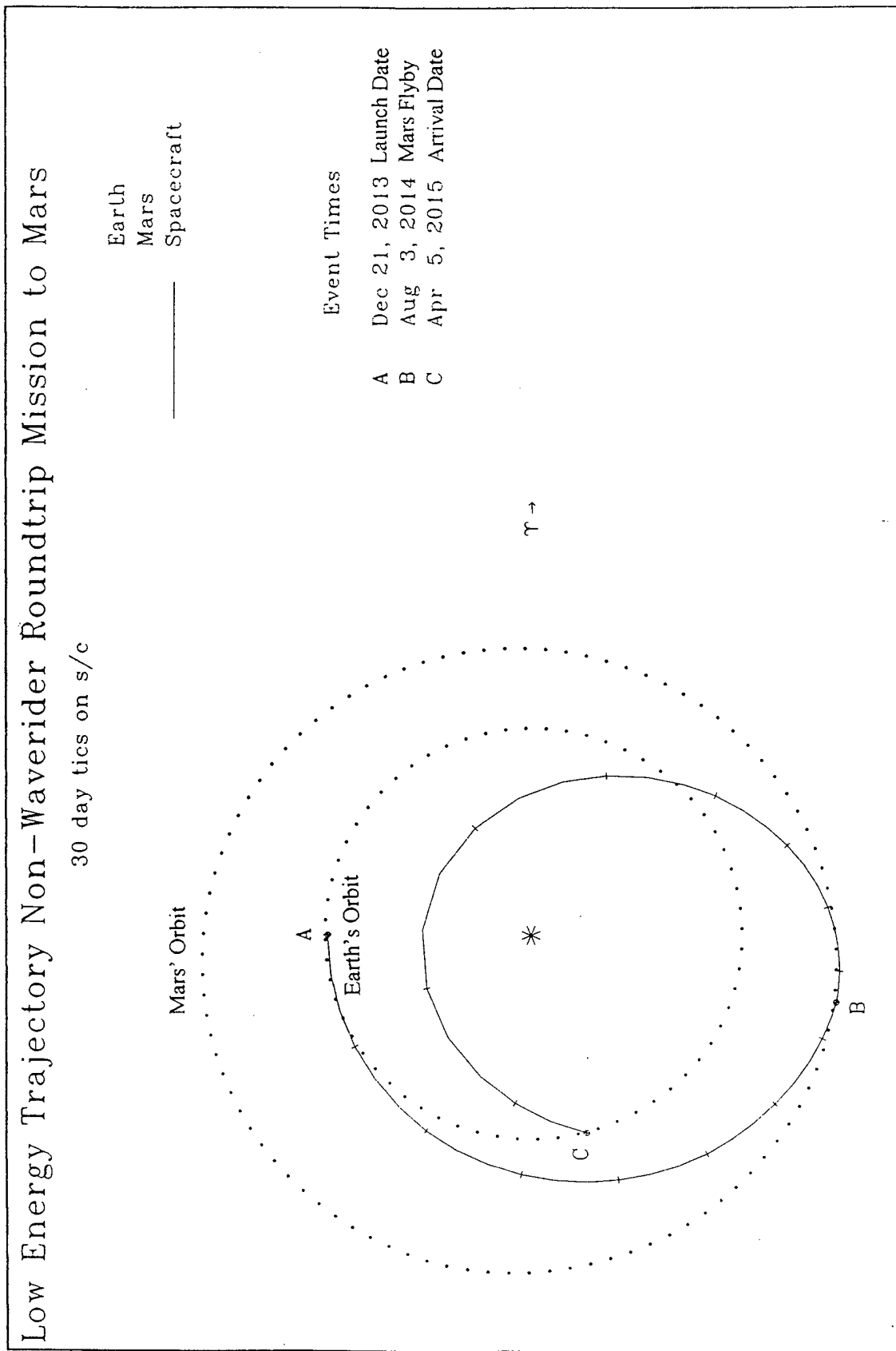
Figure 2.5 Trajectory Plot of the Low Energy Trajectory for a Non-Waverider Roundtrip Mission to Mars

25

5. Low Energy Trajectory for a Non-Waverider Roundtrip Mission to Mars

Figure 2.5 shows a typical low energy trajectory for a roundtrip mission to Mars. This mission is for a non-waverider and utilizes GA only. It will be used to compare flight times, propellant requirements, and launch energies with the waverider roundtrip mission to Mars. The highlights of this mission include: launching on December 21, 2013, flying by Mars on August 3, 2014, and returning to Earth orbit on April 5, 2015.

According to the MIDAS results shown in Appendix B, this mission has a relatively low launch energy requirement (c3) of 12.07 km^2/s^2, and a total ΔV requirement (veq) of 17262 m/s. These figures compare closely to the waverider mission where the launch energy requirement was found to be 11.04 km^2/s^2, but the total ΔV requirement was 4654 m/s. The flight times differed by just ten days between these two missions.

6. Non-Waverider Roundtrip Mission to Mars Departing on the Same Day as the Waverider

This mission shown on the next page (Fig. 2.6) is another GA comparison with the waverider roundtrip mission to Mars. From the results in Appendix B, this mission departs on November 28, 2011, with a launch energy requirement (c3) of 10.84 km^2/s^2. It will flyby Mars on July 20, 2012, and return to Earth on March 2, 2013. The total ΔV requirement for this mission was 19692 m/s, while the flight time was 460 days, the same as the waverider mission.

Non−Wvrdr Traj Roundtrip To Mars Leaving Same Day as Wvrdr

30 day tics on s/c

Mars' Orbit

Earth's Orbit

Earth
Mars
——— Spacecraft

Event Times

A   Nov 28, 2011   Launch Date
B   Jul 20, 2012   Mars Flyby
C   Mar 2, 2013   Arrival Date
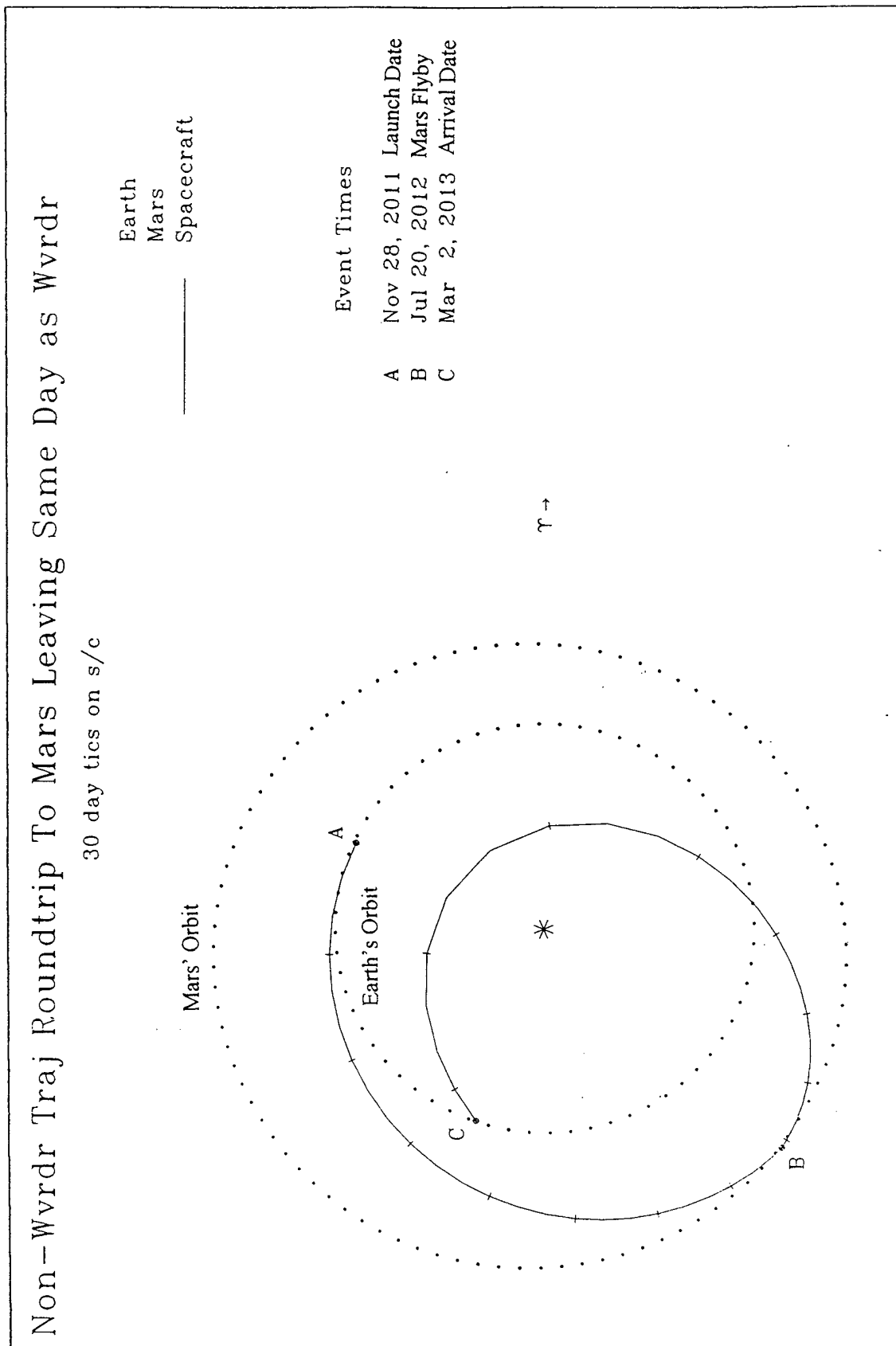
Figure 2.6 Trajectory Plot of the Non-Waverider Trajectory for a Roundtrip Mission to Mars
Departing on the Same Day as the Waverider

7. Low Energy Trajectory for a Non-Waverider Mission to Saturn

Figure 2.7 shows the trajectory plot for a GA mission to Saturn. It will be used for comparing it to the waverider mission to Saturn. This trajectory is known as a VEEGA (Venus-Earth-Earth-Gravity-Assist) trajectory. It was set to launch on September 24, 1992 with a launch energy requirement (c3) of 13.82 km^2/s^2. By flying by Venus on December 23, 1993, the spacecraft will receive a gravity assist boost from the planet. After two Earth flybys on March 4, 1995, and July 10, 1997, the spacecraft has enough energy to reach Saturn on January 10, 2002.

This mission has an especially low total ΔV requirement (veq) of 5270 m/s, but the flight time (fty) is over nine years according to the MIDAS results in Appendix B. In contrast, the waverider mission flight time is just over seven years, while the total ΔV requirement is 8511 m/s.

8. Non-Waverider Mission to Saturn Departing on the Same Day as the Waverider

This mission is also a GA comparison against the waverider mission to Saturn. Figure 2.8 shows the trajectory plot for this mission. It is set to launch on October 26, 2011, with a launch energy requirement (c3) of 37.36 km^2/s^2. This is much higher than the launch energy requirement for the waverider mission to Saturn which was only 13.48 km^2/s^2. The spacecraft will flyby Mars on June 8, 2012, and by Jupiter on September 12, 2014. It is due to arrive at Saturn on December 8, 2018. The flight time is the same for both missions, but the total ΔV requirement for this mission is 30956 m/s, whereas it is only 8511 m/s for the waverider mission. This will make a significant difference in total propellant requirements.

Low Energy Trajectory for a non–Waverider Mission to Saturn

30 day tics on s/c

Earth
Saturn
Venus
——— Spacecraft

Event Times

A   Sep 24, 1992   Launch Date
B   Dec 23, 1993   Venus Flyby
C   Mar 4, 1995   Earth Flyby
D   Jul 10, 1997   Earth Flyby
E   Jan 15, 2002   Arrival Date

Saturn's Orbit

E

Earth's Orbit
Venus' Orbit
C
B   D
A

Figure 2.7 Trajectory Plot of the Low Energy Trajectory for a Non-Waverider Mission to Saturn

Non−Wvrdr Traj to Saturn Leaving on the Same Day as the Wvrdr

30 day tics on s/c

Earth
Saturn
Mars
Jupiter
———— Spacecraft

Event Times

A Oct 26, 2011 Launch Date
B Jun 8, 2012 Mars Flyby
C Sep 12, 2014 Jupiter Flyby
D Dec 8, 2018 Arrival Date

Saturn's Orbit

Jupiter's Orbit

Mars' Orbit

Earth's Orbit

A

B

C

D
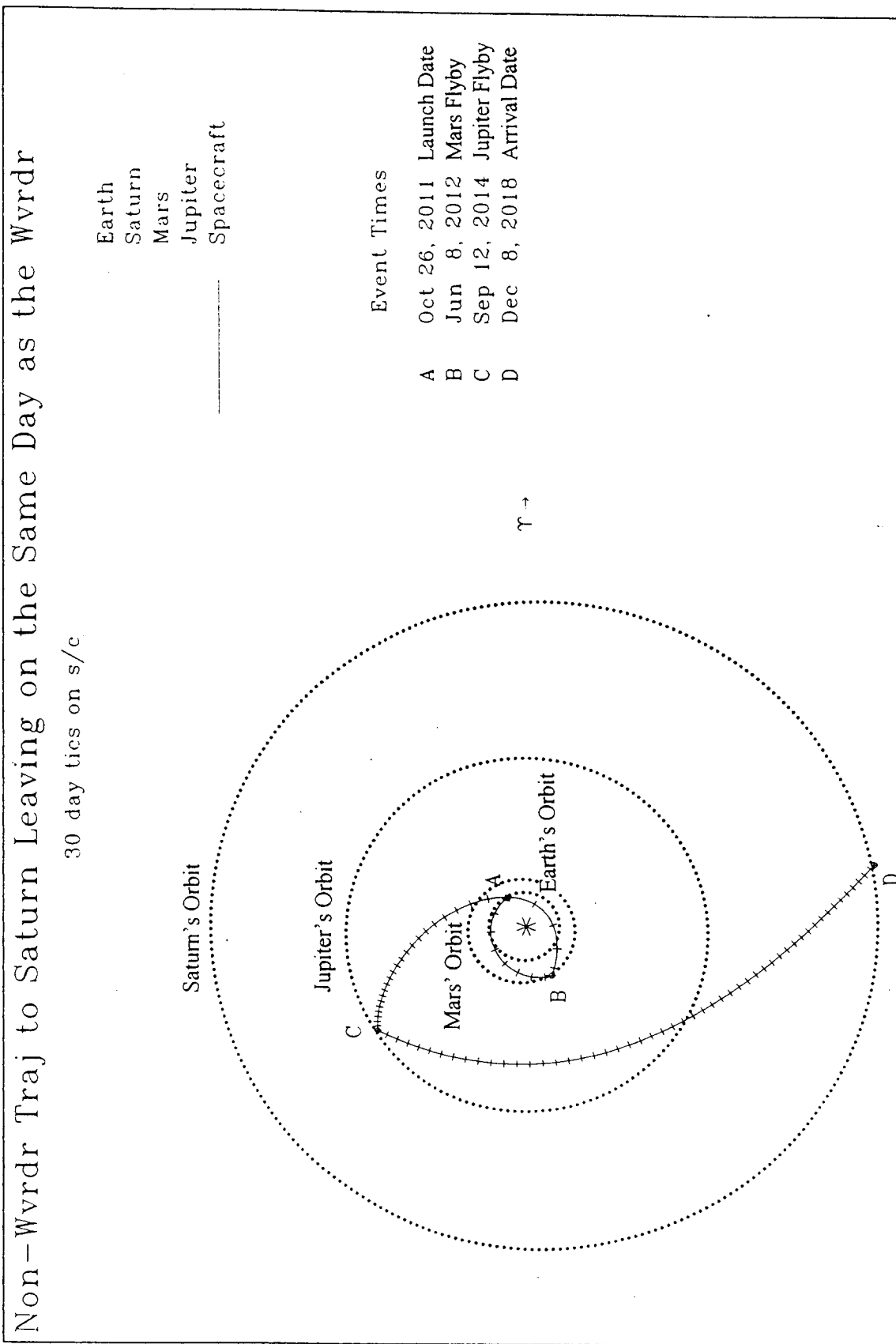
Figure 2.8 Trajectory Plot of the Non-Waverider Trajectory to Saturn Departing on the Same Day as the Waverider

9. Low Energy Trajectory for a Non-Waverider Mission to Neptune

Figure 2.9 shows the trajectory plot for this GA mission to Neptune. It will be used to compare with the waverider mission to Neptune. Launch date is set for July 10, 2003, with a launch energy requirement (c3) of 14.9 km^2/s^2. The waverider mission has a launch energy requirement of 17.1 km^2/s^2.

Mars flyby will be on February 18, 2004, and the Jupiter flyby is set for March 17, 2006. The spacecraft will reach Neptune on September 26, 2011. The total flight time is only 78 days longer than the waverider mission which will take eight years. However, the total ΔV (veq) for this mission is 36231 m/s, while the waverider mission has a total ΔV requirement of 33390 m/s. This is not a significant reduction in total ΔV, and as will be shown in a later chapter it will require that the waverider vehicle's mass be totally made up of propellant. Therefore, it seems that this mission is better suited for a conventional GA trajectory.

10. Non-Waverider Mission to Neptune Departing on the Same Day as the Waverider

Figure 2.10 shows the trajectory plot for this GA mission which is used for another comparison against the waverider mission to Neptune. This mission is set to launch on June 27, 2003 with a launch energy requirement (c3) of 11.74 km^2/s^2. It will flyby Mars on February 12, 2004, before flying by Jupiter on March 2, 2006. Arrival at Neptune is slated for June 27, 2011, making the flight time eight years. The total ΔV requirement (veq) is 38065 m/s making this mission impractical since the propellant requirement (as will be shown in a later chapter) will be too large.

Low Energy Trajectory for a non-Waverider Mission to Neptune

30 day tics on s/c

Earth
Neptune
Mars
Jupiter
————— Spacecraft
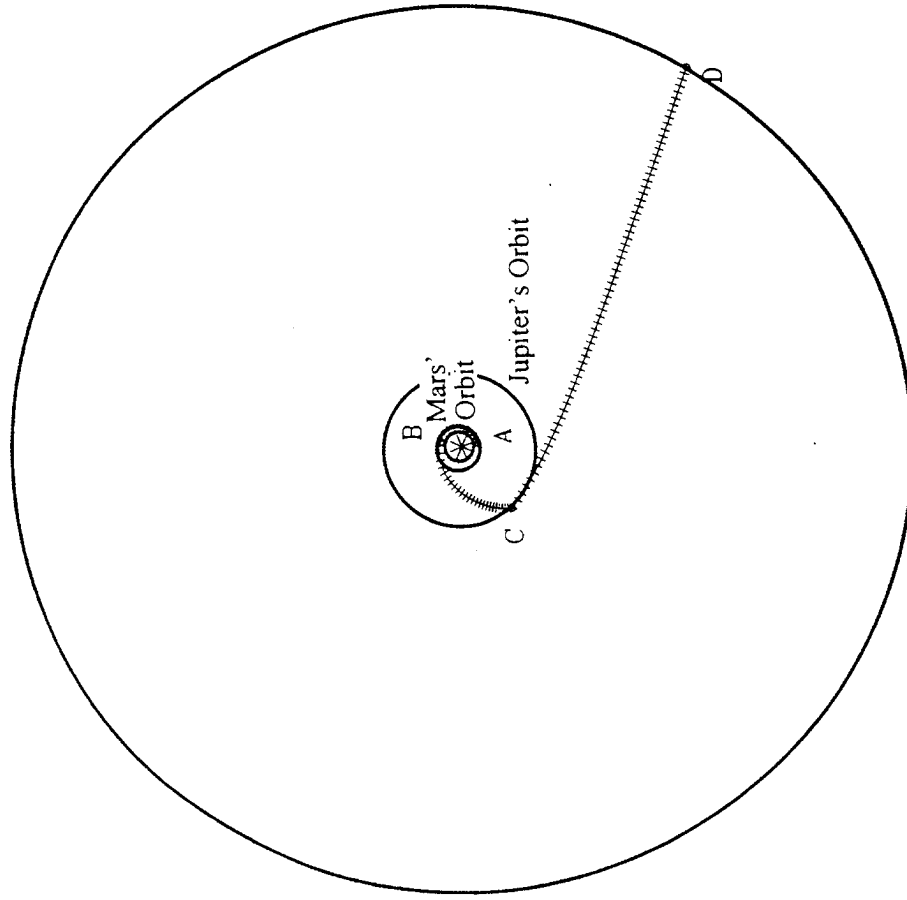
Event Times

A   Jul 10, 2003   Launch Date
B   Feb 18, 2004   Mars Flyby
C   Mar 17, 2006   Jupiter Flyby
D   Sep 26, 2011   Arrival Date

Neptune's Orbit

Mars' Orbit

Jupiter's Orbit

B

A

C

D

♈ →

Figure 2.9 Trajectory Plot of the Low Energy Trajectory for a Non-Waverider Mission to Neptune

Non-Wvrdr Traj to Neptune Leaving Same Day as the Wvrdr

30 day tics on s/c

Earth
Neptune
Mars
Jupiter
———— Spacecraft

Event Times

A   Jun 27, 2003   Launch Date
B   Feb 12, 2004   Mars Flyby
C   Mar 2, 2006   Jupiter Flyby
D   Jun 27, 2011   Arrival Date

Neptune's Orbit

Jupiter's Orbit

Mars' Orbit
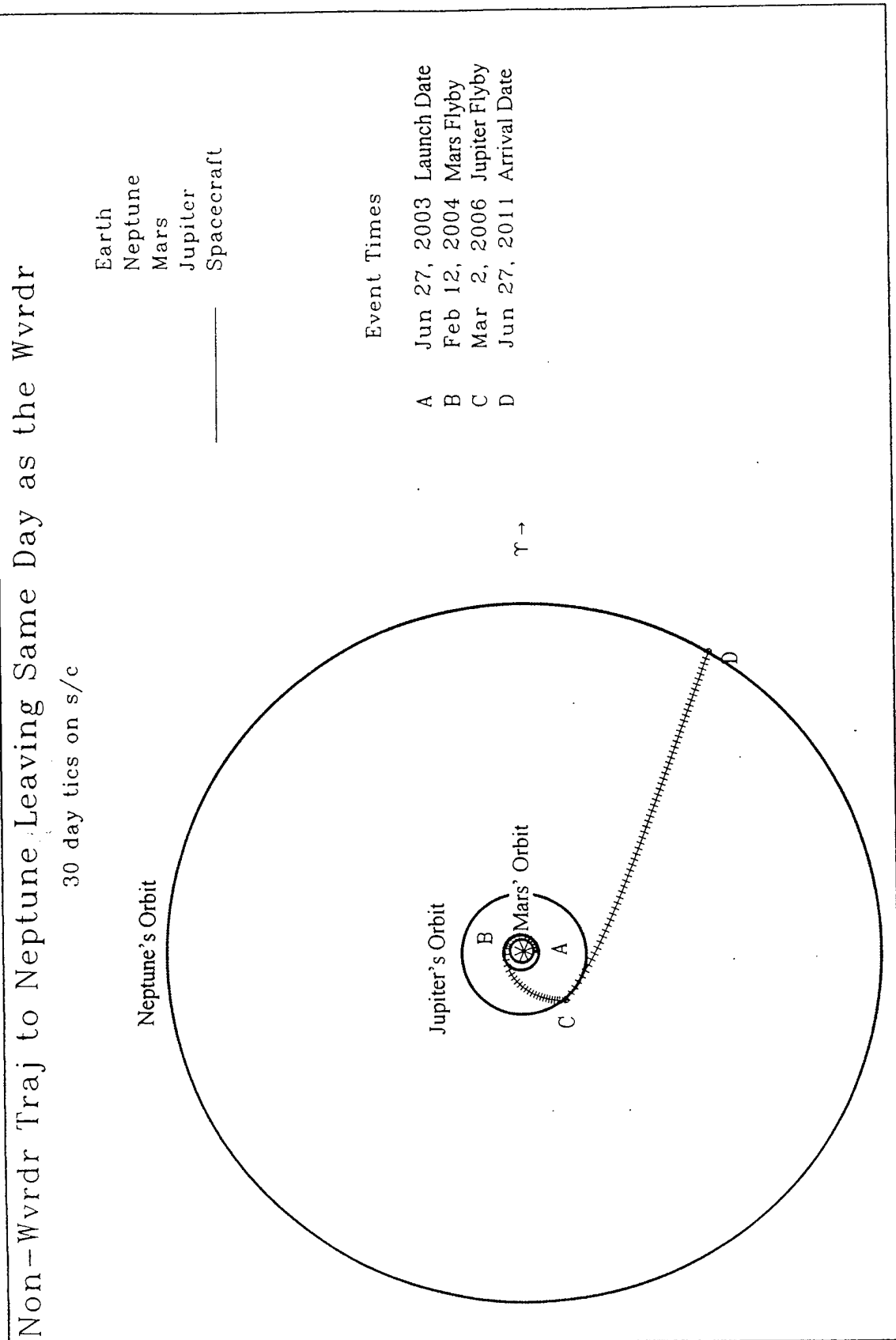
Figure 2.10   Trajectory Plot of the Non-Waverider Trajectory to Neptune Departing on the Same Day as the Waverider

Non−Wvrdr Traj Roundtrip to Saturn Leaving Same Day as Wvrdr

30 day tics on s/c

Earth
Mars
Jupiter
Saturn
————— Spacecraft

Event Times

A	Mar 14, 2014	Launch Date
B	Dec 19, 2014	Mars Flyby
C	Apr 24, 2017	Jupiter Flyby
D	Mar 20, 2021	Saturn Flyby
E	Feb 24, 2025	Arrival Date

Saturn's Orbit

Jupiter's Orbit

Mars' Orbit

Earth's Orbit
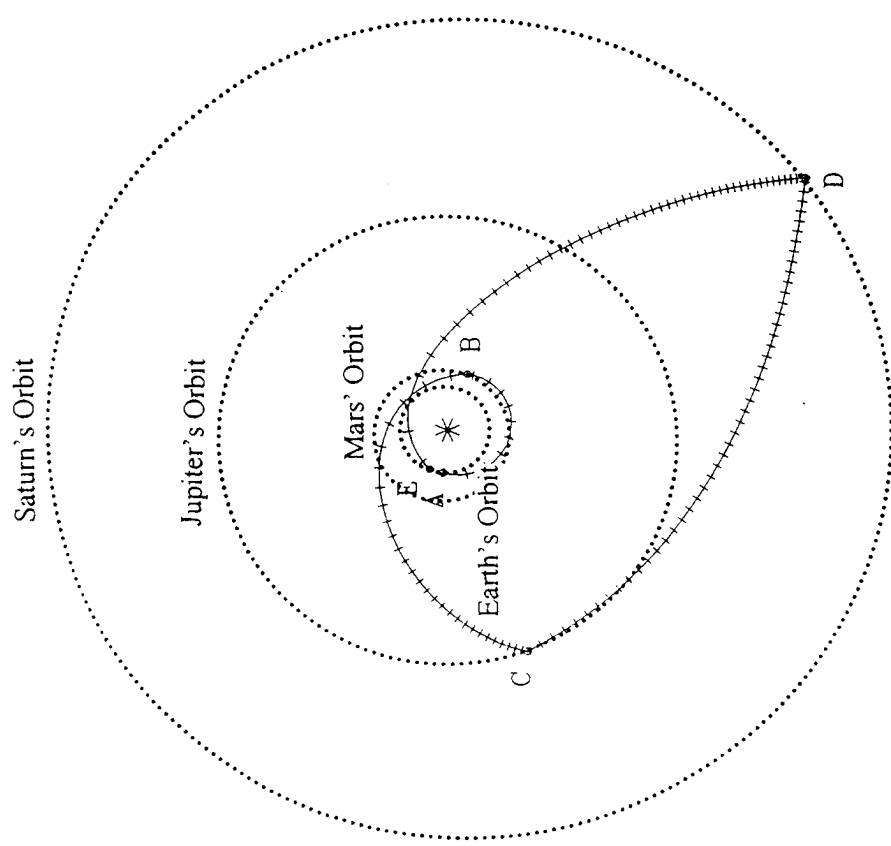
Figure 2.11 Trajectory Plot of the Non-Waverider Trajectory for a Roundtrip Mission to Saturn Departing on the Same Day as the Waverider

11. Non-Waverider Trajectory for a Roundtrip Mission to Saturn Departing on the Same Day as the Waverider

Figure 2.11 shows a trajectory plot for a GA roundtrip mission to Saturn to be used to compare with the waverider roundtrip mission to Saturn. A typical low energy mission could not be found using MIDAS. The launch date is the same as the waverider mission. It will flyby Mars on December 19, 2014, before flying by Jupiter on April 24, 2017. After turning 139° around Saturn on March 20, 2021, the spacecraft will be heading back towards Earth and arrive there on February 24, 2025.

The launch energy requirement (c3) for this mission is 46.95 km^2/s^2, and the total ΔV requirement (veq) is 38588 m/s. The waverider mission requires a launch energy of 9.78 km^2/s^2, and a total ΔV requirement of 16120 m/s. The flight times for both of these missions is just under 11 years.

12. AGA vs. GA Comparisons

The following three figures summarize the previous discussion comparing the waverider missions using AGA and the conventional GA missions. Three results were especially interesting to compare: launch energy (C_3, or c3 in the MIDAS code), flight times, and total ΔV. These results are important because they are the items that most mission planners would like to minimize or reduce.

It is best to look at the bar charts for each mission individually. Looking at the E-M-E missions, Fig 2.12 shows that the launch energy for each mission is about the same. Furthermore, the flight time and total ΔV are about the same, leading to the conclusion

that due to the relative short length of this mission, the AGA effects do not greatly reduce

any of these three parameters.
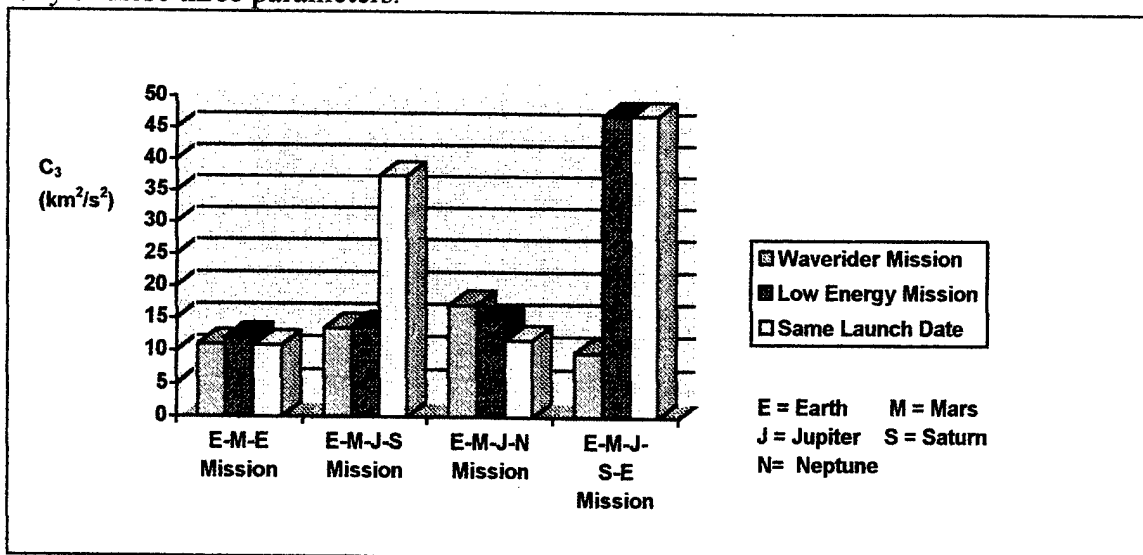
Figure 2.12 Comparison of C₃ Launch Energies
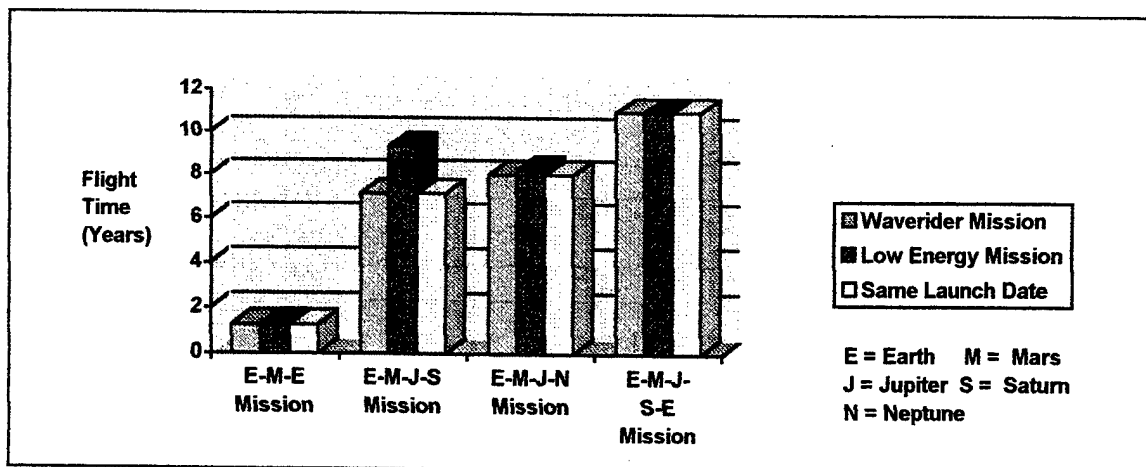
Figure 2.13 Comparison of Flight Times
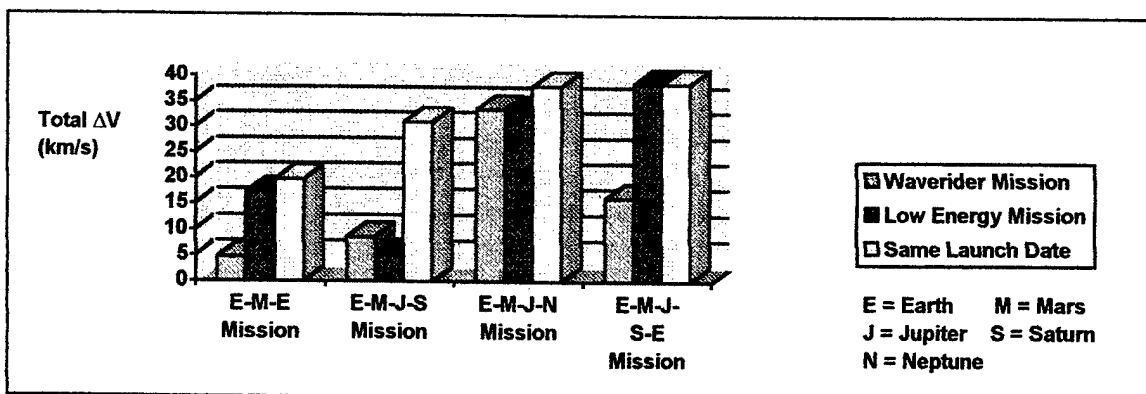
Figure 2.14 Comparison of Total ΔV

Comparing the three missions going to Saturn shows that the C_3 launch energy for the waverider and the low energy mission are about the same, but the spacecraft leaving on the same day as the waverider requires much more launch energy. The main advantage gained by using AGA for this mission is in the reduction of flight time from 9.3 years to 7.1 years while keeping the total ΔV requirement small.

The E-M-J-N missions show that sometimes AGA is not the best way to go to another planet. As can be seen in the three charts, the waverider mission requires a higher launch energy, while the flight times and total ΔVs are about the same for each mission. This is another reason why this particular waverider mission may not be feasible.

The last mission to be analyzed is the E-M-J-S-E mission. From the previous three figures, the use of AGA has significantly reduced the C_3 requirement, and the total ΔV required for the waverider mission. This mission is the most promising of the four waverider missions because of these significant reductions. Note that the low energy mission and the same launch date mission are the same for this comparison because a typical low energy roundtrip mission to Saturn could not be found using MIDAS.

The launch windows for the waverider missions are increased because the mission planner has the "free" parameter of the bending angle (ϕ, or bend in the MIDAS code) when using the AGA maneuver at Mars. If the mission is delayed or moved up on the launch schedule, the mission planner simply has to adjust the amount of bending needed at the AGA planet (Mars, in this study) in order to send the spacecraft to its next destination.

III. WAVERIDER GENERATION AND OPTIMIZATION

Waverider configurations for each mission were developed by using the Waverider code developed by the Systems Analysis Branch at the NASA Ames Research Center. The Waverider code was developed as a subset of the Hypersonic Aircraft Vehicle Optimization Code, or HAVOC and is currently configured to run on a Silicon Graphics Iris workstation [Ref. 8] at the Naval Postgraduate School (NPS). Many previous projects have been completed using the code at NPS (Price in 1993, and Cedrun in 1994, e.g.), but the analysis done for this study required some modifications to the code. The Waverider code was originally written for the analysis of vehicles operating within the Earth's atmosphere. However, the missions discussed in this thesis needed to use a Martian atmosphere. After the transport properties (c_p, μ, k, etc.) of the gaseous constituents for the Martian atmosphere were entered into the code, the user was given the option of choosing either using the Earth's atmosphere or the Martian atmosphere. Additionally, the Waverider code was written to optimize the product of L/D and I_{sp}, with the specific impulse (I_{sp}) found from analyzing air-breathing scramjets and ramjets. Since the waveriders analyzed in this report would not require an air-breathing engine, the code was altered to optimize the shape for L/D. The addition of a liquid rocket engine was added later and will be discussed in Chapt. IV. All references to the files needed to run the Waverider code are case sensitive, and are correctly written in this discussion.

A. WAVERIDER GENERATION

A waverider shape is generated by the HAVOC Waverider code by solving for a shape that is defined by a known flow field. The flow field is defined by a generating

cone which forms a conical shock as shown in Fig 3.1. A generating curve cuts through the conical shock forming the waverider's upper surface, with the lower vehicle surface defined by the resulting flow field behind the shock. The equation for the generating curve is shown in Eq. 3.1.

$$x = c_1\tan\theta + c_2 y + 10c_3 y^2 + 100c_4 y^3 + 1000c_5 y^4 + 10000c_6 y^6 + c_7\cos[(\pi c_8 y)/(2\tan\theta)] \quad (3.1)$$

In Eq. 3.1, the shock angle is defined by the angle θ.

free stream

cone defining flow field

leading edges defined arbitrarily on shock

stream surface (shape used as wing lower surface)

shock

CONSTRUCTION FROM KNOWN FLOW FIELD

wing shape

shock

RESULTING WING AND SHOCK
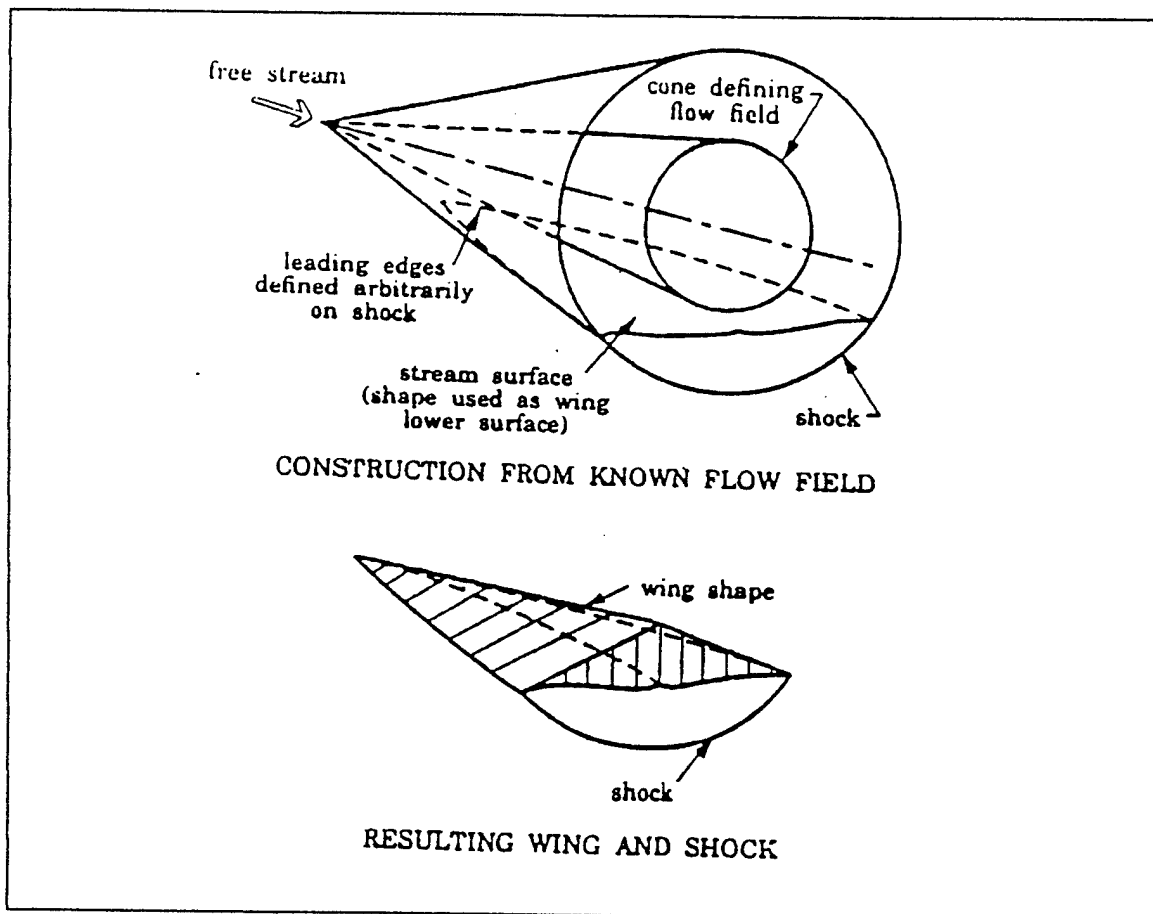
Figure 3.1 The Conical Waverider. From Ref. 8.

B. WAVERIDER OPTIMIZATION

In order to consider a number of waverider shapes for optimization, the waverider code uses a file called **wave.dat** which contains all the constraints and parameters for

optimization. This file can be altered by changing the constraints of the optimization routine to speed up the process. The code uses NASA Ames CODES-COMMIN iterative method as a methodology to calculate the optimum shape. Once the code has converged to a solution, the flow field results are stored in the file **FLWFLD.SUM**. The user can define the maximum number of iterative solutions that the optimizer will process; otherwise, the code could conceivably run forever. Initial data for the code is entered into the file **WAVRDR.DAT**. Parameters such as dynamic pressure and flight Mach number are typical of the data entered in this file. In order to have L/D's greater than five, the length of each waverider must be of the order of tens of meters [Ref. 4]. A length of 80 meters was selected for each waverider (the Space Shuttle Orbiter is only 37.2 m in length). The Waverider code also has the ability to run one solution from the file **WAVRDR1.DAT**, so that the user can become familiar with the program. This ability can also be used once the optimizer has found a solution and the output variables are stored in **WAVRDR1.DAT** so that the data is readily accessible.

C. METHODOLOGY

An iterative method (Fig. 3.2) was used to solve for certain performance parameters and geometric characteristics of each waverider. The method involved using the equations derived in the first chapter to find the altitude for waverider flight. Specifically, Eq. 1.2 was used in a MATLAB program called **vloss.m** (written by the author and shown in Appendix C) to solve for the altitude and plot a graph of L/D versus the heliocentric velocity out of the Martian atmosphere. This plot was based on the lift

41

parameter (Eq. 1.6) and the velocity loss through the atmosphere due to aerodynamic

drag (Eq. 1.5).

1. Lift Parameter

The lift parameter value defined in Eq. 1.6 was arbitrarily chosen and entered into

vloss.m along with the heliocentric velocity into the Martian atmosphere (vhi from the

Enter a new lift parameter, vho, and vhi into **vloss.m**

↓ Outputs

ρ, M and q required for the AGA maneuver

↓

Enter ρ, M, & q from vloss.m into WAVRDR.DAT & run Waverider code

↓ Outputs

mass (m), lift coefficient (C_L), & planform Area (S) of the waverider

↓

Solve for the lift parameter (Eq. 1.6) from the Waverider Code's Outputs

→

No

Is this lift parameter equal to the initially specified lift parameter

Yes → Done

ρ = density of the Martian atmosphere at the AGA altitude
M = flight Mach number during the AGA maneuver
q = the dynamic pressure during the AGA maneuver = $\frac{1}{2}\rho V_\infty^2$

Figure 3.2 Lift Parameter Iteration Method

42

MIDAS output) and the heliocentric velocity out of the Martian atmosphere (vho from the MIDAS output). The program (**vloss.m**) solves for the atmospheric density, Mach number, and dynamic pressure at which the AGA maneuver needs to be performed. This data is then entered into the **WAVRDR.DAT** file so that the Waverider code could compute the waverider mass, lift, and wing area from which one could solve for the lift parameter. If the calculated lift parameter was not the same as the initially specified lift parameter in **vloss.m**, then this would be the new arbitrary lift parameter and be reentered into **vloss.m**. Once the lift parameter converged then one had the final results for Mach number, dynamic pressure, and altitude at which to fly the AGA maneuver. These could then be entered into the **WAVRDR.DAT** file to optimize for L/D.

2. Drag Losses

As was shown in Fig. 1.2, there will be losses due to drag when flying through the Martian atmosphere. These losses were computed by using **vloss.m** to graph L/D versus the heliocentric velocity out of the atmosphere. The program simply solved for the ΔV_∞ that was lost due to drag from Eq. 1.5 for a range of L/D and subtracted that from the entered value of the vho (the ideal heliocentric velocity out of the atmosphere). The four figures on the following pages (Figs. 3.3 to 3.6) show the plots of L/D versus vho for the four waverider missions. As would be expected, as L/D approaches infinity, the drag losses decrease towards zero.

Figure 3.3 to 3.6 show the plots of the heliocentric velocity after an AGA maneuver at Mars vs. L/D. Figure 3.3 represents this plot for the E-M-E waverider mission. Once the lift parameter has converged to a value the Mach number, altitude,

dynamic pressure and velocity for the AGA maneuver are known. By holding the Mach number and altitude constant, **vloss.m** finds the heliocentric velocity after the AGA maneuver for a range of L/D values. For example, the L/D value for the E-M-E waverider was found to be 6.24 with at a Mach number of 19.23 flying through the Martian atmosphere at a constant altitude of 46 km. According to the MIDAS results from Appendix B, the heliocentric velocity (vho) after flying by Mars is 7.45 km/s. But due to the atmospheric drag losses it will be less. By referring to Fig 3.3, and by drawing a vertical line up from an L/D value of 6.24 to the curve, and then by drawing a horizontal line from that point to the vertical axis, the actual heliocentric velocity after the AGA maneuver turns out to be about 7.22 km/s. This difference must be made up by a rocket burn during the maneuver. The average value for velocity loss for all four missions during the AGA maneuver as can be seen in the table below is less than 500 m/s. Therefore, a more conservative estimate of 1000 m/s was chosen for the propellant analysis discussed in the next chapter.

MISSION (Figure) (all speeds in km/s)	vhi (from MIDAS)	vho (from MIDAS)	L/D (from the Waverider code)	vhout (from Figs. 3.3-3.6)	ΔV_∞
E-M-E (3.3)	3.903	7.45	6.24	7.22	0.230
E-M-J-S (3.4)	4.444	16.84	5.86	16.35	0.490
E-M-J-N (3.5)	4.993	13.98	5.84	13.45	0.530
E-M-J-S-E (3.6)	5.245	12.83	5.90	12.63	0.200

Table 3.1 Summary of Atmospheric Drag Losses
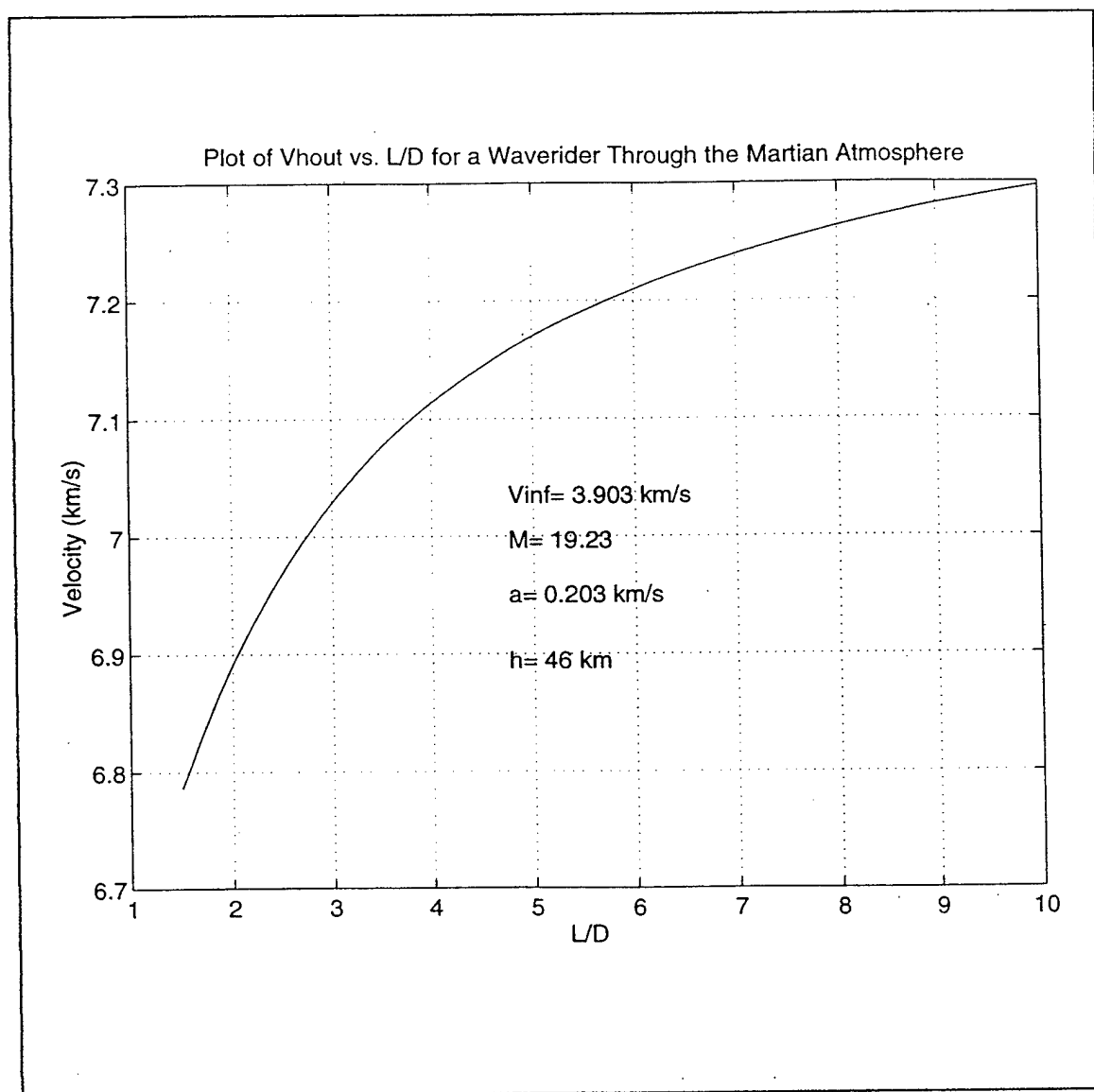
Figure 3.3 Drag Losses for the Earth-Mars-Earth Waverider Mission

Plot of Vhout vs. L/D for a Waverider Through the Martian Atmosphere

Vinf= 4.444 km/s

M= 21.89

a= 0.203 km/s

h= 46 km
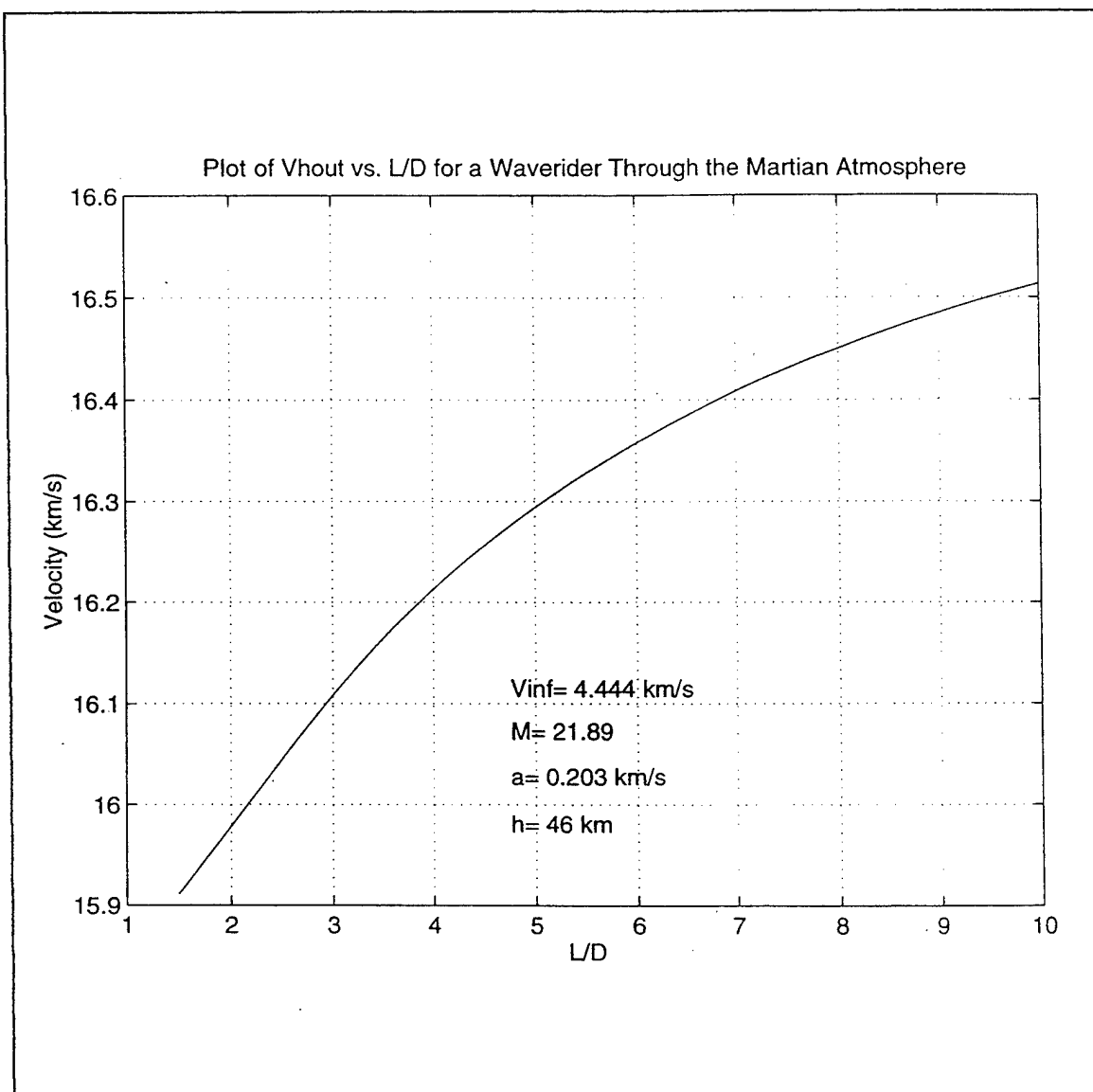
Figure 3.4 Drag Losses for the Earth-Mars-Jupiter-Saturn Waverider Mission
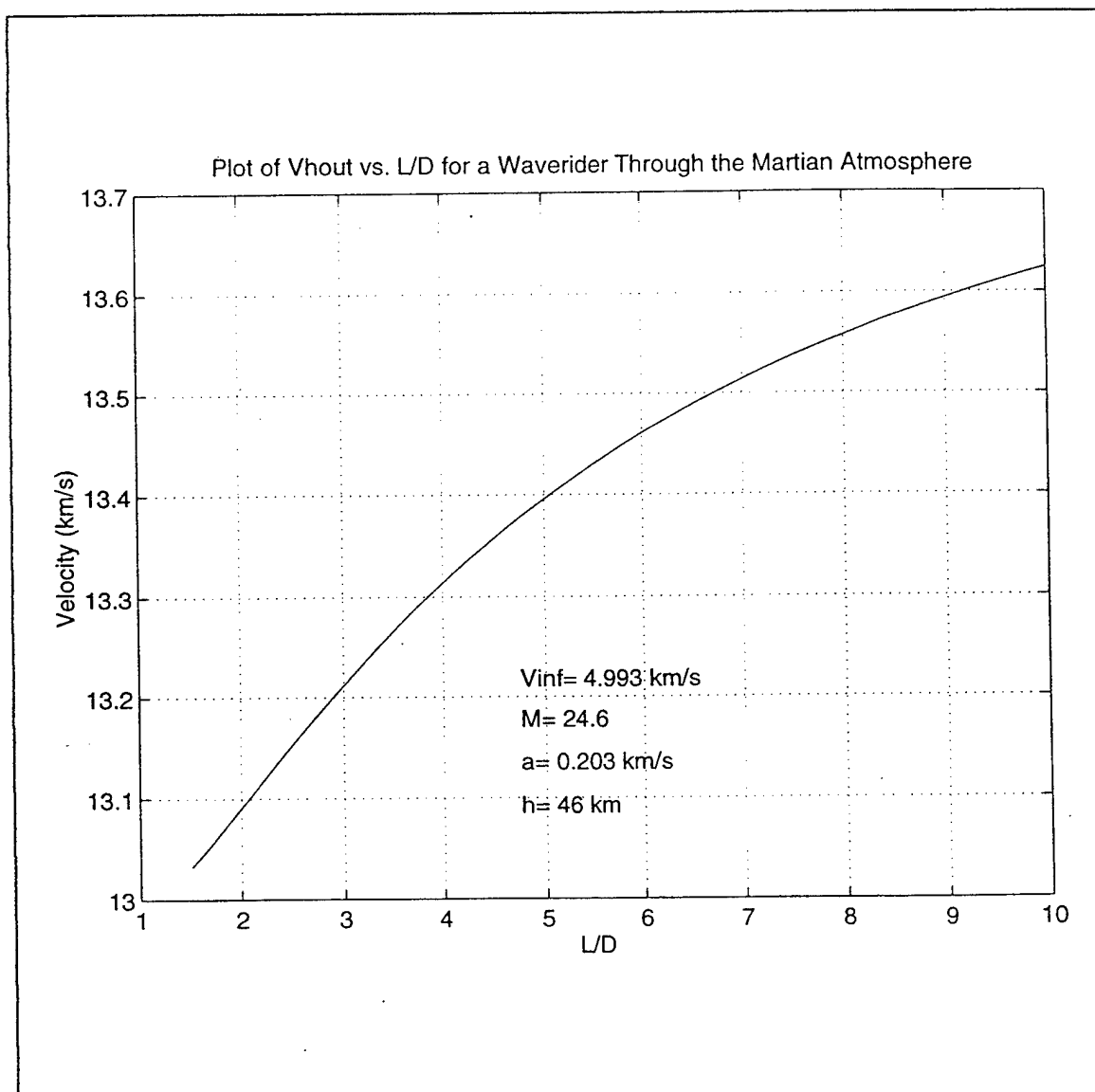
Figure 3.5 Drag Losses for the Earth-Mars-Jupiter-Neptune Waverider Mission
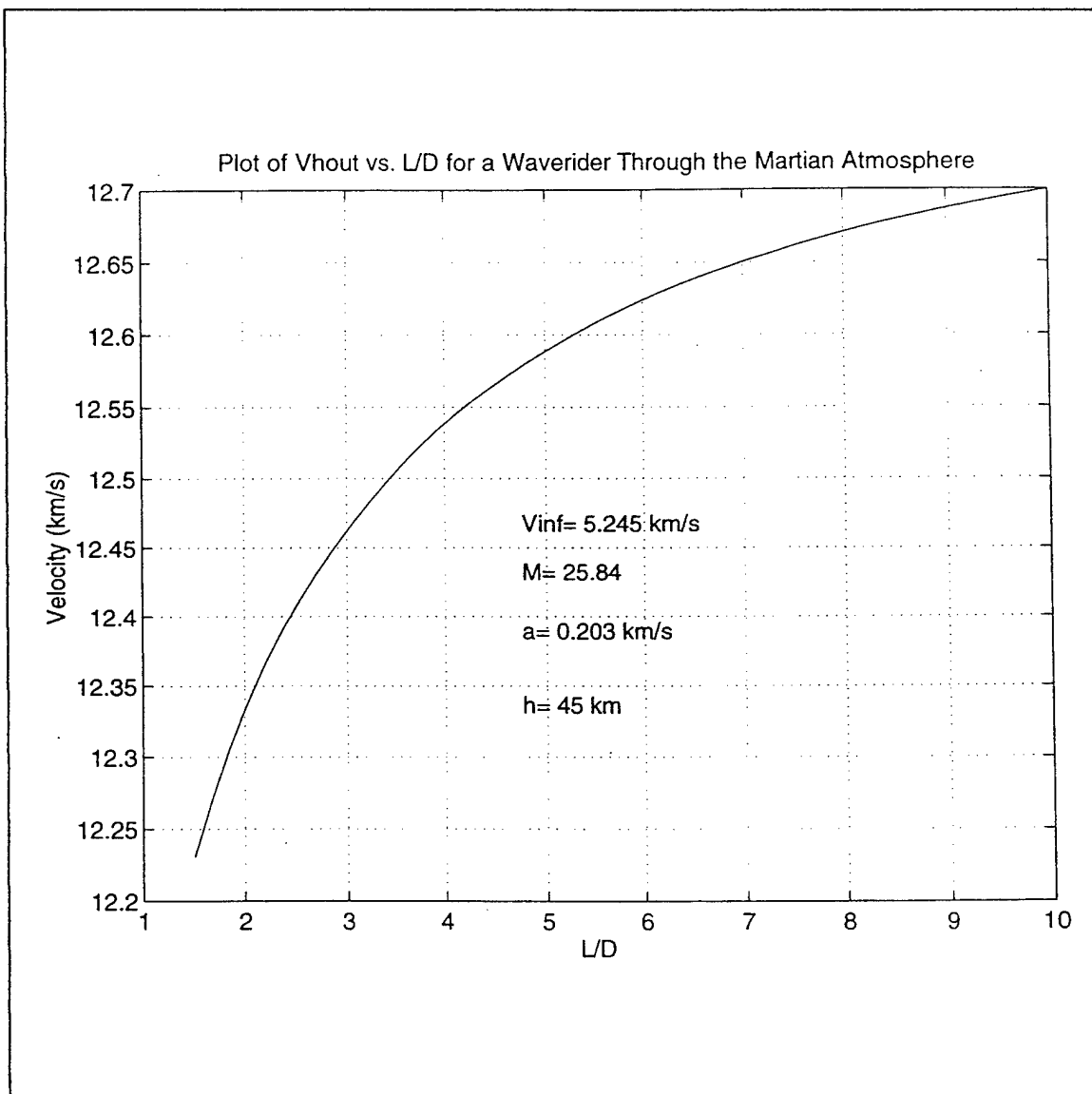
Figure 3.6 Drag Losses for the Earth-Mars-Jupiter-Saturn-Earth Waverider Mission

IV. OPTIMIZATION RESULTS

After the lift parameter converged to a value and the Waverider code optimized a design for L/D, the information was stored in a file called **FLWFLD.SUM**. The file included the waverider's geometry, mass, volume, planform area, L/D, and other information so that it can be readily accessible. This information was then written into separate files for each waverider so that it could easily be copied into **WAVRDR1.DAT**. This data file contains the "C" values corresponding to the values of C in the equation for the generating curve (Eq. 3.1). It also contains the flight parameters (Mach number and dynamic pressure) required for the AGA maneuver. **WAVRDR1.DAT** is read by the Waverider code's "one-shot" subroutine so that the user does not have run the optimization routine every time. One restriction of the Waverider code is that it only optimizes for a specific flight condition based on altitude and zero degrees angle of attack. The off design analysis for each waverider based on angle of attack, altitude, and Mach number will be discussed in the next chapter.

A. WAVERIDER GEOMETRY

Table 4.1 shows the "C" values of all four waveriders based on the output file **FLWFLD.SUM**. The generating curve for constructing a waverider can be found by placing these "C" values into Eq. 3.1. Table 4.2 shows the four waveriders configuration characteristics along with the Space Shuttle orbiter for comparison. The actual initial data files for **WAVRDR1.DAT** and the **FLWFLD.SUM** results are shown in Appendix D.

Waverider Mission	E-M-E	E-M-J-S	E-M-J-N	E-M-J-S-E
C1	0.798078	0.818714	0.892159	0.660501
C2	0.183043	0.343838	0.499986	0.217144
C3	0.518058	0.464864	0.0	0.508518
C4	0.137306	0.070586	-0.143161	0.107411
C5	0.020426	-0.023052	-0.135785	0.005622
C6	-0.000577	-0.000257	-0.033579	0.000784
C7	0.0	0.0	0.0	0.0
C8	0.0	0.0	0.0	0.0

Table 4.1 Waverider Geometry Output

Waverider Mission	E-M-E	E-M-J-S	E-M-J-N	E-M-J-S-E	Space Shuttle
Lift Parameter (kg/m^2)	516	463	432	468	50
Mass (kg)	632201	633226	621609	651909	94016
Volume (m^3)	4386	4393	4312	4523	934 (est.)
Vehicle Length (m)	80	80	80	80	37.2
Wing Span (m)	30	30	32	25	23.8
Wing Area (m^2)	1628	1490	1517	1361	367
Wing Loading (kg/m^2)	388	425	410	479	256
Dynamic Pressure (N/m^2)	1478	1915	2418	2985	N/A
Flight Altitude (km)	46	46	46	45	N/A
Flight Mach Number	19.23	21.89	24.6	25.84	N/A
L/D	6.24	5.86	5.84	5.90	N/A

Table 4.2 Waverider Configuration Characteristics

The data for the Space Shuttle orbiter was provided by Mr. Sergio Carrion at Rockwell, Inc. in Los Angeles, California. At almost twice the length of the Space Shuttle, the waveriders outweigh the Space Shuttle by a factor of seven. One reason for this is that most of the waveriders mass is made up of propellant; whereas, the orbiter carries only a fraction of the propellant. Table 4.2 indicates that although the wing spans are comparable, the interplanetary waveriders are longer, much larger (volume), and much heavier (mass) than the Space Shuttle Orbiter. As it turns out, the mass of each of the waveriders is about the same due to their lengths and vehicle densities (an input for

the **WAVRDR1.DAT** file) being equal. An item that must be noted is that the Waverider code assumes that lift and gravity are in opposite directions. However, the waveriders used in an AGA maneuver would fly "upside-down" relative to the planet, i.e., lift and gravity would be in the same direction.

The next four figures show four different views of the waveriders. Figure 4.1 shows the E-M-E waverider shape. It is a long, slender vehicle with a rounded upper surface (defined by Eq. 3.1). The generating shock angle (θ, in Eq. 3.1) which defines the flowfield was selected as 7.0478° by the optimization routine. In addition, its height is quite small compared to its length. The Waverider code found the leading edge radius to be 2.26 cm. This was a tradeoff because as the leading edge gets smaller, the temperature increases, but the drag decreases.

Similar results are shown in Figs. 4.2 to 4.4. In Fig 4.2, the E-M-J-S waverider does not have as round an upper surface as the E-M-E waverider. The leading edge radius is 2.62 cm with a generating shock angle of 7.56°. Figure 4.3 is the E-M-J-N waverider. It is characterized by its sharp edges and caret-shaped upper surface. The leading edge radius is 3.05 cm and the generating shock angle is 7.61°. Figure 4.4 shows the E-M-J-S-E waverider. It is much more rounded and thicker than the other waveriders, making the volume larger than the others. It also has the smallest wing span at 25 m. The leading edge radius is 3.05 cm and the generating shock angle is 7.7°.

30 meters

80 meters

PLAN VIEW

SIDE VIEW

ANGLED VIEW

AFT VIEW
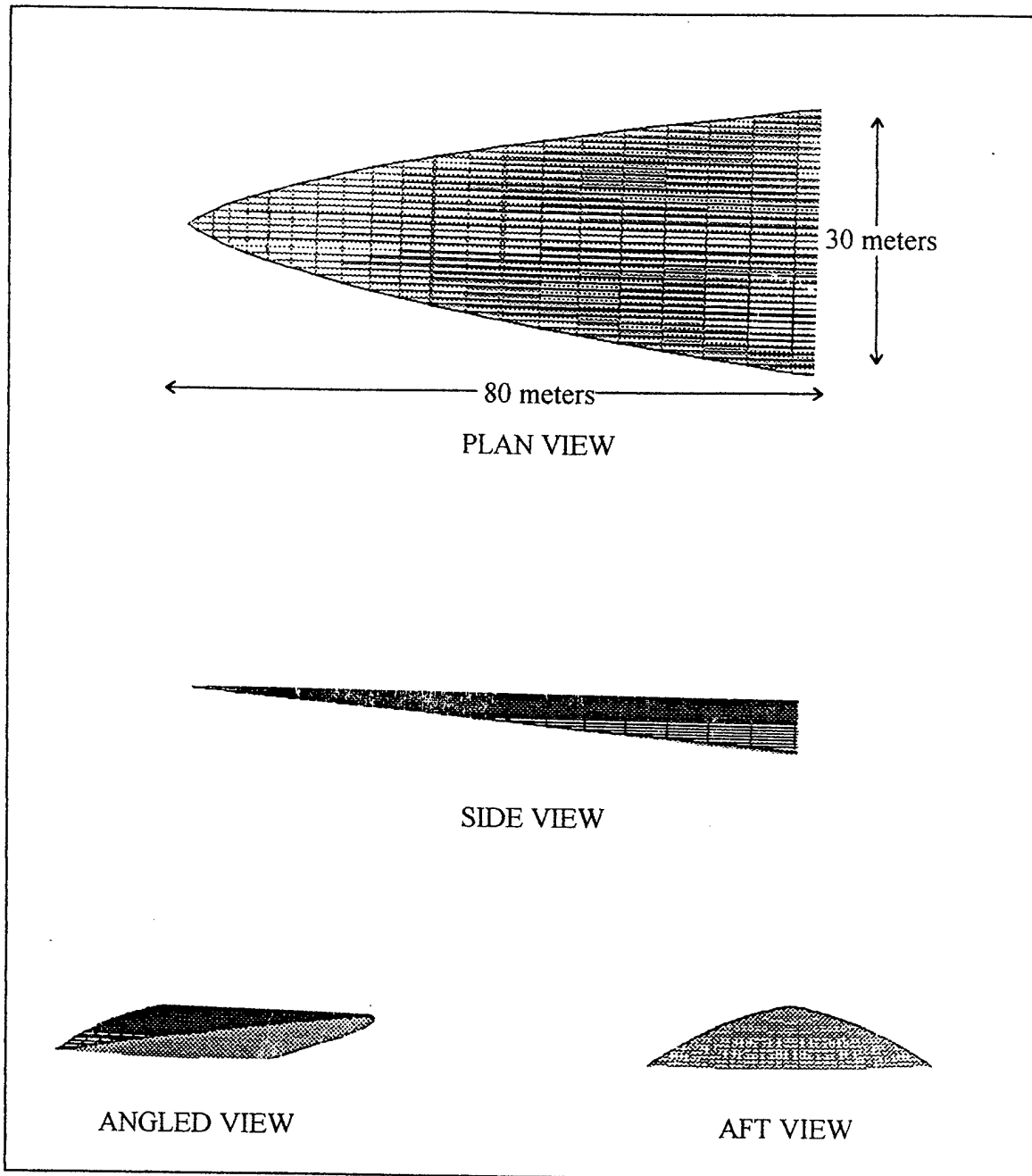
Figure 4.1 The Earth-Mars-Earth Waverider

30 meters

80 meters

PLAN VIEW

SIDE VIEW

ANGLED VIEW

AFT VIEW
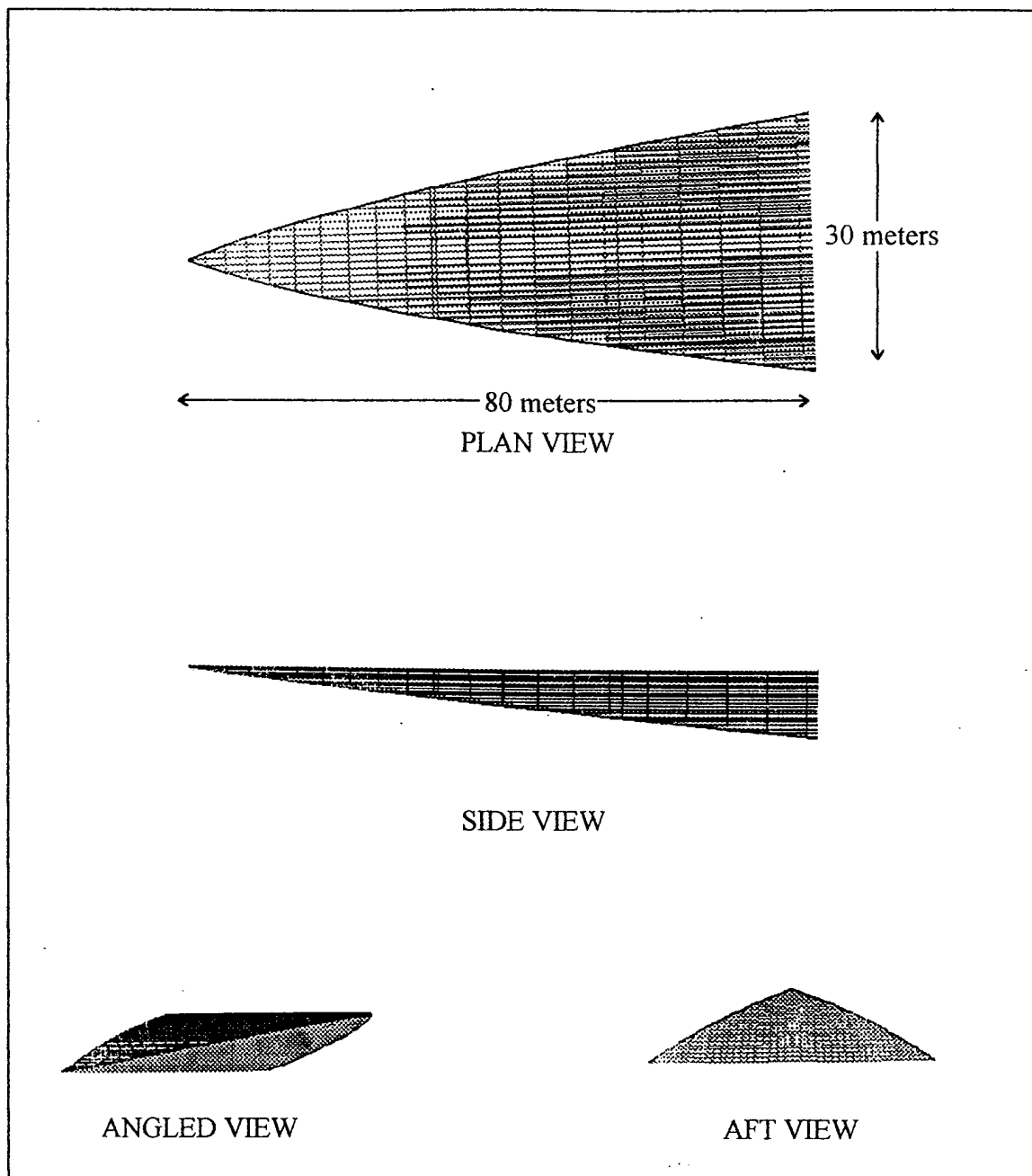
Figure 4.2 The Earth-Mars-Jupiter-Saturn Waverider

32 meters

← 80 meters →

PLAN VIEW

SIDE VIEW

ANGLED VIEW

AFT VIEW
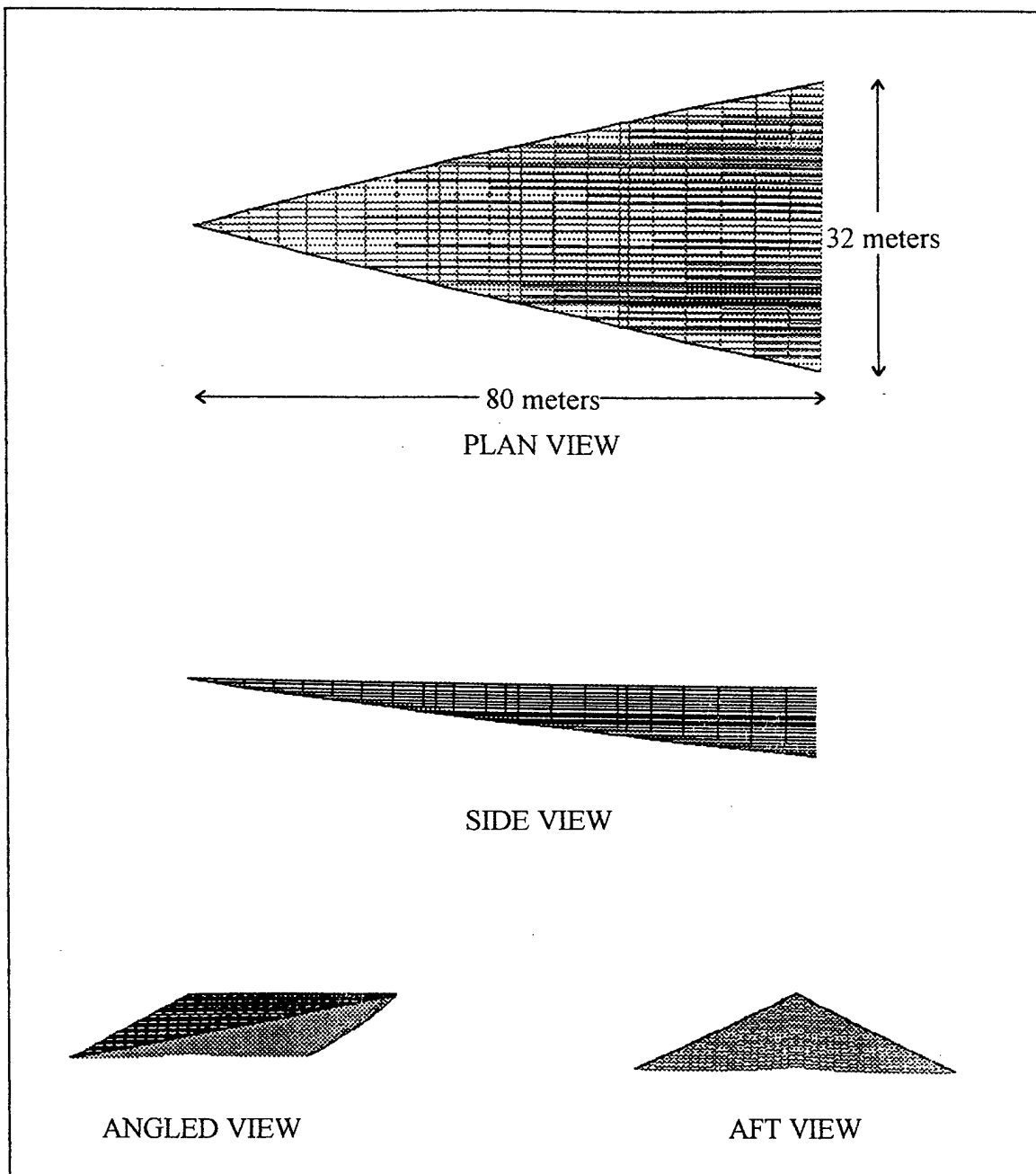
Figure 4.3 The Earth-Mars-Jupiter-Neptune Waverider

25 meters

←————80 meters————→

PLAN VIEW

SIDE VIEW

ANGLED VIEW   AFT VIEW
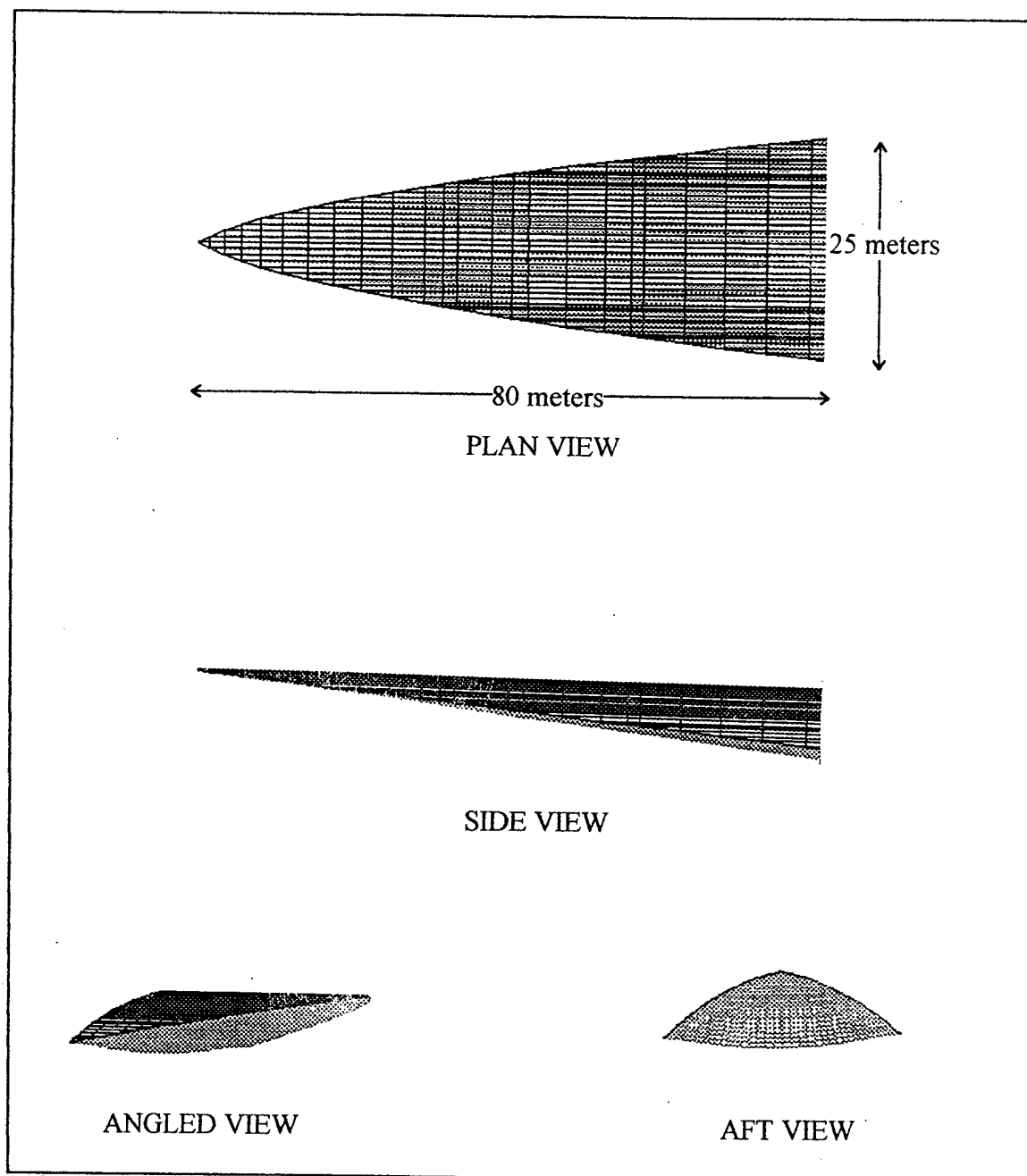
Figure 4.4 The Earth-Mars-Jupiter-Saturn-Earth Waverider

B. WAVERIDER PROPULSION SYSTEM CONSIDERATIONS

Having determined the waverider configurations that will provide the L/Ds required for the AGA maneuver, corresponding propulsion systems must be sized for the respective waverider energy requirements. All four waveriders are long slender vehicles with no engine fairings or inlets. An engine was chosen to be imbedded within the waverider structure so that it would not contribute any drag. This procedure enabled the author to use the Waverider code without having a specified engine and still have valid results. Since engine technology should improve in the future, one of the most powerful engines was selected for all four missions. The Space Shuttle's Main Engine is a high performance hydrogen-oxygen rocket engine that delivers a specific impulse of about 450 seconds with an approximate fuel density of 260 kg/m^3 [Ref. 9]. This engine was used for the fuel requirements analysis. A spreadsheet was developed to easily calculate and display the mass and volume of fuel required.

The amount of rocket propellant required for each burn was calculated from the ΔV output from MIDAS using the rocket equations shown on the top of Table 4.3 [Ref. 9]. The initial waverider mass before each burn is defined as m_o, while the mass after each burn is defined as m_f. The propellant mass is the difference between the two (m_p). Initial masses for each vehicle were calculated from the Waverider code discussed in the previous sections.

The results on the following page are conservative estimates since the amount of propellant required for an AGA maneuver is dependent on many things including the bending angle (ϕ), speed through the atmosphere, altitude, etc. A nominal value of 1000

m/s was taken as the ΔV required for the AGA maneuver at Mars. This value was determined by the author because it represents the approximate velocity loss due to atmospheric drag when flying through the Martian atmosphere for all four waverider missions plus a little extra for navigational errors. In addition, for the two missions returning to Earth, it was assumed that another AGA maneuver would be accomplished to aerocapture the vehicle thus requiring a minimum amount of fuel. From a low Earth orbit, the returned waveriders could be refurbished for another mission.

Table 4.3 shows the amount of propellant required for each burn during the waverider's mission. The E-M-E mission begins in a low Earth orbit and requires ΔV of 3654 m/s to leave the orbit and begin its mission. The amount of propellant needed for to achieve this ΔV was found by using the rocket equations shown on the top of the table. A propellant mass of 355903 kg is required for this burn. During the AGA maneuver at Mars, the waverider requires a ΔV of 1000 m/s, resulting in a burn of 123535 kg of propellant. There is no need for a propellant burn upon the waverider's return to Earth because of the aerocapture maneuver. Thus the total propellant mass required for this mission is about 480000 kg. This will take up to 42% of the waverider's volume and almost 76% of its initial mass.

The mission to Saturn requires an initial burn to leave a low Earth orbit resulting in a loss of 366210 kg of propellant. The next burn takes place during the AGA maneuver at Mars resulting in a loss of 119385 kg of propellant. Only 10098 kg of propellant is needed for the burn at Jupiter, while 51189 kg is necessary to slow the waverider enough to achieve a circular orbit around Saturn. The total amount of

propellant required for this mission is about 547000 kg. This will make up 48% of the waverider's volume and over 86% of its initial mass.

The E-M-J-N mission shows that the total propellant needed is 621609 kg, which is also its total initial mass. This means that the mission is not practical for a waverider. The vehicle density could be altered in the Waverider code to produce a more reasonable result, but the percent of propellant mass would still be over 98%. Note that the propellant required at Jupiter is much larger than for the other two missions that flyby the planet.

The final mission to be analyzed for propellant considerations is the E-M-J-S-E mission. It requires about the same amount of propellant for the first two burns at Earth and Mars. A ΔV of 2136 m/s is needed at Jupiter resulting in a burn of 26304 kg of propellant. The final burn takes place as the waverider swings around Saturn to put it on course for Earth. At Saturn, a ΔV of 9345 m/s results in a burn of 102485 kg of propellant. The total propellant mass needed for this mission is 623000 kg which makes up 95.6% of the waverider's initial mass.

The values of fuel percentages as a function of total mass shown in Table 4.3 are comparable to today's long range space flights, a promising result. Although, the Neptune mission would have to be altered slightly since the entire mass of the vehicle is made up of fuel. But, the mission to Saturn and back to Earth could be accomplished with a percent fuel mass of less than 96%. With the development of new engines and lighter weight materials, it does seem possible to create a family of waverider vehicles

for interplanetary travel. There is some concern about off design performance of these vehicles and that is the subject of the next chapter.

Constants				Equations Used
Gravity at Mars $(m/s^2) = 3.75$ M= Mars				$m_p = m_o - m_f$
at Jupiter $= 26.0$ J = Jupiter				$m_o/m_f = e^{\Delta V/(Isp\ g)}$
at Saturn $= 13.7$ S = Saturn				m_p = propellant mass
at Neptune $= 2.27$ N = Neptune				m_o = initial mass
at Earth $= 9.81$ E = Earth				m_f = final mass
I_{sp} (seconds) $= 450$ Fuel Density $(kg/m^3) = 260$				

Waverider Mission	E-M-E	E-M-J-S	E-M-J-N	E-M-J-S-E
Initial Mass (lb)	1394003	1396263	1370648	1437460
Initial Mass (kg)	632201	633226	621609	651909
Volume (ft^3)	154889	155140	152294	159718
Volume (m^3)	4389	4396	4316	4526
ΔV at Earth (m/s)	3654	3812	3968	3651
m_p for ΔV (kg)	355903	366210	368592	366804
ΔV at Mars (m/s)	1000	1000	1000	1000
m_p for ΔV (kg)	123535	119385	113125	127473
ΔV at Jupiter (m/s)		829	11993	2136
m_p for ΔV (kg)	0	10098	89699	26304
ΔV at Saturn (m/s)		2870		9345
m_p for ΔV (kg)	0	51189	0	102485
ΔV at (m/s)			16860	
m_p for ΔV (kg)	0	0	50191	0
Total m_p (kg)	479438	546883	621609	623066
Percent Volume	42.01	47.84	55.40	52.95
Percent Mass	75.84	86.36	100.00	95.58

Table 4.3 Waverider Fuel Analysis

V. OFF-DESIGN ANALYSIS

AEROSA (AERO Stand Alone) is a code used for off-design analysis of aerodynamic shapes developed by the NASA Ames Research Center. A series of spatial coordinates defining the vehicle's shape are read via a data file into the code for the off-design computations. The code is able to compute the shape generated by the Waverider code, convert it to an X-Y-Z reference frame through a transformation code (**wave2xyz**), and analyze each point or coordinate on the surface. By analyzing each point at various Mach numbers, pressures, and angles of attack, a good off-design representation of the shape can be realized. Several approximate methods for calculated the pressure coefficient on the windward surfaces are available to the user [Ref. 10]. The user is able to use any of the following methods: Newtonian, tangent wedge, tangent cone, or a combination of tangent wedge and tangent cone. In order to calculate pressure coefficients on the leeward surfaces, the user can use one of the following methods: Newtonian, high Mach base pressure, or Prandtl-Meyer expansion.

From the calculated pressure coefficient, the incremental area, and the unit normal of the incremental area, the code can compute the lift and pressure drag coefficients. Skin friction drag is computed using various reference-enthalpy methods [Ref. 11]. For the study discussed herein, the combination tangent wedge/tangent cone method was used for windward surfaces while the Prandtl-Meyer expansion method was used for the leeward surfaces. The AEROSA code had a restriction in that it was initially modeled solely for the Earth's atmosphere. However, all the vehicles in this study need

to fly through Mars' atmosphere. Therefore, the AEROSA code was provided, by NASA Ames, with a Mars atmosphere module.

A. THE MODIFIED AEROSA CODE

Since the original AEROSA code could not simulate the Martian atmosphere, the modified AEROSA code was developed by the Systems Analysis Branch at the NASA Ames Research Center for use in analyzing vehicles operating in any planetary atmosphere. Allowing the molecular weight of the fluid medium (CO_2 for Mars) through which the vehicle will be traveling to vary, the code can now be used to study a variety of different types of atmospheres. This atmospheric module modification enables the AEROSA user to investigate the possible use of other potential AGA planets (Venus, e.g.) once γ and the other appropriate transport properties for the atmosphere are entered into the code. None of the other computational aspects of AEROSA were changed. The entry data file for AEROSA is called **aero.dat** and contains angles of attack, Mach numbers, static pressure values, and the pressure coefficient calculation methods. The exit data file is called **aero.out**. The primary results of interest for this study are the AEROSA computed L/D ratios for the off-design flights of the waveriders developed for the four AGA missions.

For this study, the angle of attack was varied from -10° to +10° (each waverider was designed for $\alpha=0°$), and the Mach number was varied between ±5 from the optimized value for each mission. By changing the values for static pressure, the altitude was varied between ±10 km from the optimized value. With a known L/D ratio, the AEROSA user can utilize following graphs (Figs 5.1-5.4) of L/D versus the various

parameters (AOA, Mach number, and pressure) to analyze the off-design performance of each waverider. The sensitivity of the waveriders to each parameter was evaluated one at a time. In order to calculate the waverider performance if two or more parameters are off-design, the sensitivity to each parameter must be combined.

B. EARTH-MARS-EARTH WAVERIDER MISSION

Figure 5.1 depicts the sensitivity of the E-M-E waverider configuration if the vehicle is not flown at the design condition. The design condition for this mission was determined by MIDAS, the MATLAB program **vloss.m**, and the Waverider code. The waverider for this mission was determined to be flying at 46 km, Mach 19.23 and $0°$ angle of attack during its AGA maneuver at Mars. The results of Fig. 5.1 are very encouraging.

As illustrated in Fig 5.1a, the L/D ratio continues to rise from an angle of attack of $-6°$ through the design condition of $\alpha=0°$ before starting to drop off at $\alpha=2°$. The altitude sensitivity is shown in Fig. 5.1b. The design condition value of 46 km is a little more optimistic than what was calculated by AEROSA in that the Waverider code L/D ratio was calculated to be larger. Surprisingly, the L/D ratio does not increase appreciably at lower altitudes where the density and pressure are higher. As altitude decreases, the flight Reynold's number increases making the skin friction drag decrease and the L/D ratio increase. When the altitude becomes low enough some turbulence begins to appear resulting in an increase in the skin friction drag and a leveling off of the L/D curve. It has been noted by Lewis, et. al., [Ref. 4] that it would be best to fly as low as possible above the terrain in order to gain more lift. The data here suggests that it may be best to fly as

low as possible before the atmospheric drag exceeds the gains in lift a waverider will have at the lower altitudes. The Mach number sensitivity analysis, shown in Fig. 5.1c, behaves as expected for the waverider. As the Mach number is increased, the L/D ratio increases almost linearly, yet at a very small rate. Note that even if the waverider is at Mach 15, the L/D ratio has dropped only one-half of one percent from its largest value at Mach 24.5.

C. EARTH-MARS-JUPITER-SATURN WAVERIDER MISSION

Figure 5.2 shows the results of the off-design sensitivity for the E-M-J-S mission. The design condition for the AGA maneuver at Mars for this mission was calculated to be Mach 21.89, at an altitude of 46 km, with an L/D ratio of 5.86. Many of the same characteristics from the E-M-E mission shown in Fig. 5.1 can be seen in Fig. 5.2: the L/D ratio is increasing until 2° angle of attack is reached (Fig. 5.2a), a linear drop in L/D above the design altitude of 46 km with a converging value of L/D at lower altitudes (Fig. 5.2b), and a linear relationship between L/D and Mach number (Fig. 5.2c). It should be noted that there is a discontinuity at Mach 20 for which the author can not account. It is most likely that the modified AEROSA code has some errors in it when evaluated such high Mach numbers. In fact, when the temperature of the waverider is found to be above 5000° R, the code does accumulate some errors. However, all these designs were kept below 4500° R.
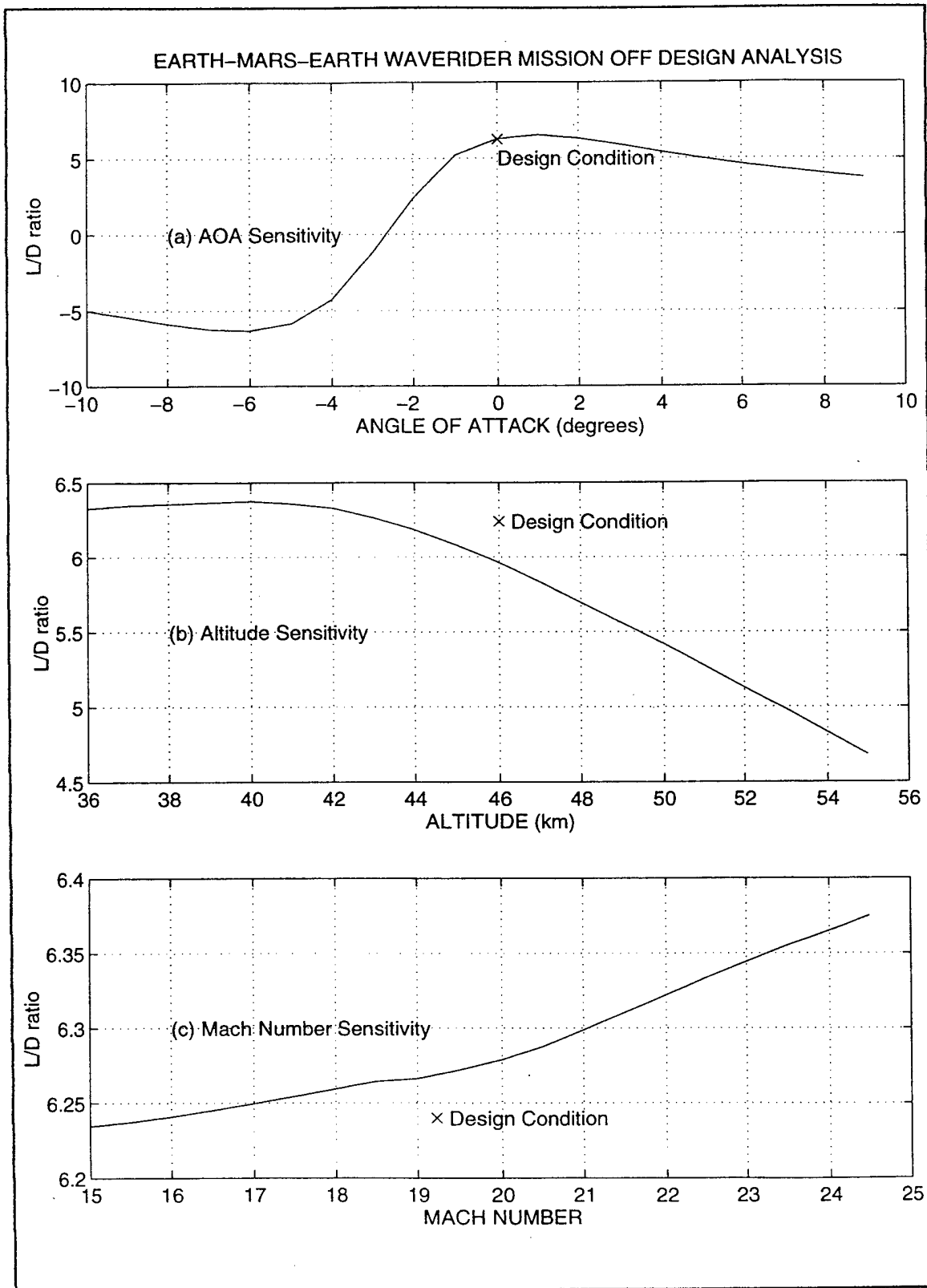
Figure 5.1 Off-Design Analysis for the Earth-Mars-Earth Waverider Mission
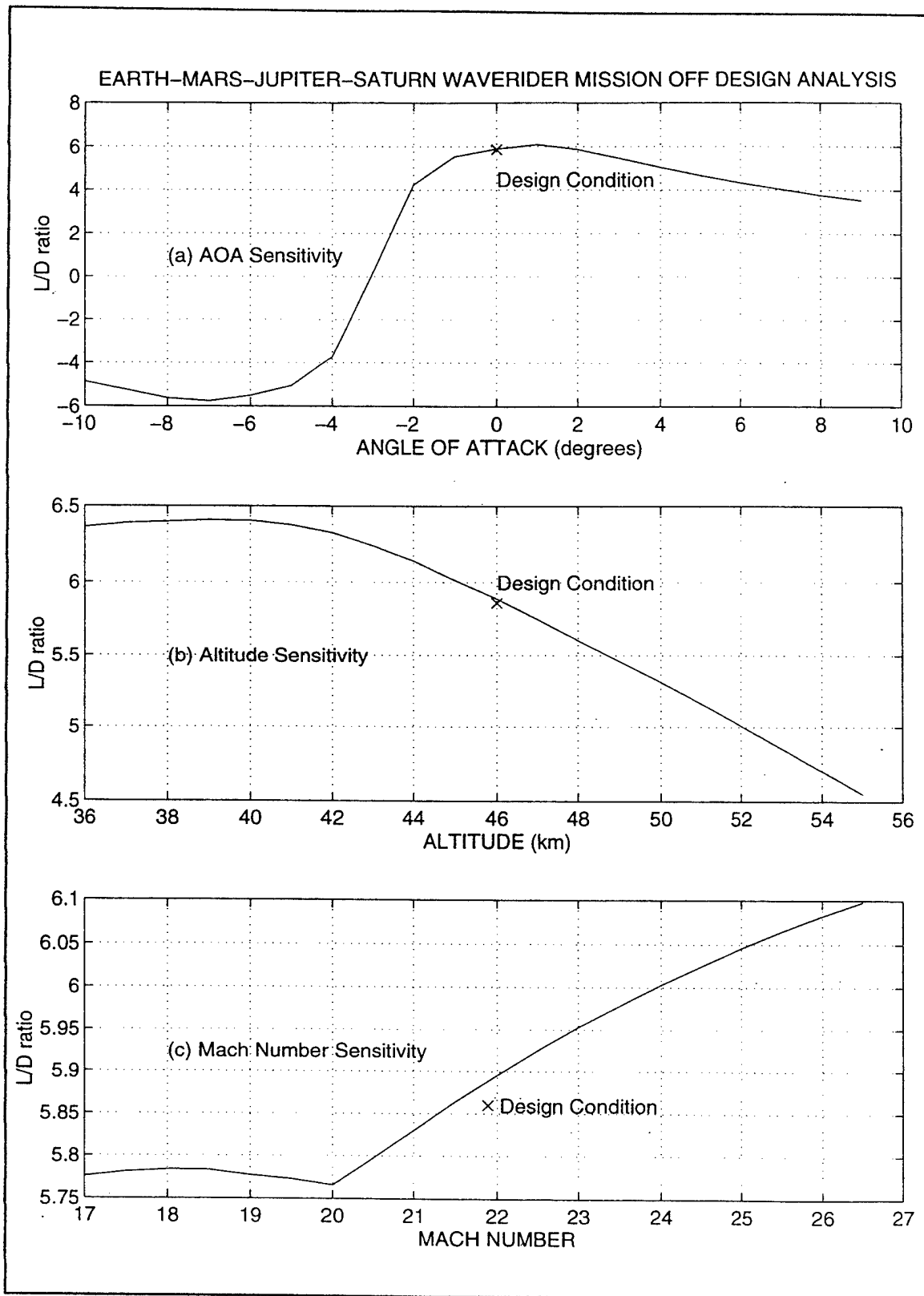
Figure 5.2 Off-Design Analysis for the Earth-Mars-Jupiter-Saturn Waverider Mission
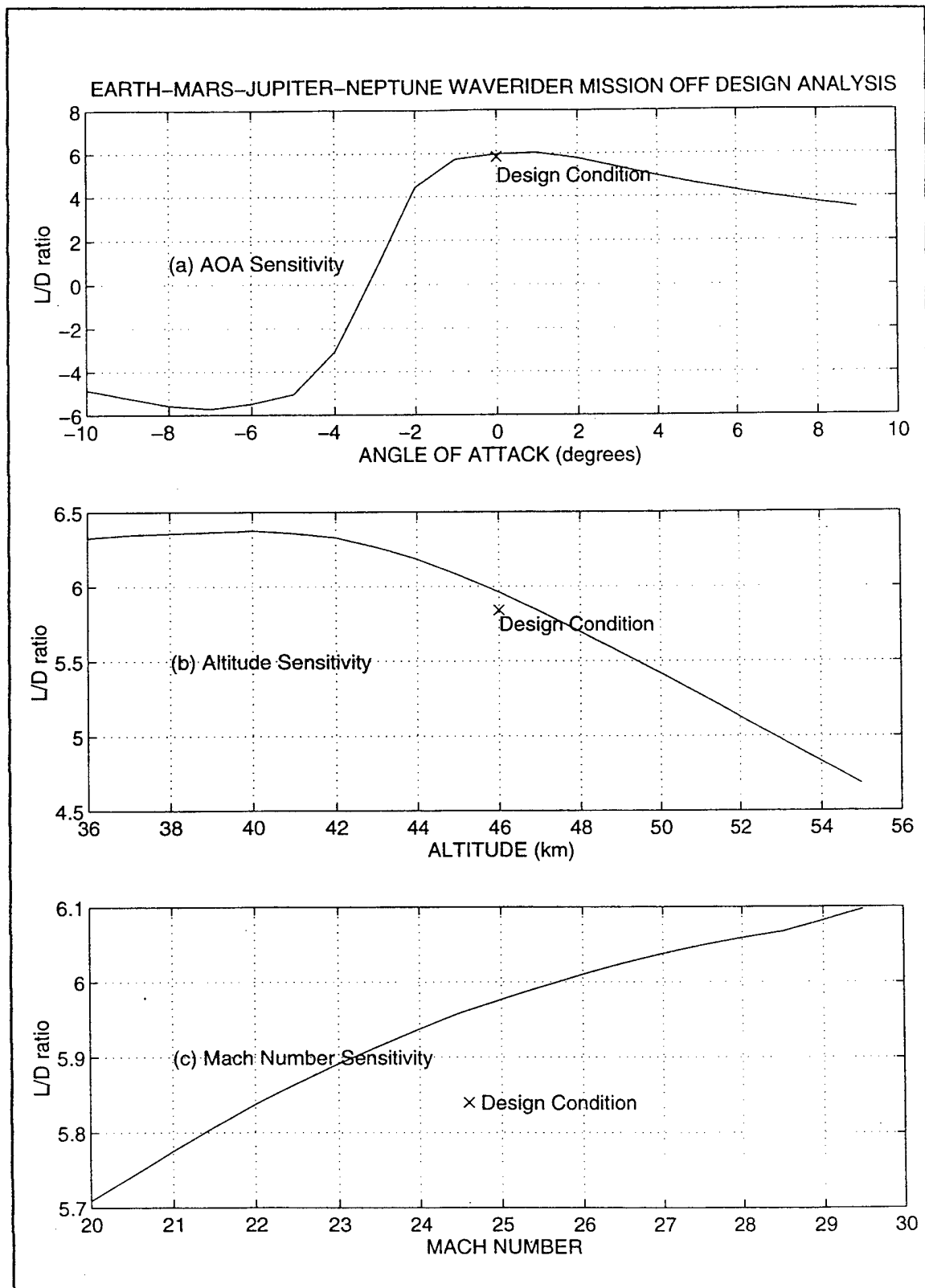
Figure 5.3 Off-Design Analysis for the Earth-Mars-Jupiter-Neptune Waverider Mission

D. EARTH-MARS-JUPITER-NEPTUNE WAVERIDER MISSION

Figure 5.3 represents the off-design sensitivity for the E-M-J-N mission. A Mach number of 24.6 at an 46 km with an L/D ratio of 5.84 was found to be the design condition for the AGA maneuver at Mars. Again, the same characteristics are present in these three graphs of L/D as in the previous two figures. The increase in L/D from -6° angle-of-attack to 2° angle-of-attack is shown in Fig. 5.3a, a linear drop in L/D above design altitude with a converging value of L/D at lower altitudes as shown in Fig. 5.3b, and a linear relationship between L/D and Mach number as shown in Fig. 5.3c.
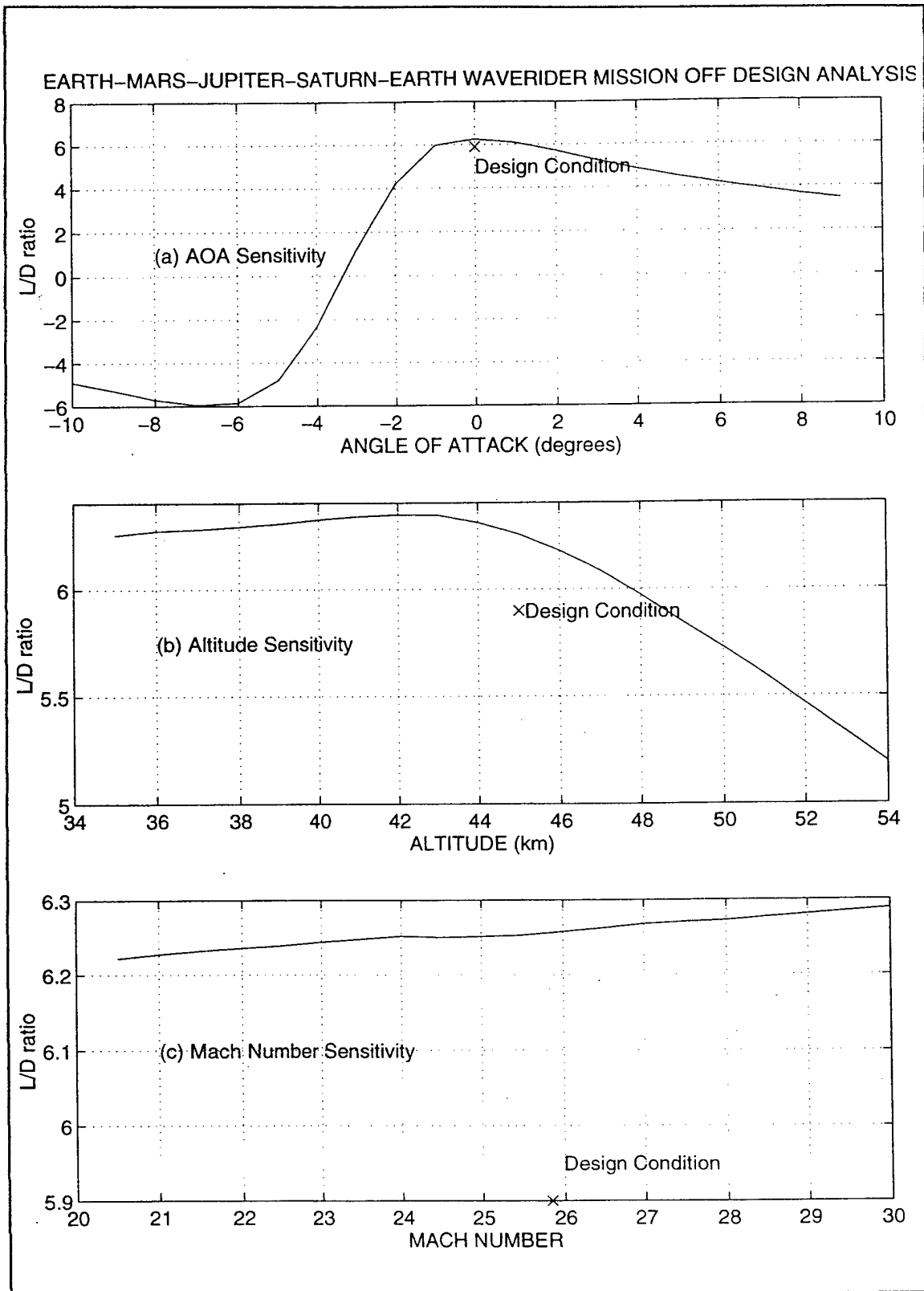
Figure 5.4 Off-Design Analysis for the Earth-Mars-Jupiter-Saturn-Earth Waverider Mission

E. EARTH-MARS-JUPITER-SATURN-EARTH WAVERIDER MISSION

Figure 5.4 displays the off design analysis for the E-M-J-S-E mission. The design condition for the AGA maneuver at Mars was determined to be Mach 25.84, at an altitude of 45 km with an L/D ratio of 5.90. Figure 5.4a displays the increase in L/D -6° to 2° angle-of-attack just as in the previous figures. Again, the altitude sensitivity displayed in Fig. 5.4b shows the same characteristic shape as in the previous figures as does the Mach number sensitivity analysis from Fig. 5.4c.

The results from the four figures in this chapter are closely related. Of special interest is the accuracy of the design condition which was found through the results of three different codes compared to the design condition calculated by the modified AEROSA code. This accuracy of less than 10% between the modified AEROSA code's design condition and the Waverider code's design condition is what is so encouraging from these results. Furthermore, the results show that as long as the waverider is close to 0° angle-of-attack, and at or below the design AGA altitude, the speed (Mach number) of the vehicle is not too important. The waverider loses a large amount of performance if the angle-of-attack is less than -1°, or if its altitude is any higher than the design altitude.

F. KUCHEMANN'S CURVE

Kuchemann [Ref. 12] suggested that the maximum L/D available at a given Mach number could be determined from Eq. 5.1. While Hunt [Ref. 13] proposed that Eq. 5.2 or 5.3 might be a better model for finding the maximum L/D. Figure 5.5 on the following page plots the Mach number vs. maximum L/D for these three equations along with the

L/D's from the four waveriders discussed in this study. Since the waveriders studied in this thesis have an L/D of approximately 6, it seems Eq. 5.3 provides the best model.

$$\left(L/D\right)_{max} = 3 + \frac{9}{M} \qquad (5.1)$$

$$\left(L/D\right)_{max} = 4 + \frac{12}{M} \qquad (5.2)$$

$$\left(L/D\right)_{max} = 6 + \frac{12}{M} \qquad (5.3)$$
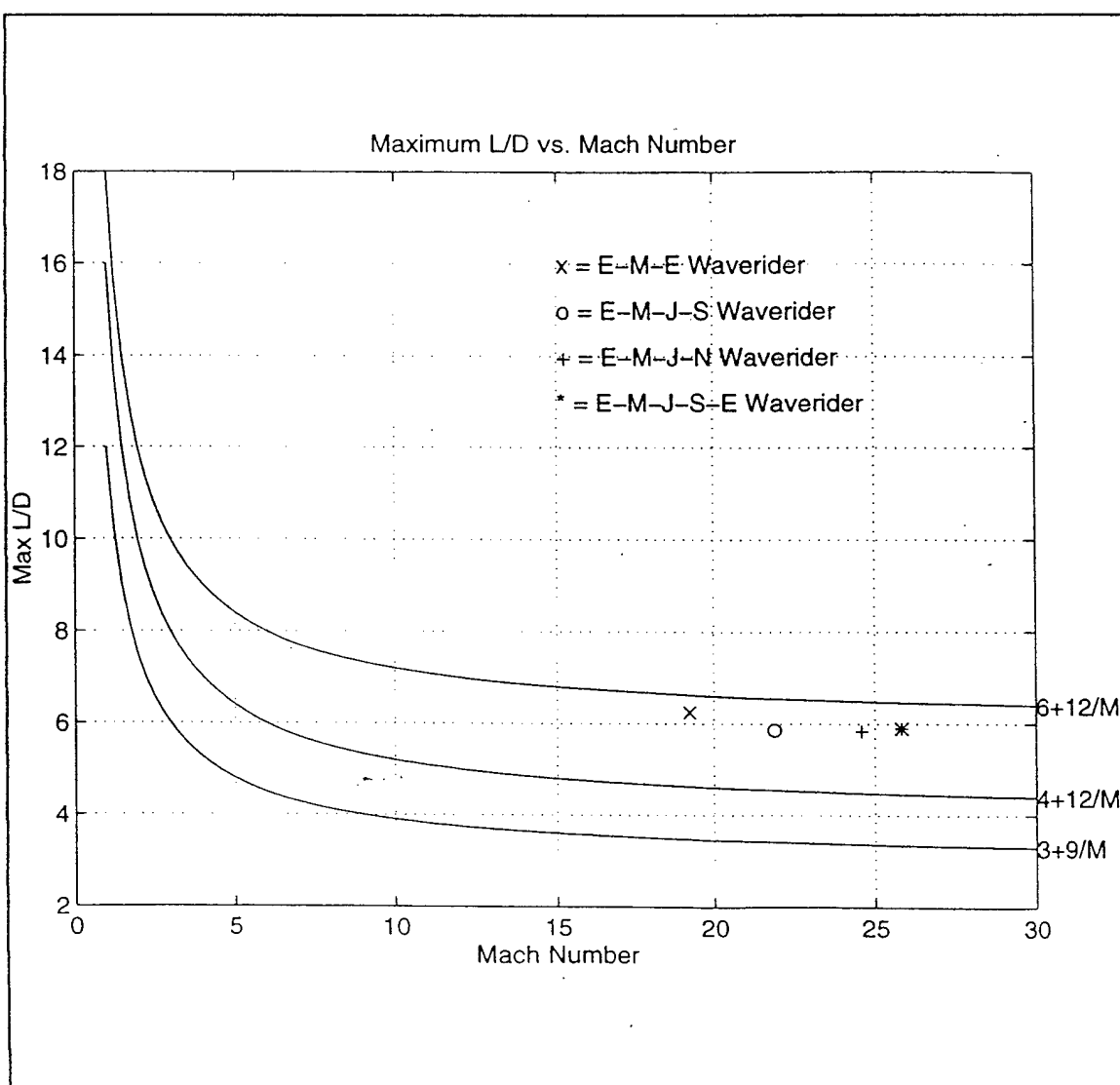
Figure 5.5 Kuchemann's Curve

VI. FOLLOW-ON RESEARCH

A. RECENT DEVELOPMENTS

Most of the current research related to the applications of AGA is being performed at JPL's Section 312 in Pasadena, California under the leadership of Dr. Angus McRonald and Dr. James Randolph. Additionally, at the University of Maryland, supported by the influence of Dr. Mark Lewis has also provided insights into the AGA concept. One of the interplanetary flights being studied by JPL is the Solar Probe Mission [Ref. 14]. This mission would measure the near sun physics environment at just four solar radii. Currently, the trajectory requires the spacecraft to use gravity assist at Jupiter to turn the spacecraft directly towards the sun. Although the mission would require a five year flight time (a desirable parameter according to Randolph, et. al.), the launch energy of 118 km^2/s^2 is too high for today's launch vehicle performance. Besides, decreasing the flight time would require a further increase in the launch energy.

In order to alleviate the launch vehicle problem for the Solar Probe, an AGA maneuver at Venus or Earth has been proposed as an alternative solution. The results of JPL's research show that the flight time would be reduced to four to 6 months depending on the trajectory used. Furthermore, the launch energy would be decreased to less than 70 km^2/s^2.

Aerospace companies, such as Lockheed, have expressed an interest in AGA technology, according to Dr. Randolph. In fact, Lockheed is redesigning a spacecraft configuration for a mission to Venus so that it can use AGA at Venus in order for the vehicle to return to Earth without using its small fuel supply. It seems as more

companies review the AGA concept, more research may be performed, and the general public will see new designs for interplanetary spacecraft.

B. OTHER AREAS FOR RESEARCH

One important waverider topic of research not addressed in this thesis is the problem of heat transfer. As a waverider enters an atmosphere it will experience extreme heat loads that could cause ablation of the leading edges as well as deterioration of the composite materials that are being proposed for these vehicles.

From elementary thermodynamic and heat transfer equations, stagnation point heating rates can be reduced by increasing the leading edge or nose radius. The four missions discussed in this thesis had an upper limit of 4500° R imposed on the leading edges. This heat load can be handled by current technology in composite materials for short time periods and for small surface areas, but this may not be sufficient due to the flight times in the Martian atmosphere. Carbon-carbon or beryllium composites in thin strips along the leading edge have been proposed to combat the waverider's leading edge heat loads. It is hoped that advances in material science technology will provide other solutions to the heat transfer problem.

Another interplanetary travel option is to design one waverider for all missions. The design would have to be generic enough to accommodate a wide range of Mach numbers. Perhaps it would look like Nonweiler's caret wing of Fig. 1.1. An analysis could be done with the software tools used in this thesis to determine whether or not this generic waverider would be a viable option for a number of missions. This would be of some interest to an Earth-Mars-Earth reusable shuttle vehicle.

Other missions should be investigated to determine if they can utilize the advantages of AGA maneuvering. Missions using both Venus and Mars for AGA are currently being studied. The advantage of using Venus as an AGA planet is that it requires less launch energy than a mission using Mars as its initial AGA planet. After performing the AGA maneuver at Venus, the vehicle would head towards Mars and perform another AGA maneuver and continue on its voyage. The problems of designing a vehicle for two different atmospheres would have to be addressed as well as the affects of ablation and leading edge deterioration associated with one AGA maneuver upon a second maneuver. For these reasons, the author chose only Mars as an AGA planet for this study. Another reason for choosing Mars is that it is generally close to most trajectories to the outer planets. A mission planner should take advantage of Mars' proximity to the intended flight path.

VII. CONCLUSIONS

This thesis has discussed the advantages of waveriders for interplanetary missions using the relatively new concept of aero-gravity-assist (AGA) maneuvering instead of gravity-assist (GA) maneuvering. It has been shown that using this maneuver with a well designed waverider would shorten flight times by as much as 25%, increase the launch windows by varying the bending angle (ϕ) at the AGA planet, and reduce fuel loads by 30%. This idea could bring about the development of a new breed of space vehicles.

Most of today's satellites and interplanetary vehicles are designed to fit within the payload volume of a launch vehicle without much concern about their deployed configuration. With budget cuts in today's space program, designers should be concerned about design economics. Designs using even a few of the AGA benefits would help the mission planners and program managers develop better space vehicles. Aero-gravity-assist is an untapped energy source that should be further explored.

APPENDIX A - MIDAS INPUTS

A. WAVERIDER MISSION INITIAL DATA FILES

1. Earth-Mars-Earth Waverider Mission

the1.inp
```
$input head='2011 Earth-Mars-Earth Waverider Mission'
shota='earth'
bulsi='earth'
body='mars'
jdl=2011,11,15
re=6878.,rp=6408.,rcb=.001,tend=460.,rn=-.1,.1
varyi='jdate','tpb'
jdate=0,tpb=178 $
$ end
```

2. Earth-Mars-Jupiter-Saturn Waverider Mission

the2.inp
```
$input head='2011 Earth-Mars-Jupiter-Saturn Waverider Mission'
shota='earth'
bulsi='saturn'
body='mars','jupiter'
jdl=2011,6,23
ndb=2,2
rp=2.2,ra=7951432,rcb=.0001,140000,tend=2600.,rn=-.2,.2,.2
varyi='jdate','tpb','tpc'
jdate=0,tpb=234.,tpc=1200 $
$ end
```

3. Earth-Mars-Jupiter-Neptune Waverider Mission

the3.inp
```
$input head='2003 Earth-Mars-Jupiter-Neptune Waverider Mission'
shota='earth'
bulsi='neptune'
body='mars','jupiter'
jdl=2003,6,14
ndb=2,2
rp=2,ra=3,rcb=.0001,140000,tend=2922.,rn=-.1,.1,.1
varyi='jdate','tpb','tpc'
jdate=0,tpb=132.4,tpc=700 $
$ end
```

4. Earth-Mars-Jupiter-Saturn-Earth Waverider Mission

satrtn1.inp
$input head='2014 Earth-Mars-Jupiter-Saturn-Earth Waverider Mission'
shota='earth'
bulsi='earth'
body='mars','jupiter','saturn'
jdl=2014,6,23
ndb=2,2,2
rp=2.2,ra=2.,rcb=.0001,140000,660000,tend=4000.,rn=-.2,.2,.2,.5
varyi='jdate','tpc','tpd'
jdate=0,tpb=180.,tpc=1200.,tpd=2600. $
$end

B. GA COMPARISON MISSION INITIAL DATA FILES

1. Low Energy Trajectory for a non-Waverider Roundtrip Mission to Mars

themar1.inp
$input head ='Low Energy Trajectory Non-Waverider Roundtrip Mission to Mars'
shota='earth',bulsi='earth',body='mars'
jdl=2013,3,19
re=6878.,rp=6408.,rcb=9397.,tend=470.,rn=-.1,.1
varyi='jdate','tpb'
jdate=349.6,tpb=541.0, $
$ end

2. Non-Waverider Trajectory for a Roundtrip Mission to Mars Departing on the Same Day as the Waverider

themar2.inp
$input head='Non-Wvrdr Traj Roundtrip Mission to Mars Leaving Same Day as Wvrdr'
shota='earth'
bulsi='earth'
body='mars'
jdl=2011,11,28
re=6878.,rp=6408.,rcb=2.,tend=460.,rn=-.1,.1
varyi='tpb'
jdate=0,tpb=178 $
$end

3. Low Energy Trajectory for a non-Waverider Mission to Saturn

thesat1.inp
$input head='Low Energy Trajectory for a non-Waverider Mission to Saturn'
shota='earth'
bulsi='saturn'
body='venus','earth','earth'
ndb=2,2,2
jdl=1992,9,23
tpb=450,900,1750
altb=300,12000,300
rn=-1.4,.4,.8
tend=3400
jdate=-6
varyi='tpb','tpc','tpd','jdate'
ra=7951432,rp=2.2
nda=2 $
$end

4. Non-Waverider Trajectory to Saturn Departing on the Same Day as the Waverider

thesat2.inp
$input head='Non-Wvrdr Traj to Saturn Leaving on the Same Day as the Wvrdr'
shota='earth'
bulsi='saturn'
body='mars','jupiter'
jdl=2011,10,26
ndb=2,2
rp=2.2,ra=7951432,rcb=2.,140000,tend=2600.,rn=-.2,.2,.2
varyi='tpb','tpc'
jdate=0,tpb=234.,tpc=1200 $
$ end

5. Low Energy Trajectory for a non-Waverider Mission to Neptune

thenep1.inp
$input head='Low Energy Trajectory for a non-Waverider Mission to Neptune'
shota='earth'
bulsi='neptune'
body='mars','jupiter'
jdl=2003,6,15
ndb=2,2,2
rp=2,ra=3,rcb=2.,140000,.1,tend=3000.,rn=-.1,.1,.1
varyi='tpb','tpc','jdate'
jdate=0,tpb=200,tpc=660 $
$end

6. Non-Waverider Trajectory to Neptune Departing on the Same Day as the Waverider

thenep2.inp
$input head='Non-Wvrdr Traj to Neptune Leaving Same Day as Wvrdr'
shota='earth'
bulsi='neptune'
body='mars','jupiter'
jdl=2003,6,27
ndb=2,2,2
rp=2,ra=3,rcb=2.,140000,.1,tend=2922.,rn=-.1,.1,.1
varyi='tpb','tpc'
jdate=0,tpb=200,tpc=660 $
$end

7. Non-Waverider Trajectory for a Roundtrip Mission to Saturn Departing on the Same Day as the Waverider

thertn1.inp
$input head='Non-Wvrdr Traj Roundtrip to Saturn Leaving Same Day as Wvrdr'
shota='earth'
bulsi='earth'
body='mars','jupiter','saturn'
jdl=2014,6,23
ndb=2,2,2
rp=2.2,ra=2.,rcb=2.0,140000,660000,tend=4000.,rn=-.2,.2,.2,.5
varyi='jdate','tpc','tpd'
jdate=0,tpb=180.,tpc=1200.,tpd=2600. $
$end

APPENDIX B - MIDAS RESULTS

A. EARTH-MARS-EARTH WAVERIDER MISSION

2011 Earth-Mars-Earth Waverider Mission   Jan 11, 1996   17:24:54

Epoch= 2011 11 15 0 0 0   2455880.500   Earth Ecliptic and Equinox of 2000
                                           and Body Equator and Equinox of Date
      Earth   Earth   Mars
Set no= 2

   nt= 1.01 iter= 25 kgo= 2 flags 0 0 0 nm= 0 nmt= 1 ndl= 2 nda= 2 ndb= 2
   veq= 20.3430   grad= .000000   dvt= 20.3430   dvmt= 4.3716   dvpl= 16.6888
   tend= 460.000   fty= 1.2594   hca= .45 .82

jdate= 13.9   2011 11 28 22 17   dvl= 3.6542   c3= 11.0357   dla= 19.484
                                                   rla= 132.641   re 6878.0
tpb= 249.6   2012 7 21 13 22   dvb= 4.3716   vhi= 3.903   vho= 7.446
                                                   bend= 50.460   rcb= 11541.
trp= 415.7   2013 1 3 15 44   rp= .4572   xmp= .3453
                                  ymp= .2996   zmp= -.0004
adate= 473.9   2013 3 2 22 17   dva= 12.3172   vhp= 16.8463   dap= 12.910
                                  rap= 148.353   rp 6408.0

Input File: the1.inp   Cumulative run time= 0.30 sec   Step= .100E-01^L

****

B. EARTH-MARS-JUPITER-SATURN WAVERIDER MISSION

2011 Earth-Mars-Jupiter-Saturn Waverider Mission   Jan 2, 1996   14:27:23
Epoch= 2011 6 23 0 0 0   2455735.500   Earth Ecliptic and Equinox of 2000
                                     and Body Equator and Equinox of Date
   Earth   Saturn   Mars   Jupiter
Set no= 1

   nt= 1.01 iter= 48 kgo= 2 flags 0 0 0 nm= 0 nmt= 1 ndl= 2 nda= 2 ndb= 2 2
  veq= 9.8693   grad= .000000   dvt= 9.8693 dvmt= 3.1869 dvpl= 6.0570
  tend= 2600.00   fty= 7.1184   hca= .52 .75 .42

jdate= 125.9 2011 10 26 21 57   dvl= 3.8123   c3= 13.4779   dla= -6.399
                                         rla= 149.109   re 6618.1
trp= 144.4 2011 11 14 9 46   rp= .9819   xmp= .5826
                        ymp= .7903 zmp= -.0118
tpb= 380.9 2012 7 7 20 39   dvb= 2.3577   vhi= 4.444   vho= 16.838
                        bend= 136.657 rcb= 27.162
trp= 472.2 2012 10 7 3 36   rp= .7843   xmp= .6065
                      ymp= -.4971 zmp= -.0095
tpc= 1242.0 2014 11 16 0 23   dvc= .8293   vhi= 6.799   vho= 10.765
                        bend= 135.631 rcc= 1.961
adate= 2725.9 2018 12 8 21 57 dva= 2.8701 vhp= 11.6329 dap= -25.570
                        rap= 287.308 rp 2.200

Input File: the2.inp   Cumulative run time= 0.59 sec   Step= .100E-01^L

****

C. EARTH-MARS-JUPITER-NEPTUNE WAVERIDER MISSION

2003 Earth-Mars-Jupiter-Neptune Waverider Mission   Jan 2, 1996   14:40:01
Epoch= 2003 6 14 0 0 0   2452804.500   Earth Ecliptic and Equinox of 2000
                                and Body Equator and Equinox of Date

Earth	Neptune	Mars	Jupiter

Set no= 1

nt= 1.01 iter= 42 kgo= 2 flags 0 0 0 nm= 0 nmt= 0 ndl= 2 nda= 2 ndb= 2 2
veq= 33.3930   grad= .000000   dvt= 33.3930   dvmt= 12.5658   dvpl= 29.4253
tend= 2922.00   fty= 8.0000   hca= .27 .53 .35

jdate=   13.8   2003 6 27 20 10   dvl= 3.9677   c3= 17.0991   dla= -19.069
                                               rla= 337.313   re 6618.1
tpb=   135.6   2003 10 27 13 28   dvb= .5730   vhi= 4.993   vho= 13.978
                                               bend= 165.396   rcb= 3.875
trp=   189.5   2003 12 20 12 36   rp= 1.2011   xmp= .5863
                                    ymp= 1.0478   zmp= -.0302
tpc=   787.3   2005 8 9 7 15   dvc= 11.9927   vhi= 10.636   vho= 19.561
                                               bend= 157.710   rcc= 1.961
adate= 2935.8   2011 6 27 20 10   dva= 16.8595   vhp= 24.6985   dap= 27.792
                                               rap= 112.236   rp 2.000

Input File: the3.inp   Cumulative run time= 0.55 sec   Step= .100E-01^L

****

D. EARTH-MARS-JUPITER-SATURN-EARTH WAVERIDER MISSION

2009 Earth-Mars-Jupiter-Saturn-Earth Waverider Mission   Apr 1, 1996   14:06:00
Epoch= 2014 6 23 0 0 0   2456831.500   Earth Ecliptic and Equinox of 2000
                                    and Body Equator and Equinox of Date

	Earth	Earth	Mars	Jupiter	Saturn

Set no= 1

  nt= 1.01   iter= 47   kgo= 2   flags 0 0 0   nm=0   nmt=1   ndl=2   nda=2   ndb=2 2 2

veq= 27.6093   grad= .000000   dvt= 27.6093   dvmt= 16.0157   dvpl= 23.9581

tend= 4000.00   fty= 10.9514   hca= .60 .60 .30 .45

jdate= -149.5   2014 1 24 11 34   dvl= 3.6513   c3= 9.7764   dla= 20.824

                                              rla= 212.928   re 6618.1

tra= 93.4   2014 9 24 10 47   ra= 1.4813   xma= .6648

                                          yma= -1.3238   zma= .0098

tpb= 180.0   2014 12 20 0 0   dvb= 4.5296   vhi= 5.245   vho= 12.827

                                            bend= 53.282   rcb= 488.61

trp= 240.4   2015 2 18 9 25   rp= 1.1367   xmp= .9126

                             ymp= .6774   zmp= -.0168

tpc= 1016.3   2017 4 4 6 19   dvc= 2.1362   vhi= 6.888   vho= 6.014

                                            bend= 165.549   rcc= 1.961

trp= 1197.3   2017 10 2 7 21   rp= 5.2902   xmp= -4.1848

                             ymp= -3.2345   zmp= .1085

tpd= 2439.8   2021 2 25 18 26   dvd= 9.3499   vhi= 9.233   vho= 7.896

                                            bend= 141.777   rcd= 11.000

trp= 3850.4   2025 1 6 8 32   rp= .9833   xmp= -.2690

                             ymp= .9458   zmp= -.0001

adate= 3850.5   2025 1 6 11 34   dva= 7.9424   vhp= 10.7677   dap= -.963

                                              rap= 197.046   rp 14032.

Input File: satrtn1.inp   Cumulative run time= 0.38 sec   Step= .100E-01^L

****

E. LOW ENERGY TRAJECTORY FOR A NON-WAVERIDER ROUNDTRIP MISSION TO MARS

2013 Earth-Mars Roundtrip   Mar 2, 1996   14:01:33
Epoch= 2013 3 19 0 0 0   2456370.500   Earth Ecliptic and Equinox of 2000 and
                                                 Body Equator and Equinox of Date
    Earth   Earth   Mars
Set no= 1

nt= 1.01 iter= 28 kgo= 2 flags 0 0 0 nm= 0 nmt= 2 ndl= 2 nda= 2 ndb= 2
veq= 17.2618   grad= .000000   dvt= 17.2618   dvmt= 3.2877   dvpl= 13.5618
tend= 470.000   fty= 1.2868   hca= .46 .83

jdate= 277.9   2013 12 21 22 2   dvl= 3.7000   c3= 12.0703   dla= -36.485
                                                  rla= 159.831   re 6878.0
trp= 278.3   2013 12 22 6 51   rp= .9837   xmp= -.0073
                                 ymp= .9837   zmp= -.0005
tpb= 503.0   2014 8 3 23 57   dvb= 3.2877   vhi= 5.005   vho= 7.378
                                                  bend= 39.350   rcb= 9397.0
trp= 684.6   2015 2 1 13 44   rp= .5190   xmp= .1179
                                 ymp= .5054   zmp= .0078
adate= 747.9   2015 4 5 22 2   dva= 10.2741   vhp= 14.3323   dap= -2.026
                                                  rap= 180.171   rp 6408.0

Input File: themar1.inp   Cumulative run time= 0.23 sec   Step= .100E-01^L

****

F. NON-WAVERIDER TRAJECTORY FOR A ROUNDTRIP MISSION TO MARS DEPARTING ON THE SAME DAY AS THE WAVERIDER

2011 Earth-Mars Roundtrip   Mar 2, 1996   15:43:34
Epoch= 2011 11 28 0 0 0   2455893.500 Earth Ecliptic and Equinox of 2000
                                             and Body Equator and Equinox of Date
      Earth   Earth   Mars
Set no= 1

   nt= 1.01 iter= 11 kgo= 2 flags 0 0 0 nm= 0 nmt= 1 ndl= 2 nda= 2 ndb= 2
 veq= 19.6923   grad= .000000   dvt= 19.6923   dvmt= 3.7485   dvpl= 16.0469
 tend= 460.000   fty= 1.2594   hca= .45 .82

jdate=   .0   2011 11 28 0 0   dvl= 3.6454   c3= 10.8386   dla= 19.913
                                                    rla= 133.735   re 6878.0
   tpb= 235.3   2012 7 20 7 45   dvb= 3.7485   vhi= 3.946   vho= 7.412
                                                    bend= 51.471   rcb= 6794.4
   trp= 401.7   2013 1 2 17 20   rp= .4590   xmp= .3502
                                     ymp= .2967   zmp= -.0006
   adate= 460.0   2013 3 2 0 0   dva= 12.2984   vhp= 16.8238   dap= 13.213
                                                    rap= 147.586   rp 6408.0

Input File: themar2.inp   Cumulative run time= 0.07 sec   Step= .100E-01^L

****

G. LOW ENERGY TRAJECTORY FOR A NON-WAVERIDER MISSION TO SATURN

Low Energy Trajectory for a non-Waverider Mission to Saturn   Mar 2, 1996 14:32:59

Epoch= 1992 9 23 0 0 0   2448888.500   Earth Ecliptic and Equinox of 2000

                               and Body Equator and Equinox of Date

     Earth   Saturn   Venus   Earth   Earth

nt= 1.02 iter= 15 kgo= 2 flags 0 0 0 nm=0 nmt=2 ndl=2 nda=2 ndb= -0 2 2

veq= 5.2704   grad= .000000   dvt= 5.2704 dvmt= .4318 dvpl= 1.4436

tend= 3400.00   fty= 9.3087   hca= -1.71 .74 1.35 .40

jdate=   1.4 1992 9 24 9 11   dvl= 3.8269   c3= 13.8151   dla= -20.263
                                          rla= 298.071   re 6618.1

tra= 10.9 1992 10 3 22 32   ra= 1.0059 xma= .9908
                             yma= .1736 zma= .0002

trp= 147.8 1993 2 17 18 16   rp= .6438 xmp= -.6342
                           ymp= -.1111 zmp= -.0002

tra= 284.6 1993 7 4 14 0   ra= 1.0059 xma= .9908
                           yma= .1736 zma= .0002

trp= 421.4 1993 11 18 9 44   rp= .6438 xmp= -.6342
                           ymp= -.1111 zmp= -.0002

tpb= 456.7 1993 12 23 16 55 dvb= .0000   vhi= 7.137 betb= 13.656
                                    bend= 60.135 rcb= 6352.0

tra= 700.8 1994 8 24 19 56   ra= 1.7337 xma= .6077
                           yma= 1.6237 zma= .0028

tpc= 892.6 1995 3 4 15 16 dvc= .0180   vhi= 12.519 vho= 12.530
                                    bend= 14.029 rcc= 18378.

trp= 935.4 1995 4 16 8 33   rp= .8240 xmp= -.5910
                           ymp= -.5741 zmp= .0000

tra= 1320.4 1996 5 5 10 21   ra= 2.4647 xma= 1.7678
                           yma= 1.7174 zma= .0000

trp= 1705.5 1997 5 25 12 8   rp= .8240 xmp= -.5910
                           ymp= -.5741 zmp= .0000

tpd= 1751.9 1997 7 10 21 2 dvd= .4138   vhi= 12.550 vho= 13.011
                                    bend= 32.304 rcd= 6678.1

adate= 3401.4 2002 1 15 9 11 dva= 1.0118 vhp= 6.3047 dap= 5.615
                                  rap= 10.673 rp 2.200

Input File: thesat1.inp   Cumulative run time= 0.97 sec   Step= .100E-01^L

****

H. NON-WAVERIDER TRAJECTORY TO SATURN DEPARTING ON THE SAME DAY AS THE WAVERIDER

2011 Earth-Mars-Jupiter-Saturn   Mar 2, 1996   16:02:10
Epoch= 2011 10 26 0 0 0   2455860.500   Earth Ecliptic and Equinox of 2000
                                        and Body Equator and Equinox of Date
    Earth   Saturn   Mars   Jupiter
Set no= 1

nt= 1.01 iter= 38 kgo= 2 flags 0 0 0 nm= 0 nmt= 2 ndl= 2 nda= 2 ndb= 2 2
veq= 30.9559   grad= .000000   dvt= 30.9559   dvmt= 23.5168   dvpl= 26.1542
tend= 2600.00   fty= 7.1184   hca= .49 .77 .43

jdate=   .0   2011 10 26 0 0   dvl= 4.8017   c3= 37.3575   dla= 51.464
                                             rla= 191.710   re 6618.1
trp=   21.8   2011 11 16 19 14   rp= .9751   xmp= .5355
                                            ymp= .8128   zmp= .0576
tpb= 226.9   2012 6 8 20 29   dvb= 22.8513   vhi= 6.220   vho= 18.523
                                             bend= 143.647   rcb= 6794.4
trp= 319.0   2012 9 8 23 53   rp= .6788   xmp= .4834
                              ymp= -.4765   zmp= -.0078
tpc= 1052.4   2014 9 12 10 18   dvc= .6655   vhi= 7.320   vho= 10.502
                                            bend= 134.502   rcc= 1.961
adate= 2600.0   2018 12 8 0 0   dva= 2.6374   vhp= 11.0895   dap= -25.923
                                             rap= 285.898   rp 2.200

Input File: thesat2.inp   Cumulative run time= 0.29 sec   Step= .100E-01

****

I. LOW ENERGY TRAJECTORY FOR A NON-WAVERIDER MISSION TO NEPTUNE

2003 Earth-Mars-Jupiter-Neptune   Mar 2, 1996   15:00:42

Epoch= 2003 6 15 0 0 0   2452805.500   Earth Ecliptic and Equinox of 2000

                                     and Body Equator and Equinox of Date

      Earth   Neptune   Mars   Jupiter

Set no= 1

    nt= 1.01 iter= 45 kgo=2 flags 0 0 0 nm= 0 nmt= 0 ndl=2 nda= 2 ndb= 2 2

    veq= 36.2313   grad= .000000   dvt= 36.2313   dvmt= 14.8649   dvpl= 32.3578

    tend= 3000.00   fty= 8.2136   hca= .41 .40 .30

    jdate= 25.4   2003 7 10 10 2   dvl= 3.8735   c3= 14.8974   dla= 5.115

                                             rla= 336.840   re 6618.1

    tpb= 248.0   2004 2 18 0 18   dvb= 6.9980   vhi= 3.076   vho= 6.821

                                       bend= 141.802   rcb= 6794.4

    tpc= 1006.5   2006 3 17 11 11   dvc= 7.8669   vhi= 7.209   vho= 18.847

                                       bend= 147.581   rcc= 1.961

    adate= 3025.4   2011 9 26 10 2   dva= 17.4929   vhp= 25.4607   dap= 27.513

                                       rap= 114.079   rp 2.000

Input File: thenep1.inp   Cumulative run time= 0.27 sec   Step= .100E-01^L

****

J. NON-WAVERIDER TRAJECTORY TO NEPTUNE DEPARTING ON THE SAME DAY AS THE WAVERIDER

2003 Earth-Mars-Jupiter-Neptune   Mar 2, 1996   15:25:59
Epoch= 2003 6 27 0 0 0   2452817.500   Earth Ecliptic and Equinox of 2000
                                             and Body Equator and Equinox of Date
       Earth   Neptune   Mars   Jupiter
Set no= 1

    nt= 1.01 iter= 35 kgo= 2 flags 0 0 0 nm= 0 nmt= 0 ndl=2 nda=2 ndb= 2 2
    veq= 38.0650   grad= .000000   dvt= 38.0650   dvmt= 15.8535   dvpl= 34.3278
    tend= 2922.00   fty= 8.0000   hca= .44 .40 .31

jdate=   .0   2003 6 27 0 0   dvl= 3.7371   c3= 11.7427   dla= 13.459
                                                   rla= 340.031   re 6618.1
  tpb= 230.5   2004 2 12 11 5   dvb= 7.0319   vhi= 3.089   vho= 6.977
                                                   bend= 137.712   rcb= 6794.4
  tpc= 979.0   2006 3 2 1 2   dvc= 8.8216   vhi= 7.444   vho= 19.952
                                                   bend= 147.861   rcc= 1.961
adate= 2922.0   2011 6 27 0 0   dva= 18.4743   vhp= 26.6284   dap= 27.555
                                                   rap= 113.816   rp   2.000

Input File: thenep2.inp   Cumulative run time= 0.25 sec   Step= .100E-01^L

****

```
*************************************************************************
```
There were no low energy transfers found for a mission to Saturn with a return to Earth
```
*************************************************************************
```

K. NON-WAVERIDER TRAJECTORY FOR A ROUNDTRIP MISSION TO SATURN DEPARTING ON THE SAME DAY AS THE WAVERIDER

2014 Earth-Mars-Jupiter-Saturn-Earth   Apr 2, 1996   09:30:47
Epoch= 2014 6 23 0 0 0   2456831.500   Earth Ecliptic and Equinox of 2000
                                             and Body Equator and Equinox of Date
        Earth   Earth   Mars   Jupiter   Saturn
Set no= 1

    nt= 1.01 iter= 52 kgo=2 flags 0 0 0 nm=0 nmt=3 ndl=2 nda=2 ndb= 2 2 2
    veq= 38.5878   grad= .000000   dvt= 38.5878 dvmt= 20.1997 dvpl= 33.4100
    tend= 4000.00   fty= 10.9514   hca= .46 .61 .30 .58

jdate= -100.2   2014 3 14 19 1   dvl= 5.1779   c3= 46.9496   dla= -38.997
                                                       rla= 172.855 re 6618.1
tra=   94.5   2014 9 25 12 45   ra= 1.4973   xma= .7178
                                   yma= -1.3039   zma= -.1630
tpb= 180.0   2014 12 20 0 0   dvb= 9.0807   vhi= 6.619   vho= 12.743
                                                       bend= 57.268 rcb= 6794.4
trp= 240.5   2015 2 18 12 45   rp= 1.1377   xmp= .9134
                                   ymp= .6781   zmp= -.0175
tpc= 1036.0   2017 4 24 0 45   dvc= 2.0444   vhi= 6.633   vho= 5.871
                                                       bend= 166.352 rcc= 1.961
trp= 1208.9   2017 10 13 22 42   rp= 5.3073   xmp= -4.1723
                                   ymp= -3.2784   zmp= .1078
tpd= 2462.9   2021 3 20 22 3   dvd= 9.0746   vhi= 9.112   vho= 7.949
                                                       bend= 139.048 rcd= 11.000
trp= 3869.6   2025 1 25 15 16   rp= .8413   xmp= -.2721
                                   ymp= .7960   zmp= .0112
adate= 3899.8 2025 2 24 19 1   dva= 13.2103   vhp= 16.7981 dap= -3.650
                                                       rap= 182.509 rp 14032.

Input File: thertn1.inp   Cumulative run time= 0.34 sec   Step= .100E-01^L


```
*************************************************************************
```

APPENDIX C-MATLAB PROGRAMS

A. VLOSS.M

```
%This program will figure out the altitude via the density to fly a
%Waverider at plus plot the outgoing hyperbolic excess velocity vs. L/D

clear
mcla=input('Enter the factor m/clA in kg/m^2 ');
planet=input('Enter the AGA planet: 1 for Venus, 2 for Earth, or 3 for Mars ');

%Some constants of Venus Earth and Mars
rp=[6050 6378 3410];
g=[8.73 9.8 3.69];
mu=[324850 398604 42930];

%Set initial values
rho=0;
cl=linspace(0,1,11);
ld=linspace(1.5,10,50);
vinf=input('Enter vhi from MIDAS (km/s) ');
vvv=num2str(vinf);
vho=input('Enter vho from MIDAS (km/s) ');
phideg=input('Enter the bend angle from MIDAS in degrees ');
phi=phideg*pi/180;
diff=12;

%Density values for Venus (1st column), Earth (2nd column), Mars (3rd column)
%values are from 33 km to 100 km in steps of 1 km (kg/m^3)

rhov=1e-3*[8041 7420 6831 6274 5762 5276 4823 4404 4015 3646 3303 2985 2693 ...
2426 2186 1967 1769 1594 1432 1284 1153 1032 920.7 818.3 721.2 628.9 544.8 ...
469.4 405.3 341.1 292.7 244.3 208.6 172.9 146.95 121.0 102.5 83.93 70.84 ...
57.75 48.54 39.33 32.98 26.63 22.24 17.84 14.85 11.86 9.793 7.725 6.326 ...
4.926 4.007 3.088 2.493 1.898 1.525 1.151 .9173 .6836 .5416 .3995 .3155 ...
.2314 .1831 .1347 .1068 .0789]';

rhoe=1e-6*[11573 9887.4 8463.4 7257.9 6235.5 5366.6 4626.7 3995.7 3456.4 ...
2994.8 2598.9 2258.9 1966.3 1714.1 1469.5 1316.7 1162.8 1026.9 906.9 800.97 ...
710.29 631.37 560.75 497.62 441.21 390.86 345.94 305.92 270.28 239.31 212.52 ...
188.37 166.65 147.13 129.64 113.99 100.00 87.535 76.442 66.593 57.866 50.151 ...
43.35 37.36 32.10 27.50 23.49 19.99 16.62 13.82 11.50 9.563 7.955 6.617 5.504 ...
4.579 3.810 3.170 2.598 2.137 1.763 1.459 1.211 1.008 .8415 .7044 .5911 .4974]';
```

rhom=1e-6*[719 647 582 524 471 423 379 340 304 272 243 217 194 173 154 137 122 ...
108 96.0 85.2 75.5 66.9 59.2 52.3 46.3 40.9 36.1 31.8 28.0 24.7 21.7 19.1 16.8 ...
14.8 13.0 11.4 9.97 8.73 7.65 6.70 5.85 5.12 4.47 3.91 3.42 2.99 2.62 2.29 2.0 ...
1.75 1.53 1.34 1.17 1.03 .897 .785 .687 .601 .526 .461 .403 .353 .309 .271 .237 ...
.208 .182 .159]';

%Speed of sound values for 33 km to 100 km in steps of 1 km in km/s

avenus=1e-3*[335 332 329 327 324 322 319 316 314 312 309 306 304 302 299 297 295
292 ...
288 284 281 277 273 270 267 263 260 256 254 252 251 250 249 248 246 244 243 241 ...
240 238 237 235 234 232 231 229 227 225 223 222 220 219 217 216 214 212 210 209 ...
209 210 210 211 211 212 212 212 213 213]';

aearth=zeros(68,1); % imcomplete data for now

amars=1e-3*[211 210 210 209 208 207 207 206 205 205 204 203 203 202 202 201 200
200 ...
199 199 198 197 197 196 196 195 195 194 194 194 193 193 193 192 192 192 192 192 ...
191 191 191 191 191 191 191 191 191 191 191 191 191 191 191 191 191 191 191 191 ...
191 191 191 191 191 191 191 191 191 191]';

%group values of density and speed of sound into matrices
rhoall=[rhov rhoe rhom];
aall=[avenus aearth amars];

%set initial tolerance for finding the appropriate density to fly an AGA maneuver
error=[.0001,1e-6,12e-6];

%iterate to find the density
for a=1:length(ld);
        row=0;
        while (abs(diff)>error(planet));
                diff
                row=row+1;
                h=33+row;
                r=h+rp(planet);
                guess=rhoall(row,planet);
                aspeed=aall(row,planet);
                vo=sqrt(mu(planet)/r);
                vatmos=sqrt(2*vo^2+vinf^2);
                vc=sqrt(g(planet)*r/1000);
%   check rho vs. r
                rho=(1-(vc/vatmos)^2)*2*mcla/(1000*r);
                diff=(guess-rho);

96

```
            end

        dv(a)=1-exp((-phi/ld(a))*(1+(vc/vinf)^2));
        vhout(a)=vho-dv(a);
end

%Calculate values of Mach number, dynamic pressure, altitude, etc...
Mach=vinf/aspeed;
Mch=num2str(Mach);
sound=num2str(aspeed);
hhh=num2str(h);
vinfcol=vinf*ones(1,length(ld));

%List values of L/D, delta V, vinf and vhout to the screen
sprintf=('   Cl/Cd    dv      vinf    vhout')

results=[ld',dv',vinfcol',vhout']
qinf=.5*guess*(vinf*1000)^2
english=qinf/1.4882
Mach
h

%Plot vhout vs. L/D
figure(1)
plot(ld,vhout),grid,xlabel('L/D'),ylabel('Velocity (km/s)')
title('Plot of Vhout vs. L/D for a Waverider Through an Atmosphere')
avgx=(max(ld)+min(ld))/2;
text(avgx-1,vhout(10),['Vinf= ',vvv,' km/s'])
text(avgx-1,vhout(8),['or at Mach ',Mch])
text(avgx-1,vhout(6),['Flying at an altitude of ',hhh,' km'])
text(avgx-3,vhout(4),['Where the speed of sound is ',sound,' km/s'])
text(0,vinf,['------------------Vinf = ',vvv,' km/s---------------'])
```

APPENDIX D - WAVERIDER DESIGN RESULTS

A. EARTH-MARS-EARTH MISSION

1. WAVRDR1.DAT Input

THE1.DAT

```
$CONSTANTS
  C1 = 0.798078,   ! C1 - C8: Coeff. of the waverider generating curve
  C2 = 0.183043,
  C3 = 0.518058,
  C4 = 0.137306,
  C5 = 0.020426,
  C6 = -0.000577,
  c7 = 0.00,
  c8 = 0.00,
  ESMILE = 0.0, ! Engine smile angle, rad. (measured from cone axis)
  ZR1 = 0.35,    ! 1st ramp location, body length
  RMP1 = 0.0,    ! 1st ramp angle, deg.
  ZR2 = 0.45,    ! 2nd ramp location, body length
  RMP2 = 0.0,    ! 2nd ramp angle
  ZSHDR = 0.62,   ! shoulder (combustor entrance) location, body length
  ZC1 = 0.58,    ! cowl lip location, body length
  XLCOWL = 0.0,  ! cowl length, body length
  DELNOZ = 0.0, ! nozzle expansion angle, deg.
  XNZEND = 0.00,   ! nozzle end point, body length
$END
$indat
  m1 = 19.2266,       ! Free stream Mach no.
  gama = 1.31,       ! specific heat ratio
  thesdg = 7.0478,    ! conical shock angle, deg.
  lb =263.,        ! veh. length, ft
  hthrin = 5.,      ! combustor throat height, in
  lcmbft = 4.      ! combustor length, ft
  repft = 20283.31, ! Reynold no./ft
  ibltyp = 1,       ! boundary layer flag
  slice = 'ARC',     ! grid type
  alpha = 2.0,      ! used only when grid type slice="POW"
  ncut = 22,        ! number of grid lines
  mcut = 1,         ! additional grid lines near the tip
  qinf = 992.9046,     ! free stream dynamic pressure, psf
  vehden = 9.0,     ! vehicle density, lp/ft^3
  rlein = 0.8878
  iair = 2              !iair=1 Earth's atmos.; iar=2 Mars' atmos
```

```
$end
$PARABOLADAT
  ZFAIR2 = 1.0
  INITANG = 15.
  LINEAR = .F.
  XCLOSE = 0.0
$END
$COCKPITDAT
  THETASC = 15        ··
$END
```

2. FLWFLD.SUM Results

THE1.SUM

ESMILE = 0.00000

VOL	SPLAN	WS	ALT	WEIGHT	CMBWID	AC0	A_thr
154889.22	17523.62	79.55	42165.43	1394003.00	0.0000	0.0000	0.0000

THRUST	DRAG	LIFT	WALT	TIPANG	TLERAD	LELIFT	LEDRAG
0.00	65277.31	407348.88	-652957.31	8.39	4517.52	1836.52	1783.45

C1-C8: 0.798078 0.183043 0.518058 0.137306 0.020426-0.000577 0.000000 0.000000

ZR1	RMP1	ZR2	RMP2	ZSHDR	ZC1	LC	NZANGL
0.35000	0.00000	0.45000	0.00000	0.62000	0.58000	0.32000	0.00000

QINF	ESMILE	RLE	VEH.DEN	SHCK ANGL	NOSE ANGL	L/D_AERO
992.9	0.0000	0.8878	9.0000	7.0478	5.1228	6.2403

L/D	VOLFTR	TIPDEG	PENLTY	S/L	TLERAD
6.38694	0.00851	8.38663	0.00000	0.41318	4517.52

L/D_t	XCWLSH	Eff.Isp	OBJCRU	RLE
6.2403	0.0000	0.0000	6.2403	0.8878

B. EARTH-MARS-JUPITER-SATURN MISSION

1. WAVRDR1.DAT Input

THE2.DAT

```
$CONSTANTS
   C1 = 0.818714,   ! C1 - C8: Coeff. of the waverider generating curve
   C2 = 0.343838,
   C3 = 0.464864,
   C4 = 0.070586,
   C5 = -0.023052,
   C6 = -0.000257,
   c7 = 0.00,
   c8 = 0.00,
   ESMILE = 0.0, ! Engine smile angle, rad. (measured from cone axis)
   ZR1 = 0.35,    ! 1st ramp location, body length
   RMP1 = 0.0,    ! 1st ramp angle, deg.
   ZR2 = 0.45,    ! 2nd ramp location, body length
   RMP2 = 0.0,    ! 2nd ramp angle
   ZSHDR = 0.62,   ! shoulder (combustor entrance) location, body length
   ZC1 = 0.58,    ! cowl lip location, body length
   XLCOWL = 0.0,  ! cowl length, body length
   DELNOZ = 0.0, ! nozzle expansion angle, deg.
   XNZEND = 0.0,   ! nozzle end point, body length
$END
$indat
   m1 = 21.8916,          ! Free stream Mach no.
   gama = 1.31,        ! specific heat ratio
   thesdg = 7.5587,     ! conical shock angle, deg.
   lb =263.,        ! veh. length, ft
   hthrin = 5.,      ! combustor throat height, in
   lcmbft = 4.       ! combustor length, ft
   repft = 23094.26,  ! Reynold no./ft
   ibltyp = 1,       ! boundary layer flag
   slice = 'ARC',     ! grid type
   alpha = 2.0,      ! used only when grid type slice="POW"
   ncut = 22,        ! number of grid lines
   mcut = 1,         ! additional grid lines near the tip
   qinf = 1287.2,    ! free stream dynamic pressure, psf
   vehden = 9.0,     ! vehicle density, lp/ft^3
   rlein = 1.0305
   iair = 2                 !iair=1 Earth's atmos.; iar=2 Mars' atmos
$end
$PARABOLADAT
```

```
    ZFAIR2 = 1.0
    INITANG = 15.
    LINEAR = .F.
    XCLOSE = 0.0
$END
$COCKPITDAT
    THETASC = 15
$END
```

2. FLWFLD.SUM Results

THE2.SUM

ESMILE = 0.00000

VOL	SPLAN	WS	ALT	WEIGHT	CMBWID	AC0	A_thr
155140.34	16041.89	87.04	42166.30	1396263.13	0.0000	0.0000	0.0000

THRUST	DRAG	LIFT	WALT	TIPANG	TLERAD	LELIFT	LEDRAG
0.00	100381.08	588663.81	*	13.67	4518.36	3255.39	2098.65

C1-C8: 0.818714 0.343838 0.464864 0.070586-0.023052-0.000257 0.000000 0.000000

ZR1	RMP1	ZR2	RMP2	ZSHDR	ZC1	LC	NZANGL
0.35000	0.00000	0.45000	0.00000	0.62000	0.58000	0.32000	0.00000

QINF	ESMILE	RLE	VEH.DEN	SHCK ANGL	NOSE ANGL	L/D_AERO
1287.2	0.0000	1.0305	9.0000	7.5587	5.8574	5.8643

L/D	VOLFTR	TIPDEG	PENLTY	S/L	TLERAD
5.95664	0.00853	13.67131	0.00000	0.40146	4518.36

L/D_t	XCWLSH	Eff.Isp	OBJCRU	RLE
5.8643	0.0000	0.0000	5.8643	1.0305

C. EARTH-MARS-JUPITER-NEPTUNE MISSION

1. WAVRDR1.DAT Input

THE3.DAT

```
$CONSTANTS
  C1 = 0.892159,   ! C1 - C8: Coeff. of the waverider generating curve
  C2 = 0.499986,
  C3 = 0.0,
  C4 = -0.143161,
  C5 = -0.135785,
  C6 = -0.033579,
  c7 = 0.00,
  c8 = 0.00,
  ESMILE = 0.0, ! Engine smile angle, rad. (measured from cone axis)
  ZR1 = 0.35,    ! 1st ramp location, body length
  RMP1 = 0.0,    ! 1st ramp angle, deg.
  ZR2 = 0.45,    ! 2nd ramp location, body length
  RMP2 = 0.0,    ! 2nd ramp angle
  ZSHDR = 0.62,  ! shoulder (combustor entrance) location, body length
  ZC1 = 0.0,     ! cowl lip location, body length
  XLCOWL = 0.0,  ! cowl length, body length
  DELNOZ = 0.0,  ! nozzle expansion angle, deg.
  XNZEND = 0.0,    ! nozzle end point, body length
$END
$indat
  m1 = 24.5961,        ! Free stream Mach no.
  gama = 1.31,      ! specific heat ratio
  thesdg = 7.6055,    ! conical shock angle, deg.
  lb =263.,        ! veh. length, ft
  hthrin = 5.,      ! combustor throat height, in
  lcmbft = 4.      ! combustor length, ft
  repft = 25947.5, ! Reynold no./ft
  ibltyp = 1,      ! boundary layer flag
  slice = 'ARC',   ! grid type
  alpha = 2.0,     ! used only when grid type slice="POW"
  ncut = 22,       ! number of grid lines
  mcut = 1,        ! additional grid lines near the tip
  qinf = 1624.9,    ! free stream dynamic pressure, psf
  vehden = 9.0,    ! vehicle density, lp/ft^3
  rlein = 1.2
  iair = 2                !iair=1 Earth's atmos.; iar=2 Mars' atmos
$end
$PARABOLADAT
```

```
  ZFAIR2 = 1.0
  INITANG = 15.
  LINEAR = .F.
  XCLOSE = 0.00
$END
$COCKPITDAT
  THETASC = 15
$END
```

2. FLWFLD.SUM Results

THE3.SUM

```
ESMILE =  0.00000
    VOL    SPLAN    WS    ALT        WEIGHT   CMBWID    AC0    A_thr
152294.23 16331.72  83.93 42166.06  1370648.13  0.0000  0.0000  0.0000
  THRUST   DRAG    LIFT   WALT  TIPANG  TLERAD  LELIFT  LEDRAG
   0.00   133830.98 781773.75  *     20.84   4575.17  5760.75  3736.96

C1-C8: 0.892159 0.499986 0.000000-0.143161-0.135785-0.033579 0.000000 0.000000
   ZR1    RMP1    ZR2    RMP2   ZSHDR   ZC1    LC    NZANGL
 0.35000  0.00000  0.45000  0.00000  0.62000   0.58000  0.32000  0.00000
  QINF   ESMILE   RLE   VEH.DEN  SHCK ANGL  NOSE ANGL  L/D_AERO
 1624.9  0.0000   1.2000   9.0000    7.6055     6.0377     5.8415
   L/D   VOLFTR   TIPDEG   PENLTY    S/L    TLERAD
 5.96538  0.00837  20.83794  0.00000  0.45842  4575.17
   L/D_t   XCWLSH   Eff.Isp   OBJCRU   RLE
 5.8415   0.0000   0.0000   5.8415   1.2000
```

D. EARTH-MARS-JUPITER-SATURN-EARTH MISSION

1. WAVRDR1.DAT Input

THE4.DAT

```
$CONSTANTS
  C1 = 0.660501,   ! C1 - C8: Coeff. of the waverider generating curve
  C2 = 0.217144,
  C3 = 0.508518,
  C4 = 0.107411,
  C5 = 0.005622,
  C6 = 0.000784,
  c7 = 0.00,
  c8 = 0.00,
  ESMILE = 0.0, ! Engine smile angle, rad. (measured from cone axis)
  ZR1 = 0.35,    ! 1st ramp location, body length
  RMP1 = 0.0,    ! 1st ramp angle, deg.
  ZR2 = 0.45,    ! 2nd ramp location, body length
  RMP2 = 0.0,    ! 2nd ramp angle
  ZSHDR = 0.62,   ! shoulder (combustor entrance) location, body length
  ZC1 = 0.0,     ! cowl lip location, body length
  XLCOWL = 0.0,  ! cowl length, body length
  DELNOZ = 0.0, ! nozzle expansion angle, deg.
  XNZEND = 0.0,    ! nozzle end point, body length
$END
$indat
  m1 = 25.8374,        ! Free stream Mach no.
  gama = 1.31,       ! specific heat ratio
  thesdg = 7.7,    ! conical shock angle, deg.
  lb =263.,         ! veh. length, ft
  hthrin = 5.,      ! combustor throat height, in
  lcmbft = 4.      ! combustor length, ft
  repft = 29985.80, ! Reynold no./ft
  ibltyp = 1,        ! boundary layer flag
  slice = 'ARC',     ! grid type
  alpha = 2.0,      ! used only when grid type slice="POW"
  ncut = 22,        ! number of grid lines
  mcut = 1,          ! additional grid lines near the tip
  qinf = 2005.7,     ! free stream dynamic pressure, psf
  vehden = 9.0,     ! vehicle density, lp/ft^3
  rlein  = 1.2
  iair = 2                !iair=1 Earth's atmos.; iar=2 Mars' atmos
$end
$PARABOLADAT
```

```
    ZFAIR2 = 1.0
    INITANG = 15.
    LINEAR = .F.
    XCLOSE = 0.00
$END
$COCKPITDAT
    THETASC = 15
$END
```

2. FLWFLD.SUM Results

THE4.SUM

VOL	SPLAN	WS	ALT	WEIGHT	CMBWID	AC0	A_thr
159717.73	14646.36	98.14	38374.71	1437459.63	0.0000	0.0000	0.0000
THRUST	DRAG	LIFT	WALT	TIPANG	TLERAD	LELIFT	LEDRAG
0.00	154905.42	913216.50	*	10.79	5625.55	4626.72	3279.61

C1-C8: 0.660501 0.217144 0.508518 0.107411 0.005622 0.000784 0.000000 0.000000

ZR1	RMP1	ZR2	RMP2	ZSHDR	ZC1	LC	NZANGL
0.35000	0.00000	0.45000	0.00000	0.62000	0.58000	0.32000	0.00000

QINF	ESMILE	RLE	VEH.DEN	SHCK ANGL	NOSE ANGL	L/D_AERO
2005.7	0.0000	1.2000	9.0000	7.7000	6.2549	5.8953

L/D	VOLFTR	TIPDEG	PENLTY	S/L	TLERAD
5.99241	0.00878	10.78951	0.00000	0.34575	5625.55

L/D_t	XCWLSH	Eff.Isp	OBJCRU	RLE
5.8953	0.0000	0.0000	5.8953	1.2000

APPENDIX E-AEROSA RESULTS

A. EARTH-MARS-EARTH WAVERIDER MISSION

1. Angle of Attack Analysis

AOA Degree	MINF	TINF R	PINF psf	CL	CDP	CDF	CDTOT	L/D	CM	Tupr R	Tlow R
-10.00	19.23	280.80	0.11	-0.06730	0.01160	0.00191	0.01352	-4.98340	-0.00765	924.56	565.24
-9.00	19.23	280.80	0.11	-0.05601	0.00861	0.00177	0.01039	-5.39862	-0.00634	904.74	565.24
-8.00	19.23	280.80	0.11	-0.04580	0.00618	0.00164	0.00782	-5.86333	-0.00517	887.23	565.24
-7.00	19.23	280.80	0.11	-0.03613	0.00423	0.00157	0.00581	-6.22336	-0.00407	878.01	600.24
-6.00	19.23	280.80	0.11	-0.02717	0.00274	0.00155	0.00429	-6.31938	-0.00305	847.56	635.90
-5.00	19.23	280.80	0.11	-0.01884	0.00167	0.00152	0.00319	-5.85301	-0.00210	819.06	677.86
-4.00	19.23	280.80	0.11	-0.01095	0.00097	0.00150	0.00248	-4.26290	-0.00121	801.16	732.71
-3.00	19.23	280.80	0.11	-0.00321	0.00065	0.00150	0.00214	-1.22540	-0.00034	766.57	755.63
-2.00	19.23	280.80	0.11	0.00451	0.00068	0.00149	0.00217	2.38140	0.00054	741.94	781.35
-1.00	19.23	280.80	0.11	0.01267	0.00107	0.00148	0.00255	5.20288	0.00146	698.67	812.16
0.00	19.23	280.80	0.11	0.02053	0.00185	0.00151	0.00335	6.26878	0.00236	666.36	831.31
1.00	19.23	280.80	0.11	0.02930	0.00303	0.00151	0.00454	6.53001	0.00337	628.44	857.88
2.00	19.23	280.80	0.11	0.03878	0.00464	0.00154	0.00618	6.30654	0.00448	588.48	882.52
3.00	19.23	280.80	0.11	0.04901	0.00674	0.00160	0.00834	5.88313	0.00567	564.69	895.08
4.00	19.23	280.80	0.11	0.05984	0.00936	0.00171	0.01107	5.40316	0.00696	564.69	914.64
5.00	19.23	280.80	0.11	0.07178	0.01257	0.00183	0.01439	4.97889	0.00839	564.69	934.91
6.00	19.23	280.80	0.11	0.08480	0.01643	0.00196	0.01839	4.59825	0.00996	564.69	953.85
7.00	19.23	280.80	0.11	0.09879	0.02098	0.00211	0.02308	4.26617	0.01166	564.69	969.96
8.00	19.23	280.80	0.11	0.11391	0.02632	0.00224	0.02855	3.97733	0.01351	564.69	983.05
9.00	19.23	280.80	0.11	0.13000	0.03247	0.00237	0.03484	3.72098	0.01550	564.69	999.63

2. Altitude Analysis

AOA Degree	MINF	TINF R	PINF psf	CL	CDP	CDF	CDTOT	L/D	CM	Tupr R	Tlow R
0.00	24.60	301.50	0.35	0.02104	0.00222	0.00109	0.00331	6.32796	0.00201	942.29	1207.87
0.00	24.60	299.00	0.31	0.02103	0.00222	0.00108	0.00330	6.34793	0.00201	925.59	1187.66
0.00	24.60	296.60	0.28	0.02103	0.00222	0.00108	0.00330	6.35749	0.00201	909.77	1169.18
0.00	24.60	294.50	0.25	0.02103	0.00222	0.00108	0.00330	6.36646	0.00201	894.74	1151.67
0.00	24.60	292.30	0.22	0.02103	0.00222	0.00109	0.00331	6.37586	0.00201	878.69	1133.34
0.00	24.60	290.20	0.20	0.02103	0.00222	0.00111	0.00332	6.35940	0.00201	861.39	1114.27
0.00	24.60	288.00	0.17	0.02103	0.00222	0.00114	0.00336	6.32960	0.00201	844.49	1096.40
0.00	24.60	286.20	0.15	0.02103	0.00222	0.00119	0.00340	6.26532	0.00201	827.74	1083.16
0.00	24.60	284.40	0.14	0.02103	0.00222	0.00124	0.00346	6.18495	0.00201	824.32	1065.93
0.00	24.60	282.60	0.12	0.02103	0.00222	0.00131	0.00353	6.07934	0.00201	810.94	1048.45
0.00	24.60	280.80	0.11	0.02103	0.00222	0.00139	0.00360	5.96251	0.00201	798.23	1031.33
0.00	24.60	279.00	0.10	0.02103	0.00222	0.00147	0.00369	5.83281	0.00201	786.42	1014.48
0.00	24.60	277.40	0.08	0.02103	0.00222	0.00156	0.00378	5.69545	0.00201	775.39	997.71
0.00	24.60	275.60	0.07	0.02103	0.00222	0.00166	0.00388	5.55660	0.00201	766.11	981.02
0.00	24.60	274.00	0.07	0.02104	0.00222	0.00176	0.00398	5.41880	0.00201	740.58	965.03
0.00	24.60	272.20	0.06	0.02103	0.00222	0.00188	0.00410	5.27491	0.00201	725.49	948.54
0.00	24.60	270.50	0.05	0.02103	0.00222	0.00200	0.00422	5.12854	0.00201	708.81	932.28
0.00	24.60	269.10	0.05	0.02104	0.00222	0.00213	0.00434	4.98224	0.00201	691.02	916.65
0.00	24.60	267.70	0.04	0.02103	0.00222	0.00227	0.00448	4.83136	0.00201	688.29	900.88
0.00	24.60	266.20	0.03	0.02103	0.00222	0.00241	0.00463	4.68225	0.00201	671.24	885.48

3. Mach Number Analysis

AOA Degree	MINF	TINF R	PINF psf	CL	CDP	CDF	CDTOT	L/D	CM	Tupr R	Tlow R
0.00	15.00	280.80	0.11	0.02244	0.00201	0.00167	0.00369	6.23459	0.00258	618.80	688.92
0.00	15.50	280.80	0.11	0.02214	0.00199	0.00165	0.00364	6.23724	0.00255	612.80	703.17
0.00	16.00	280.80	0.11	0.02187	0.00196	0.00162	0.00359	6.24082	0.00252	638.03	732.07
0.00	16.50	280.80	0.11	0.02162	0.00194	0.00160	0.00355	6.24502	0.00249	630.24	747.78
0.00	17.00	280.80	0.11	0.02139	0.00192	0.00158	0.00351	6.24955	0.00246	621.60	763.34
0.00	17.50	280.80	0.11	0.02118	0.00190	0.00156	0.00347	6.25448	0.00244	651.96	778.77
0.00	18.00	280.80	0.11	0.02098	0.00189	0.00154	0.00343	6.25938	0.00241	669.71	794.10
0.00	18.50	280.80	0.11	0.02079	0.00187	0.00153	0.00340	6.26429	0.00239	661.19	809.30
0.00	19.00	280.80	0.11	0.02061	0.00185	0.00151	0.00337	6.26618	0.00237	665.79	824.40
0.00	19.50	280.80	0.11	0.02045	0.00184	0.00150	0.00334	6.27197	0.00235	685.46	839.39
0.00	20.00	280.80	0.11	0.02030	0.00183	0.00148	0.00331	6.27881	0.00233	691.10	854.77
0.00	20.50	280.80	0.11	0.02016	0.00181	0.00147	0.00328	6.28762	0.00232	690.65	871.14
0.00	21.00	280.80	0.11	0.02003	0.00180	0.00145	0.00325	6.29869	0.00230	728.16	887.43
0.00	21.50	280.80	0.11	0.01990	0.00179	0.00144	0.00323	6.31053	0.00229	721.33	903.44
0.00	22.00	280.80	0.11	0.01979	0.00178	0.00142	0.00320	6.32214	0.00227	725.97	919.16
0.00	22.50	280.80	0.11	0.01968	0.00177	0.00141	0.00318	6.33366	0.00226	739.89	934.83
0.00	23.00	280.80	0.11	0.01957	0.00176	0.00139	0.00316	6.34432	0.00225	546.05	950.44
0.00	23.50	280.80	0.11	0.01948	0.00175	0.00138	0.00313	6.35536	0.00224	772.08	965.99
0.00	24.00	280.80	0.11	0.01938	0.00174	0.00137	0.00311	6.36496	0.00223	769.31	988.40
0.00	24.50	280.80	0.11	0.01930	0.00174	0.00136	0.00309	6.37496	0.00221	789.61	1003.89

B. EARTH-MARS-JUPITER-SATURN WAVERIDER MISSION

1. Angle of Attack Analysis

AOA Degree	MINF	TINF R	PINF psf	CL	CDP	CDF	CDTOT	L/D	CM	Tupr R	Tlow R
-10.00	21.89	280.80	0.11	-0.05225	0.00899	0.00174	0.01073	-4.87531	-0.00557	994.48	618.29
-9.00	21.89	280.80	0.11	-0.04324	0.00663	0.00162	0.00825	-5.24919	-0.00459	976.04	618.29
-8.00	21.89	280.80	0.11	-0.03480	0.00468	0.00151	0.00619	-5.63098	-0.00369	963.38	627.05
-7.00	21.89	280.80	0.11	-0.02651	0.00312	0.00147	0.00459	-5.76906	-0.00281	933.48	678.59
-6.00	21.89	280.80	0.11	-0.01906	0.00198	0.00145	0.00344	-5.50990	-0.00201	913.53	730.08
-5.00	21.89	280.80	0.11	-0.01310	0.00119	0.00137	0.00255	-5.06197	-0.00138	887.58	744.05
-4.00	21.89	280.80	0.11	-0.00773	0.00068	0.00130	0.00199	-3.72908	-0.00083	858.46	766.00
-3.00	21.89	280.80	0.11	-0.00003	0.00052	0.00133	0.00185	0.25297	-0.00003	831.35	832.67
-2.00	21.89	280.80	0.11	0.00773	0.00067	0.00126	0.00193	4.24724	0.00077	764.31	863.53
-1.00	21.89	280.80	0.11	0.01343	0.00119	0.00132	0.00251	5.54042	0.00134	745.51	889.48
0.00	21.89	280.80	0.11	0.01959	0.00201	0.00139	0.00340	5.88874	0.00197	729.62	913.96
1.00	21.89	280.80	0.11	0.02783	0.00322	0.00140	0.00462	6.08714	0.00281	683.70	944.63
2.00	21.89	280.80	0.11	0.03675	0.00486	0.00142	0.00629	5.86710	0.00373	635.08	967.18
3.00	21.89	280.80	0.11	0.04590	0.00691	0.00148	0.00840	5.47158	0.00467	617.89	987.25
4.00	21.89	280.80	0.11	0.05558	0.00942	0.00158	0.01100	5.04967	0.00568	617.89	1008.92
5.00	21.89	280.80	0.11	0.06732	0.01267	0.00172	0.01439	4.66816	0.00676	617.89	1030.27
6.00	21.89	280.80	0.11	0.08140	0.01684	0.00185	0.01870	4.34035	0.00839	617.89	1052.34
7.00	21.89	280.80	0.11	0.09460	0.02134	0.00197	0.02331	4.04604	0.00979	617.89	1066.14
8.00	21.89	280.80	0.11	0.10872	0.02657	0.00210	0.02866	3.78163	0.01130	617.89	1087.65
9.00	21.89	280.80	0.11	0.12331	0.03245	0.00221	0.03467	3.54662	0.01296	617.89	1103.54

2. Altitude Analysis

AOA Degree	MINF	TINF R	PINF psf	CL	CDP	CDF	CDTOT	L/D	CM	Tupr R	Tlow R
0.00	21.89	301.50	0.35	0.01959	0.00201	0.00106	0.00307	6.36327	0.00197	866.35	1082.94
0.00	21.89	299.00	0.31	0.01959	0.00201	0.00105	0.00306	6.38974	0.00197	861.07	1065.04
0.00	21.89	296.60	0.28	0.01959	0.00201	0.00105	0.00306	6.39901	0.00197	836.75	1048.50
0.00	21.89	294.50	0.25	0.01959	0.00201	0.00105	0.00306	6.40938	0.00197	827.96	1032.80
0.00	21.89	292.30	0.22	0.01959	0.00201	0.00106	0.00307	6.40602	0.00197	811.39	1020.94
0.00	21.89	290.20	0.20	0.01959	0.00201	0.00109	0.00310	6.37914	0.00197	813.11	1002.16
0.00	21.89	288.00	0.17	0.01959	0.00201	0.00113	0.00313	6.32872	0.00197	792.79	984.98
0.00	21.89	286.20	0.15	0.01959	0.00201	0.00118	0.00319	6.24162	0.00197	776.64	967.83
0.00	21.89	284.40	0.14	0.01959	0.00201	0.00124	0.00325	6.14356	0.00197	747.54	951.81
0.00	21.89	282.60	0.12	0.01959	0.00201	0.00131	0.00332	6.01453	0.00197	739.22	927.30
0.00	21.89	280.80	0.11	0.01959	0.00201	0.00139	0.00340	5.88874	0.00197	729.62	913.96
0.00	21.89	279.00	0.10	0.01959	0.00201	0.00148	0.00349	5.74874	0.00197	719.18	900.37
0.00	21.89	277.40	0.08	0.01959	0.00201	0.00157	0.00358	5.60340	0.00197	692.26	886.50
0.00	21.89	275.60	0.07	0.01959	0.00201	0.00167	0.00368	5.45691	0.00197	684.36	872.27
0.00	21.89	274.00	0.07	0.01959	0.00201	0.00178	0.00378	5.31199	0.00197	675.66	858.52
0.00	21.89	272.20	0.06	0.01959	0.00201	0.00189	0.00390	5.16121	0.00197	666.23	844.20
0.00	21.89	270.50	0.05	0.01959	0.00201	0.00201	0.00402	5.00864	0.00197	656.26	821.77
0.00	21.89	269.10	0.05	0.01959	0.00201	0.00214	0.00415	4.85684	0.00197	646.12	809.95
0.00	21.89	267.70	0.04	0.01959	0.00201	0.00228	0.00429	4.70103	0.00197	635.66	797.60
0.00	21.89	266.20	0.03	0.01959	0.00201	0.00243	0.00444	4.54792	0.00197	650.56	785.11

3. Mach Number Analysis

AOA Degree	MINF	TINF R	PINF psf	CL	CDP	CDF	CDTOT	L/D	CM	Tupr R	Tlow R
0.00	17.00	280.80	0.11	0.02060	0.00211	0.00154	0.00365	5.77555	0.00208	621.60	759.99
0.00	17.50	280.80	0.11	0.02040	0.00209	0.00152	0.00361	5.78099	0.00206	651.97	775.11
0.00	18.00	280.80	0.11	0.02018	0.00207	0.00150	0.00357	5.78350	0.00203	669.72	789.96
0.00	18.50	280.80	0.11	0.01994	0.00204	0.00149	0.00353	5.78328	0.00201	661.20	804.53
0.00	19.00	280.80	0.11	0.01968	0.00202	0.00147	0.00349	5.77713	0.00198	665.79	818.81
0.00	19.50	280.80	0.11	0.01942	0.00199	0.00145	0.00344	5.77281	0.00196	685.46	832.78
0.00	20.00	280.80	0.11	0.01915	0.00196	0.00144	0.00340	5.76584	0.00193	691.11	857.96
0.00	20.50	280.80	0.11	0.01928	0.00198	0.00143	0.00340	5.79756	0.00194	690.65	863.15
0.00	21.00	280.80	0.11	0.01940	0.00199	0.00142	0.00340	5.82986	0.00195	728.16	881.79
0.00	21.50	280.80	0.11	0.01951	0.00200	0.00140	0.00340	5.86364	0.00197	721.33	900.18
0.00	22.00	280.80	0.11	0.01961	0.00201	0.00139	0.00340	5.89564	0.00198	725.97	917.76
0.00	22.50	280.80	0.11	0.01970	0.00202	0.00138	0.00340	5.92546	0.00198	739.89	934.92
0.00	23.00	280.80	0.11	0.01978	0.00203	0.00137	0.00339	5.95316	0.00199	545.87	951.95
0.00	23.50	280.80	0.11	0.01986	0.00204	0.00136	0.00339	5.97891	0.00200	772.09	968.79
0.00	24.00	280.80	0.11	0.01993	0.00204	0.00135	0.00339	6.00325	0.00201	769.32	991.13
0.00	24.50	280.80	0.11	0.01999	0.00205	0.00134	0.00338	6.02519	0.00201	789.61	1010.35
0.00	25.00	280.80	0.11	0.02004	0.00205	0.00133	0.00338	6.04607	0.00202	789.02	1026.13
0.00	25.50	280.80	0.11	0.02009	0.00206	0.00132	0.00338	6.06490	0.00202	793.75	1036.10
0.00	26.00	280.80	0.11	0.02013	0.00206	0.00131	0.00337	6.08247	0.00203	808.59	1051.31
0.00	26.50	280.80	0.11	0.02018	0.00207	0.00130	0.00337	6.09815	0.00203	819.26	1066.34

C. EARTH-MARS-JUPITER-NEPTUNE WAVERIDER MISSION

1. Angle of Attack Analysis

AOA Degree	MINF	TINF R	PINF psf	CL	CDP	CDF	CDTOT	L/D	CM	Tupr R	Tlow R
-10.00	24.60	280.80	0.11	-0.05089	0.00881	0.00170	0.01051	-4.84694	-0.00446	1092.47	662.37
-9.00	24.60	280.80	0.11	-0.04214	0.00651	0.00159	0.00809	-5.21058	-0.00369	1074.21	662.37
-8.00	24.60	280.80	0.11	-0.03396	0.00461	0.00149	0.00609	-5.57895	-0.00296	1050.02	670.14
-7.00	24.60	280.80	0.11	-0.02599	0.00309	0.00144	0.00453	-5.72427	-0.00226	1034.14	747.23
-6.00	24.60	280.80	0.11	-0.01886	0.00199	0.00142	0.00341	-5.49115	-0.00163	1006.98	795.96
-5.00	24.60	280.80	0.11	-0.01311	0.00120	0.00135	0.00255	-5.05845	-0.00113	976.86	827.13
-4.00	24.60	280.80	0.11	-0.00644	0.00067	0.00130	0.00197	-3.06912	-0.00056	939.72	883.26
-3.00	24.60	280.80	0.11	0.00059	0.00056	0.00135	0.00191	0.59699	0.00010	903.51	921.35
-2.00	24.60	280.80	0.11	0.00825	0.00072	0.00125	0.00197	4.43680	0.00080	841.89	961.77
-1.00	24.60	280.80	0.11	0.01476	0.00134	0.00132	0.00266	5.72595	0.00141	813.96	999.27
0.00	24.60	280.80	0.11	0.02103	0.00222	0.00139	0.00360	5.96251	0.00201	798.23	1031.33
1.00	24.60	280.80	0.11	0.02932	0.00350	0.00141	0.00492	6.02659	0.00280	746.36	1050.30
2.00	24.60	280.80	0.11	0.03824	0.00521	0.00143	0.00664	5.78195	0.00367	675.13	1077.94
3.00	24.60	280.80	0.11	0.04736	0.00732	0.00151	0.00884	5.36815	0.00456	659.67	1099.10
4.00	24.60	280.80	0.11	0.05719	0.00991	0.00161	0.01152	4.96204	0.00552	659.67	1125.49
5.00	24.60	280.80	0.11	0.06784	0.01301	0.00171	0.01473	4.59858	0.00658	659.67	1146.49
6.00	24.60	280.80	0.11	0.08139	0.01713	0.00184	0.01897	4.28034	0.00792	659.67	1167.24
7.00	24.60	280.80	0.11	0.09448	0.02164	0.00196	0.02360	3.99294	0.00923	659.67	1191.21
8.00	24.60	280.80	0.11	0.10840	0.02686	0.00206	0.02892	3.73970	0.01064	659.67	1208.05
9.00	24.60	280.80	0.11	0.12308	0.03282	0.00216	0.03498	3.51018	0.01215	659.67	1232.81

2. Altitude Analysis

AOA Degree	MINF	TINF R	PINF psf	CL	CDP	CDF	CDTOT	L/D	CM	Tupr R	Tlow R
0.00	24.60	301.50	0.35	0.02104	0.00222	0.00109	0.00331	6.32796	0.00201	942.29	1207.87
0.00	24.60	299.00	0.31	0.02103	0.00222	0.00108	0.00330	6.34793	0.00201	925.59	1187.66
0.00	24.60	296.60	0.28	0.02103	0.00222	0.00108	0.00330	6.35749	0.00201	909.77	1169.18
0.00	24.60	294.50	0.25	0.02103	0.00222	0.00108	0.00330	6.36646	0.00201	894.74	1151.67
0.00	24.60	292.30	0.22	0.02103	0.00222	0.00109	0.00331	6.37586	0.00201	878.69	1133.34
0.00	24.60	290.20	0.20	0.02103	0.00222	0.00111	0.00332	6.35940	0.00201	861.39	1114.27
0.00	24.60	288.00	0.17	0.02103	0.00222	0.00114	0.00336	6.32960	0.00201	844.49	1096.40
0.00	24.60	286.20	0.15	0.02103	0.00222	0.00119	0.00340	6.26532	0.00201	827.74	1083.16
0.00	24.60	284.40	0.14	0.02103	0.00222	0.00124	0.00346	6.18495	0.00201	824.32	1065.93
0.00	24.60	282.60	0.12	0.02103	0.00222	0.00131	0.00353	6.07934	0.00201	810.94	1048.45
0.00	24.60	280.80	0.11	0.02103	0.00222	0.00139	0.00360	5.96251	0.00201	798.23	1031.33
0.00	24.60	279.00	0.10	0.02103	0.00222	0.00147	0.00369	5.83281	0.00201	786.42	1014.48
0.00	24.60	277.40	0.08	0.02103	0.00222	0.00156	0.00378	5.69545	0.00201	775.39	997.71
0.00	24.60	275.60	0.07	0.02103	0.00222	0.00166	0.00388	5.55660	0.00201	766.11	981.02
0.00	24.60	274.00	0.07	0.02104	0.00222	0.00176	0.00398	5.41880	0.00201	740.58	965.03
0.00	24.60	272.20	0.06	0.02103	0.00222	0.00188	0.00410	5.27491	0.00201	725.49	948.54
0.00	24.60	270.50	0.05	0.02103	0.00222	0.00200	0.00422	5.12854	0.00201	708.81	932.28
0.00	24.60	269.10	0.05	0.02104	0.00222	0.00213	0.00434	4.98224	0.00201	691.02	916.65
0.00	24.60	267.70	0.04	0.02103	0.00222	0.00227	0.00448	4.83136	0.00201	688.29	900.88
0.00	24.60	266.20	0.03	0.02103	0.00222	0.00241	0.00463	4.68225	0.00201	671.24	885.48

3. Mach Number Analysis

AOA Degree	MINF	TINF R	PINF psf	CL	CDP	CDF	CDTOT	L/D	CM	Tupr R	Tlow R
0.00	20.00	280.80	0.11	0.02018	0.00213	0.00149	0.00362	5.70925	0.00193	699.27	873.42
0.00	20.50	280.80	0.11	0.02032	0.00214	0.00148	0.00363	5.74121	0.00194	699.05	890.14
0.00	21.00	280.80	0.11	0.02044	0.00216	0.00147	0.00362	5.77537	0.00196	736.54	899.08
0.00	21.50	280.80	0.11	0.02055	0.00217	0.00145	0.00362	5.80751	0.00197	729.88	917.45
0.00	22.00	280.80	0.11	0.02065	0.00218	0.00144	0.00362	5.83754	0.00198	734.79	935.11
0.00	22.50	280.80	0.11	0.02074	0.00219	0.00143	0.00362	5.86517	0.00199	749.03	952.63
0.00	23.00	280.80	0.11	0.02082	0.00220	0.00142	0.00361	5.89150	0.00199	470.13	969.98
0.00	23.50	280.80	0.11	0.02089	0.00220	0.00141	0.00361	5.91475	0.00200	781.82	987.12
0.00	24.00	280.80	0.11	0.02096	0.00221	0.00140	0.00361	5.93750	0.00201	778.19	1008.51
0.00	24.50	280.80	0.11	0.02102	0.00222	0.00139	0.00361	5.95871	0.00201	798.91	1028.12
0.00	25.00	280.80	0.11	0.02108	0.00222	0.00138	0.00360	5.97644	0.00202	798.23	1044.09
0.00	25.50	280.80	0.11	0.02113	0.00223	0.00137	0.00360	5.99384	0.00202	803.08	1059.84
0.00	26.00	280.80	0.11	0.02117	0.00223	0.00136	0.00360	6.01011	0.00203	818.08	1075.37
0.00	26.50	280.80	0.11	0.02121	0.00224	0.00136	0.00359	6.02498	0.00203	828.86	1085.61
0.00	27.00	280.80	0.11	0.02125	0.00224	0.00135	0.00359	6.03802	0.00203	845.84	1100.50
0.00	27.50	280.80	0.11	0.02129	0.00224	0.00135	0.00359	6.04926	0.00204	851.82	1115.11
0.00	28.00	280.80	0.11	0.02132	0.00225	0.00134	0.00359	6.05889	0.00204	858.99	1129.44
0.00	28.50	280.80	0.11	0.02134	0.00225	0.00134	0.00359	6.06695	0.00204	866.75	1144.20
0.00	29.00	280.80	0.11	0.02137	0.00225	0.00133	0.00358	6.08180	0.00205	874.83	1160.12
0.00	29.50	280.80	0.11	0.02139	0.00225	0.00132	0.00358	6.09686	0.00205	874.09	1175.91

D. EARTH-MARS-JUPITER-SATURN-EARTH WAVERIDER MISSION

1. Angle of Attack Analysis

AOA Degree	MINF	TINF R	PINF psf	CL	CDP	CDF	CDTOT	L/D	CM	Tupr R	Tlow R
10.00	25.84	282.60	0.12	-0.06014	0.01042	0.00190	0.01232	-4.88451	-0.00715	1184.88	697.79
-9.00	25.84	282.60	0.12	-0.04969	0.00769	0.00173	0.00942	-5.27958	-0.00588	1162.26	697.79
-8.00	25.84	282.60	0.12	-0.04005	0.00547	0.00156	0.00703	-5.69643	-0.00473	1132.09	715.62
-7.00	25.84	282.60	0.12	-0.03095	0.00372	0.00148	0.00519	-5.94879	-0.00364	1106.80	780.42
-6.00	25.84	282.60	0.12	-0.02248	0.00240	0.00141	0.00381	-5.85294	-0.00264	1081.72	844.75
-5.00	25.84	282.60	0.12	-0.01428	0.00149	0.00140	0.00289	-4.80186	-0.00169	1052.41	903.94
-4.00	25.84	282.60	0.12	-0.00621	0.00099	0.00141	0.00240	-2.32461	-0.00076	1013.28	949.43
-3.00	25.84	282.60	0.12	0.00183	0.00088	0.00141	0.00229	1.14028	0.00017	975.71	993.68
-2.00	25.84	282.60	0.12	0.01005	0.00118	0.00139	0.00257	4.20189	0.00111	937.22	1032.07
-1.00	25.84	282.60	0.12	0.01885	0.00188	0.00136	0.00324	5.97255	0.00212	875.60	1068.34
0.00	25.84	282.60	0.12	0.02743	0.00303	0.00140	0.00444	6.25671	0.00311	821.25	1092.39
1.00	25.84	282.60	0.12	0.03695	0.00463	0.00145	0.00609	6.08867	0.00422	761.19	1120.40
2.00	25.84	282.60	0.12	0.04729	0.00673	0.00153	0.00826	5.71267	0.00543	697.25	1149.94
3.00	25.84	282.60	0.12	0.05818	0.00935	0.00167	0.01102	5.26228	0.00671	697.25	1176.74
4.00	25.84	282.60	0.12	0.07014	0.01257	0.00181	0.01438	4.85595	0.00814	697.25	1197.55
5.00	25.84	282.60	0.12	0.08323	0.01646	0.00197	0.01842	4.50108	0.00971	697.25	1224.95
6.00	25.84	282.60	0.12	0.09737	0.02106	0.00210	0.02316	4.19069	0.01143	697.25	1246.14
7.00	25.84	282.60	0.12	0.11251	0.02642	0.00224	0.02866	3.91303	0.01328	697.25	1273.95
8.00	25.84	282.60	0.12	0.12860	0.03261	0.00235	0.03495	3.66817	0.01527	697.25	1296.51
9.00	25.84	282.60	0.12	0.14561	0.03966	0.00241	0.04207	3.45162	0.01739	697.25	1325.02

2. Altitude Analysis

AOA Degree	MINF	TINF R	PINF psf	CL	CDP	CDF	CDTOT	L/D	CM	Tupr R	Tlow R
0.00	25.84	303.70	0.39	0.02743	0.00303	0.00134	0.00438	6.25476	0.00311	975.45	1497.43
0.00	25.84	301.50	0.35	0.02743	0.00303	0.00133	0.00436	6.27265	0.00311	960.53	1404.59
0.00	25.84	299.00	0.31	0.02743	0.00303	0.00132	0.00435	6.28044	0.00311	943.69	1320.42
0.00	25.84	296.60	0.28	0.02743	0.00303	0.00131	0.00434	6.29247	0.00311	927.87	1225.35
0.00	25.84	294.50	0.25	0.02743	0.00303	0.00130	0.00434	6.30592	0.00311	912.95	1206.73
0.00	25.84	292.30	0.22	0.02743	0.00303	0.00129	0.00433	6.32401	0.00311	897.32	1187.24
0.00	25.84	290.20	0.20	0.02743	0.00303	0.00129	0.00432	6.33824	0.00311	881.15	1167.00
0.00	25.84	288.00	0.17	0.02743	0.00303	0.00130	0.00433	6.34580	0.00311	865.86	1148.02
0.00	25.84	286.20	0.15	0.02743	0.00303	0.00132	0.00435	6.34391	0.00311	850.60	1128.90
0.00	25.84	284.40	0.14	0.02743	0.00303	0.00135	0.00439	6.31001	0.00311	836.04	1110.76
0.00	25.84	282.60	0.12	0.02743	0.00303	0.00140	0.00444	6.25671	0.00311	821.25	1092.39
0.00	25.84	280.80	0.11	0.02743	0.00303	0.00147	0.00450	6.18028	0.00311	806.56	1074.38
0.00	25.84	279.00	0.10	0.02743	0.00303	0.00155	0.00458	6.08589	0.00311	791.96	1061.77
0.00	25.84	277.40	0.08	0.02743	0.00303	0.00164	0.00467	5.97330	0.00311	777.56	1044.06
0.00	25.84	275.60	0.07	0.02743	0.00303	0.00174	0.00478	5.85115	0.00311	763.02	1026.43
0.00	25.84	274.00	0.07	0.02743	0.00303	0.00185	0.00488	5.72778	0.00311	749.08	1009.58
0.00	25.84	272.20	0.06	0.02743	0.00303	0.00197	0.00500	5.59831	0.00311	734.44	992.26
0.00	25.84	270.50	0.05	0.02743	0.00303	0.00209	0.00513	5.46574	0.00311	719.86	975.19
0.00	25.84	269.10	0.05	0.02743	0.00303	0.00223	0.00526	5.33195	0.00311	705.96	958.74
0.00	25.84	267.70	0.04	0.02743	0.00303	0.00237	0.00541	5.19285	0.00311	691.78	942.13

3. Mach Number Analysis

AOA Degree	MINF	TINF R	PINF psf	CL	CDP	CDF	CDTOT	L/D	CM	Tupr R	Tlow R
0.00	20.50	282.60	0.12	0.02859	0.00316	0.00150	0.00466	6.22222	0.00325	725.40	920.98
0.00	21.00	282.60	0.12	0.02844	0.00315	0.00149	0.00463	6.22761	0.00323	744.29	937.65
0.00	21.50	282.60	0.12	0.02831	0.00313	0.00148	0.00461	6.23209	0.00322	733.67	954.12
0.00	22.00	282.60	0.12	0.02818	0.00312	0.00146	0.00458	6.23593	0.00320	754.35	970.38
0.00	22.50	282.60	0.12	0.02806	0.00310	0.00145	0.00456	6.23907	0.00319	765.62	986.40
0.00	23.00	282.60	0.12	0.02795	0.00309	0.00145	0.00454	6.24372	0.00317	475.24	1002.11
0.00	23.50	282.60	0.12	0.02785	0.00308	0.00144	0.00452	6.24764	0.00316	774.79	1017.54
0.00	24.00	282.60	0.12	0.02775	0.00307	0.00143	0.00450	6.25161	0.00315	788.19	1035.34
0.00	24.50	282.60	0.12	0.02765	0.00306	0.00142	0.00448	6.25005	0.00314	803.22	1053.50
0.00	25.00	282.60	0.12	0.02757	0.00305	0.00142	0.00446	6.25115	0.00313	805.78	1065.00
0.00	25.50	282.60	0.12	0.02748	0.00304	0.00141	0.00445	6.25289	0.00312	811.12	1081.35
0.00	26.00	282.60	0.12	0.02740	0.00303	0.00140	0.00443	6.25770	0.00311	825.10	1097.56
0.00	26.50	282.60	0.12	0.02733	0.00302	0.00139	0.00441	6.26232	0.00310	835.68	1113.63
0.00	27.00	282.60	0.12	0.02725	0.00301	0.00139	0.00440	6.26762	0.00309	851.99	1129.55
0.00	27.50	282.60	0.12	0.02718	0.00301	0.00138	0.00438	6.27043	0.00308	858.30	1145.31
0.00	28.00	282.60	0.12	0.02712	0.00300	0.00137	0.00437	6.27256	0.00308	865.68	1160.90
0.00	28.50	282.60	0.12	0.02706	0.00299	0.00136	0.00436	6.27695	0.00307	873.59	1176.31
0.00	29.00	282.60	0.12	0.02700	0.00299	0.00136	0.00434	6.28056	0.00306	881.78	1191.53
0.00	29.50	282.60	0.12	0.02694	0.00298	0.00135	0.00433	6.28433	0.00306	881.52	1206.54
0.00	30.00	282.60	0.12	0.02689	0.00297	0.00135	0.00432	6.28842	0.00305	891.78	1221.35

LIST OF REFERENCES

1. Randolph, A. D., "AGA Characteristics," paper written for the Advanced Propulsion Conference, Jet Propulsion Laboratory, Pasadena, California, May 1994.

2. McRonald, A. D., and Randolph, J. E., "Applications of Aero-Gravity-Assist to High Energy Solar System Missions," paper presented at the AIAA/AAS Astrodynamics Conference, Portland, Oregon, 20-22 August 1990.

3. Schindel, L. H., "Waveriders," *Tactical Missile Aerodynamics, Progress in Astronautics and Aeronautics,* v. 104, pp. 198-242.

4. Lewis, M. J., and McRonald, A. D., "The Design of Hypersonic Waveriders for Aero-Assisted Interplanetary Trajectories," paper presented at the AIAA 29th Aerospace Sciences Meeting, Reno, Nevada, 7-10 January 1991.

5. Sauer, C. G., "MIDAS: Mission Design and Analysis Software for the Optimization of Ballistic Interplanetary Trajectories," *The Journal of the Astronautical Sciences,* Vol. 37, No. 3, July-September 1989, pp. 251-259.

6. Sauer, C. G., "Preliminary Draft of Users Guide to MIDAS," paper written for the Advanced Projects Group, Jet Propulsion Laboratory, Pasadena, California, 4 March 1991.

7. Diehl, R. E., and Myers, M. R., *Gravity-Assist Trajectories to the Outer Solar System,* Jet Propulsion Laboratory Document D-4677, 21 September 1987.

8. Price, D. R., *Optimization and Performance Analysis of a Supersonic Conical-Flow Waverider for a Deck-Launched Intercept Mission,* Master's Thesis, Naval Postgraduate School, Monterey, California, June 1993.

9. Sutton, G. P., *Rocket Propulsion Elements: An Introduction to the Engineering of Rockets,* Wiley-Interscience Publication: John Wiley & Sons, Inc., 1992.

10. Anderson, J. D., *Hypersonic and High Temperaure Gas Dynamics,* McGraw-Hill, Inc., 1989.

11. Pessin, D. N., *Aerodynamic Analysis of Hypersonic Waverider Aircraft,* Master's Thesis, California Polytechnic State University, San Luis Obispo, California, March 1993.

12. Kuchemann, D., *The Aerodynamic Design of Aircraft,* Pergamon Press Ltd., 1978.

13.   Bertin, J. J., *Hypersonic Aerothermodynamics,* AIAA Inc., 1994.

14.   Randolph, J. E., and McRonald, A. D., "Solar Probe Mission Status," JPL internal document No. 89-212, 1989.

15.   McRonald, A. D., and Randolph, J. E., "Hypersonic Maneuvering for Augmenting Planetary Gravity Assist," *Journal of Spacecraft and Rockets,* American Institute of Aeronautics and Astronautics, Vol. 29, No. 2, March-April 1992, pp216-222.

16.   Randolph, J. E., and McRonald, A. D., "Solar System 'Fast Mission' Scenarios Using Hypersonic Waveriders," paper presented at the AIAA 29th Aerospace Sciences Meeting, Reno, Nevada, 7-10 January 1991.

17.   McRonald, A. D., and Randolph, J. E., "Hypersonic Maneuvering to Provide Planetary Gravity Assist," paper presented at the AIAA 28th Aerospace Sciences Meeting, Reno, Nevada, 8-11 January 1990.

INITAL DISTRIBUTION LIST

1. Defense Technical Information Center   2
   8725 John J. Kingman Rd., STE 0944
   Ft. Belvoir, Virginia 22060-6218

2. Dudley Knox Library   2
   Naval Postgraduate School
   411 Dyer Rd.
   Monterey, California 93943-5101

3. Professor C. F. Newberry   5
   Dept. of Aeronautics and Astronautics
   AA/Ne
   Naval Postgraduate School
   Monterey, California 93943

4. Professor D. J. Collins   1
   Dept. of Aeronautics and Astronautics
   AA
   Naval Postgraduate School
   Monterey, California 93943

5. Mr. J. V. Bowles   5
   Systems Analysis Branch
   M. S. 237-11
   NASA Ames Research Center
   Moffett Field, California 94035

6. Dr. A. D. McRonald   1
   Advanced Projects Group
   Mission Design Section
   Jet Propulsion Laboratory
   Pasadena, California 91109-8099

7. Mr. J. E. Randolph   1
   Space Physics Program Manager
   Solar Probe Manager
   Jet Propulsion Laboratory
   Pasadena, California 91109-8099

8.   Dr. John D. Anderson, Jr.   1
        Professor
        Aerospace Engineering Department
        University of Maryland
        College Park, Maryland 20742

9.   Dr.Mark J. Lewis   1
        Assistant Professor
        Aerospace Engineering Department
        University of Maryland
        College Park, Maryland 20742

10.   Dr. Isaiah M. Blankson   1
        Manager of University Research Programs
        Office of Aeronautics
        Code RT
        NASA Headquarters
        300 E Street, S.W.
        Washington, DC 20546

11.   John L. Anderson   1
        Advanced Concepts Office
        Office of Space Access and Technology
        Code XZ
        NASA Headquarters
        Washington, DC 20546